INCREASES AND DECREASES IN THE FINE MODE FRACTION OF AEROSOL OPTICAL DEPTH WITH INCREASING RELATIVE HUMIDITY

BY

SUCHISMITA BOSE

THESIS

Submitted in partial fulfillment of the requirements
for the degree of Master of Science in Atmospheric Sciences
in the Graduate College of the
University of Illinois at Urbana-Champaign, 2011

Urbana, Illinois

Adviser:

Professor Larry Di Girolamo

ABSTRACT

The total contribution of the small (radius $\leq$ 0.35 μm) and medium (radius $\leq$ 0.7 μm) sized particles as a defined by MISR (Multi-Angle Imaging SpectroRadiometer) to the Aerosol Optical Depth (AOD) is correlated to the AERONET (Aerosol Robotic Network) fine mode fraction of AOD. According to this thesis the contribution of particles having radius $\leq$ 0.7 μm to the measured AOD can either increase or decrease with increasing relative humidity, depending on the initial function of aerosols. Instinctively it appears that since the aerosols swell up according to their hygroscopic properties with an increase in relative humidity, the contribution of particles having radius $\leq$ 0.7 μm to the AOD (defined here as fine mode fraction of AOD) should decrease. Although this is true for certain size distributions, it is not true for all size distributions. However, often the increase in fine mode fraction of AOD as derived from AERONET/ Satellite based instruments are interpreted as an increase in fine particle pollutants of anthropogenic origin and a decrease in fine mode fraction is attributed to enhanced dust activity or influence of larger marine aerosols without considering the influence of relative humidity. Although fine mode fraction will definitely change if the emission scenario of fine particles changes (e.g. if there is increased crop waste burning or a sudden surge of wind blown dust from elsewhere), but according to the work presented in this thesis, for certain size distributions relative humidity alone is sufficient to explain large increases or decreases in fine mode fraction of AOD. Hence prior to attributing increases and decreases in particle fine mode fraction to changes in emission from different sources, the role of relative humidity and the prevalent particle size distribution in the region must both be accounted for.

To my dearest mother.

ACKNOWLEDGMENTS

This thesis would not have been possible without the constant guidance and support of my adviser and mentor Prof. Larry Di Girolamo. I am really grateful to him for being so patient and understanding throughout. Larry has not only been a wonderful guide but I also cherish being a student and a TA in his courses. I am indebted to Prof. Nicole Riemer and Prof. Greg McFarquhar for building up my interest in atmospheric aerosols and helping me develop a thorough understanding of the topic. Thanks to Prof. Robert Rauber for leading such a wonderful group of faculty, students and staff that made my experience at the Department of Atmospheric Sciences at UIUC a memorable one.

This research has been partially funded by the MISR project initiative at Jet Propulsion Laboratory, California Institute of Technology.

Finally, my sincere gratitude to all my friends, family and especially my husband for always being there for me.

TABLE OF CONTENTS

LIST OF TABLES vii

LIST OF FIGURES viii

LIST OF ABBREVIATIONS xvi

CHAPTER 1 INTRODUCTION 1
1.1 Atmospheric Aerosols 1
1.2 Significance of fine aerosol particles 3
1.3 Monitoring the emission of fine aerosol particles of anthropogenic origin 5
1.4 Goal of this research 6

CHAPTER 2 RELEVANT STUDIES 8
2.1 Impact of Relative Humidity on Aerosol Optical properties: Observation and model based studies 8
2.2 Studies that have focused on sensitivity of aerosol radiative forcing to changes in relative humidity 12
2.3 Studies regarding role of relative humidity in influencing aerosol optical properties near cloud boundaries 14

CHAPTER 3 METHODOLOGY 18
3.1 Analytical Size Distribution Function 19
3.2 Aerosol Particle Model and Chemical Composition 23
3.3 Complex Index of Refraction of the Aerosol particles and its dependence on relative humidity 26
3.4 Aerosol Particle Growth Factor as a Function of Relative Humidity 28
3.5 Calculation of fine mode fraction of aerosol optical depth 32

CHAPTER 4 RESULTS AND DISCUSSION 36
4.1 Trends in the variation of fine mode fraction of AOD with positive changes in relative humidity 36
4.2 Quantification of the increases and decreases in fine mode fraction of AOD 48
4.3 Discussion of the results 52

CHAPTER 5 CONCLUSION 56
5.1 Applicability of the results to other definitions of fine mode fraction 56
5.2 Assumptions 61
5.3 Error estimation 63
5.4 Impact of RH on Angstrom Exponent 65
5.5 Conclusion 67

APPENDIX A VARIATION IN THE FINE MODE FRACTION OF AOD AS A FUNCTION OF RELATIVE HUMIDITY FOR TYPE 1 AEROSOLS 69

APPENDIX B VARIATION IN FINE MODE FRACTION OF AOD AS A FUNCTION OF RELATIVE HUMIDITY FOR TYPE 2 AEROSOLS 83

REFERENCES 97

LIST OF TABLES

3.1 Table listing different combinations of fractional volume concentration in the accumulation and coarse modes 21
3.2 Different combinations of the parameter values (R_1, R_2, $Ln\sigma_1$, $Ln\sigma_2$) that have been used in the lognormal volume distribution function to generate a variety of different dry aerosol size distributions 22
3.3 Mass fraction and critical relative humidities of the salts constituting the soluble part of the aerosol particles 24
3.4 Parameter values specifying the chemical composition of the aerosol particles in accordance to Nilsson (1979). δ_s is the mass fraction of water soluble components, δ_i is the mass fraction of water insoluble components, δ_{soot} is the mass fraction of soot and ρ represents the densities of the respective components. . . . 24
3.5 Complex refractive indices (n=n' + ik) 27
3.6 Mass fractions and parameter values corresponding to Type 1 and Type 2 aerosol compositions for calculating the growth factor 32
3.7 Van't Hoff factor i and the dissolved fraction ϵ of the water soluble components at different relative humidities. The value of i and ϵ corresponding to RH of 76% was not listed in the source (Nilsson, 1979) 34

5.1 Error estimate in fine mode fraction of AOD due to fixed microphysical cut-off radius of 0.7μm 64
5.2 Error estimate in fine mode fraction of AOD from the assumption that particles larger than 10μm do not contribute to the aerosol optical depth for the size distributions under consideration 64

LIST OF FIGURES

1.1 Different modes present in aerosol size distribution (Seinfeld & Pandis, 1998) 2

3.1 Aerosol particle model adopted from Nilsson (1979) 25
3.2 The growth factor $\left(\frac{r}{r_0}\right)$ as a function of RH for Type 1 aerosols corresponding to dry radius of 0.05 μm. 33
3.3 The growth factor $\left(\frac{r}{r_0}\right)$ as a function of RH for Type 2 aerosols corresponding to dry radius of 0.05 μm. 33

4.1 An example of continuous increase in the fine mode fraction of AOD with increase in RH 38
4.2 An example of continuous decrease in the fine mode fraction of AOD with increase in RH 38
4.3 An example of Fine mode fraction of AOD remains constant with increase in RH 39
4.4 An example of Fine mode fraction of AOD exhibits mixed behavior with increase in RH 39
4.5 Changes in Aerosol Size Distribution with increase in RH for Type 1 aerosols: Dry size distribution corresponding to the continuous increase in fine mode fraction scenario 40
4.6 Changes in Aerosol Size Distribution with increase in RH for Type 1 aerosols: Dry size distribution corresponding to the continuous decrease in fine mode fraction scenario 40
4.7 Changes in Aerosol Size Distribution with increase in RH for Type 1 aerosols: Dry size distribution corresponding to the constant fine mode fraction scenario 41
4.8 Changes in Aerosol Size Distribution with increase in RH for Type 1 aerosols: Dry size distribution corresponding to the mixed behavior in fine mode fraction scenario 41
4.9 Normalized Cumulative Aerosol Optical Depth for RH = 55%, 75%, 95% (Composition: Type 1 aerosols). Dry size distribution corresponding to continuous increase in fine mode fraction scenario. 42

4.10 Normalized Cumulative Aerosol Optical Depth for RH = 55%, 75%, 95% (Composition: Type 1 aerosols). Dry size distribution corresponding to continuous decrease in fine mode fraction scenario. 42
4.11 Normalized Cumulative Aerosol Optical Depth for RH = 55%, 75%, 95% (Composition: Type 1 aerosols). Dry size distribution corresponding to constant fine mode fraction scenario. . . . 43
4.12 Normalized Cumulative Aerosol Optical Depth for RH = 55%, 75%, 95% (Composition: Type 1 aerosols). Dry size distribution corresponding to mixed behavior in fine mode fraction scenario. 43
4.13 Extinction efficiency (λ = 550 nm) as a function of particle radius for Type 1 aerosols, using Mie theory 45
4.14 Product of extinction efficiency (λ = 550 nm) and square of particle radius as a function of radius of Type 1 aerosols 45
4.15 Change in fine mode fraction of AOD with increase in RH for dry size distribution characterized by parameters R_1=0.005μm; Lnσ_1=0.4; Lnσ_2=0.72. The value of R_2 increases steadily from 1 μm to 3 μm along the horizontal axis. Arrows indicate the accumulation mode fraction 49
4.16 Change in fine mode fraction of AOD with increase in RH for dry size distribution characterized by parameters R_1=0.05μm; Lnσ_1=0.4; Lnσ_2=0.72. The value of R_2 increases steadily from 1 μm to 3 μm along the horizontal axis. Arrows indicate the accumulation mode fraction 49
4.17 Change in fine mode fraction of AOD with increase in RH for dry size distribution characterized by parameters R_1=0.05μm; R_2=1.5μm; Lnσ_1=0.2. The value of Lnσ_2 increases steadily from 0.2 to 0.8 along the horizontal axis. Arrows indicate the accumulation mode fraction 50
4.18 Change in fine mode fraction of AOD with increase in RH for dry size distribution characterized by parameters R_1=0.05μm; R_2=1.5μm; Lnσ_1=0.4. The value of Lnσ_2 increases steadily from 0.2 to 0.8 along the horizontal axis. Arrows indicate the accumulation mode fraction 50
4.19 Change in fine mode fraction of AOD with increase in RH for dry size distribution characterized by parameters R_1=0.05μm; R_2=1.5μm; Lnσ_1=0.6. The value of Lnσ_2 increases steadily from 0.2 to 0.8 along the horizontal axis. Arrows indicate the accumulation mode fraction 51

4.20 Change in fine mode fraction of AOD with increase in RH for dry size distribution characterized by parameters R_1=0.05μm; R_2=1.5μm; Lnσ_1=0.8. The value of Lnσ_2 increases steadily from 0.2 to 0.8 along the horizontal axis. Arrows indicate the accumulation mode fraction 51

5.1 Fine mode fraction of AOD as defined by AERONET as a function of RH (R_1=0.05 μm, R_2=1.5 μm, Lnσ_1 = 0.4, Lnσ_2=0.4, $V_{t1}/V_{t1} + V_{t2} = 0.2$) 57
5.2 Fine mode fraction of AOD as defined by AERONET as a function of RH (R_1=0.05 μm, R_2=1 μm, Lnσ_1 = 0.4, Lnσ_2=0.72, $V_{t1}/V_{t1} + V_{t2} = 0.2$) 57
5.3 Fine mode fraction of AOD as defined by AERONET as a function of RH (R_1=0.05 μm, R_2=1 μm, Lnσ_1 = 0.4, Lnσ_2=0.72, $V_{t1}/V_{t1} + V_{t2} = 1$) 58
5.4 Fine mode fraction of AOD as defined by AERONET as a function of RH (R_1=0.05 μm, R_2=1.5 μm, Lnσ_1 = 0.4, Lnσ_2=0.72, $V_{t1}/V_{t1} + V_{t2} = 0.2$) 58
5.5 Fine mode fraction of AOD as defined by MODIS as a function of RH (R_1=0.05 μm, R_2=1.5 μm, Lnσ_1 = 0.4, Lnσ_2=0.4, $V_{t1}/V_{t1} + V_{t2} = 0.2$) 59
5.6 Fine mode fraction of AOD as defined by MODIS as a function of RH (R_1=0.05 μm, R_2=1 μm, Lnσ_1 = 0.4, Lnσ_2=0.72, $V_{t1}/V_{t1} + V_{t2} = 0.2$) 59
5.7 Fine mode fraction of AOD as defined by MODIS as a function of RH (R_1=0.05 μm, R_2=1 μm, Lnσ_1 = 0.4, Lnσ_2=0.72, $V_{t1}/V_{t1} + V_{t2} = 1$) 60
5.8 Fine mode fraction of AOD as defined by MODIS as a function of RH (R_1=0.05 μm, R_2=1.5 μm, Lnσ_1 = 0.4, Lnσ_2=0.72, $V_{t1}/V_{t1} + V_{t2} = 0.2$) 60
5.9 Change in Angstrom Exponent with RH for 9 different accumulation mode fracitons (dry). (Loeb & Schuster, 2008) 67

A.1 Fine mode fraction of AOD (Type 1 aerosols) as a function of RH for dry size distributions specified by the parameters R_1=0.005μm, R_2=1μm, lnσ_1=0.4,lnσ_2=0.72,$V_{t1}/(V_{t1} + V_{t2})$=1, 0.8, 0.6, 0.4, 0.2, 0.0 69
A.2 Fine mode fraction of AOD (Type 1 aerosols) as a function of RH for dry size distributions specified by the parameters R_1=0.005μm, R_2=1.5μm, lnσ_1=0.4,lnσ_2=0.72,$V_{t1}/(V_{t1} + V_{t2})$=1, 0.8, 0.6, 0.4, 0.2, 0.0 70
A.3 Fine mode fraction of AOD (Type 1 aerosols) as a function of RH for dry size distributions specified by the parameters R_1=0.005μm, R_2=2.0, lnσ_1=0.4,lnσ_2=0.72,$V_{t1}/(V_{t1} + V_{t2})$=1, 0.8, 0.6, 0.4, 0.2, 0.0 70

A.4 Fine mode fraction of AOD (Type 1 aerosols) as a function of RH for dry size distributions specified by the parameters R_1=0.005μm, R_2=2.5μm, lnσ_1=0.4,lnσ_2=0.72,$V_{t1}/(V_{t1}+V_{t2})$=1, 0.8, 0.6, 0.4, 0.2, 0.0 71
A.5 Fine mode fraction of AOD (Type 1 aerosols) as a function of RH for dry size distributions specified by the parameters R_1=0.005μm, R_2=3μm, lnσ_1=0.4,lnσ_2=0.72,$V_{t1}/(V_{t1}+V_{t2})$=1, 0.8, 0.6, 0.4, 0.2, 0.0 71
A.6 Fine mode fraction of AOD (Type 1 aerosols) as a function of RH for dry size distributions specified by the parameters R_1=0.05μm, R_2=1μm, lnσ_1=0.4,lnσ_2=0.72,$V_{t1}/(V_{t1}+V_{t2})$=1, 0.8, 0.6, 0.4, 0.2, 0.0 72
A.7 Fine mode fraction of AOD (Type 1 aerosols) as a function of RH for dry size distributions specified by the parameters R_1=0.05μm, R_2=1.5μm, lnσ_1=0.4,lnσ_2=0.72,$V_{t1}/(V_{t1}+V_{t2})$=1, 0.8, 0.6, 0.4, 0.2, 0.0 72
A.8 Fine mode fraction of AOD (Type 1 aerosols) as a function of RH for dry size distributions specified by the parameters R_1=0.05μm, R_2=2μm, lnσ_1=0.4,lnσ_2=0.72,$V_{t1}/(V_{t1}+V_{t2})$=1, 0.8, 0.6, 0.4, 0.2, 0.0 73
A.9 Fine mode fraction of AOD (Type 1 aerosols) as a function of RH for dry size distributions specified by the parameters R_1=0.05, R_2=2.5μm, lnσ_1=0.4,lnσ_2=0.72,$V_{t1}/(V_{t1}+V_{t2})$=1, 0.8, 0.6, 0.4, 0.2, 0.0 73
A.10 Fine mode fraction of AOD (Type 1 aerosols) as a function of RH for dry size distributions specified by the parameters R_1=0.05μm, R_2=3μm, lnσ_1=0.4,lnσ_2=0.72,$V_{t1}/(V_{t1}+V_{t2})$=1, 0.8, 0.6, 0.4, 0.2, 0.0 74
A.11 Fine mode fraction of AOD (Type 1 aerosols) as a function of RH for dry size distributions specified by the parameters R_1=0.05μm, R_2=1.5μm, lnσ_1=0.2,lnσ_2=0.2,$V_{t1}/(V_{t1}+V_{t2})$=1, 0.8, 0.6, 0.4, 0.2, 0.0 74
A.12 Fine mode fraction of AOD (Type 1 aerosols) as a function of RH for dry size distributions specified by the parameters R_1=0.05μm, R_2=1.5μm, lnσ_1=0.2,lnσ_2=0.4,$V_{t1}/(V_{t1}+V_{t2})$=1, 0.8, 0.6, 0.4, 0.2, 0.0 75
A.13 Fine mode fraction of AOD (Type 1 aerosols) as a function of RH for dry size distributions specified by the parameters R_1=0.05μm, R_2=1.5μm, lnσ_1=0.2,lnσ_2=0.6,$V_{t1}/(V_{t1}+V_{t2})$=1, 0.8, 0.6, 0.4, 0.2, 0.0 75
A.14 Fine mode fraction of AOD (Type 1 aerosols) as a function of RH for dry size distributions specified by the parameters R_1=0.05μm, R_2=1.5μm, lnσ_1=0.2,lnσ_2=0.8,$V_{t1}/(V_{t1}+V_{t2})$=1, 0.8, 0.6, 0.4, 0.2, 0.0 76

A.15 Fine mode fraction of AOD (Type 1 aerosols) as a function of RH for dry size distributions specified by the parameters R_1=0.05μm, R_2=1.5μm, lnσ_1=0.4,lnσ_2=0.2,$V_{t1}/(V_{t1}+V_{t2})$=1, 0.8, 0.6, 0.4, 0.2, 0.0 76
A.16 Fine mode fraction of AOD (Type 1 aerosols) as a function of RH for dry size distributions specified by the parameters R_1=0.05μm, R_2=1.5μm, lnσ_1=0.4,lnσ_2=0.4,$V_{t1}/(V_{t1}+V_{t2})$=1, 0.8, 0.6, 0.4, 0.2, 0.0 77
A.17 Fine mode fraction of AOD (Type 1 aerosols) as a function of RH for dry size distributions specified by the parameters R_1=0.05μm, R_2=1.5μm, lnσ_1=0.4,lnσ_2=0.6,$V_{t1}/(V_{t1}+V_{t2})$=1, 0.8, 0.6, 0.4, 0.2, 0.0 77
A.18 Fine mode fraction of AOD (Type 1 aerosols) as a function of RH for dry size distributions specified by the parameters R_1=0.05μm, R_2=1.5μm, lnσ_1=0.4,lnσ_2=0.8,$V_{t1}/(V_{t1}+V_{t2})$=1, 0.8, 0.6, 0.4, 0.2, 0.0 78
A.19 Fine mode fraction of AOD (Type 1 aerosols) as a function of RH for dry size distributions specified by the parameters R_1=0.05μm, R_2=1.5μm, lnσ_1=0.6,lnσ_2=0.2,$V_{t1}/(V_{t1}+V_{t2})$=1, 0.8, 0.6, 0.4, 0.2, 0.0 78
A.20 Fine mode fraction of AOD (Type 1 aerosols) as a function of RH for dry size distributions specified by the parameters R_1=0.05μm, R_2=1.5μm, lnσ_1=0.6,lnσ_2=0.4,$V_{t1}/(V_{t1}+V_{t2})$=1, 0.8, 0.6, 0.4, 0.2, 0.0 79
A.21 Fine mode fraction of AOD (Type 1 aerosols) as a function of RH for dry size distributions specified by the parameters R_1=0.05μm, R_2=1.5μm, lnσ_1=0.6,lnσ_2=0.6,$V_{t1}/(V_{t1}+V_{t2})$=1, 0.8, 0.6, 0.4, 0.2, 0.0 79
A.22 Fine mode fraction of AOD (Type 1 aerosols) as a function of RH for dry size distributions specified by the parameters R_1=0.05μm, R_2=1.5μm, lnσ_1=0.6,lnσ_2=0.8,$V_{t1}/(V_{t1}+V_{t2})$=1, 0.8, 0.6, 0.4, 0.2, 0.0 80
A.23 Fine mode fraction of AOD (Type 1 aerosols) as a function of RH for dry size distributions specified by the parameters R_1=0.05μm, R_2=1.5μm, lnσ_1=0.8,lnσ_2=0.2,$V_{t1}/(V_{t1}+V_{t2})$=1, 0.8, 0.6, 0.4, 0.2, 0.0 80
A.24 Fine mode fraction of AOD (Type 1 aerosols) as a function of RH for dry size distributions specified by the parameters R_1=0.05μm, R_2=1.5μm, lnσ_1=0.8,lnσ_2=0.4,$V_{t1}/(V_{t1}+V_{t2})$=1, 0.8, 0.6, 0.4, 0.2, 0.0 81
A.25 Fine mode fraction of AOD (Type 1 aerosols) as a function of RH for dry size distributions specified by the parameters R_1=0.05μm, R_2=1.5μm, lnσ_1=0.8,lnσ_2=0.6,$V_{t1}/(V_{t1}+V_{t2})$=1, 0.8, 0.6, 0.4, 0.2, 0.0 81

A.26 Fine mode fraction of AOD (Type 1 aerosols) as a function of RH for dry size distributions specified by the parameters R_1=0.05μm, R_2=1.5μm, lnσ_1=0.8,lnσ_2=0.8,$V_{t1}/(V_{t1}+V_{t2})$=1, 0.8, 0.6, 0.4, 0.2, 0.0 82

B.1 Fine mode fraction of AOD (Type 2 aerosols) as a function of RH for dry size distributions specified by the parameters R_1=0.005μm, R_2=1μm, lnσ_1=0.4,lnσ_2=0.72,$V_{t1}/(V_{t1}+V_{t2})$=1, 0.8, 0.6, 0.4, 0.2, 0.0 83

B.2 Fine mode fraction of AOD (Type 2 aerosols) as a function of RH for dry size distributions specified by the parameters R_1=0.005μm, R_2=1.5μm, lnσ_1=0.4,lnσ_2=0.72,$V_{t1}/(V_{t1}+V_{t2})$=1, 0.8, 0.6, 0.4, 0.2, 0.0 84

B.3 Fine mode fraction of AOD (Type 2 aerosols) as a function of RH for dry size distributions specified by the parameters R_1=0.005μm, R_2=2.0μm, lnσ_1=0.4,lnσ_2=0.72,$V_{t1}/(V_{t1}+V_{t2})$=1, 0.8, 0.6, 0.4, 0.2, 0.0 84

B.4 Fine mode fraction of AOD (Type 2 aerosols) as a function of RH for dry size distributions specified by the parameters R_1=0.005μm, R_2=2.5μm, lnσ_1=0.4,lnσ_2=0.72,$V_{t1}/(V_{t1}+V_{t2})$=1, 0.8, 0.6, 0.4, 0.2, 0.0 85

B.5 Fine mode fraction of AOD (Type 2 aerosols) as a function of RH for dry size distributions specified by the parameters R_1=0.005μm, R_2=3.0μm, lnσ_1=0.4,lnσ_2=0.72,$V_{t1}/(V_{t1}+V_{t2})$=1, 0.8, 0.6, 0.4, 0.2, 0.0 85

B.6 Fine mode fraction of AOD (Type 2 aerosols) as a function of RH for dry size distributions specified by the parameters R_1=0.05μm, R_2=1.0μm, lnσ_1=0.4,lnσ_2=0.72,$V_{t1}/(V_{t1}+V_{t2})$=1, 0.8, 0.6, 0.4, 0.2, 0.0 86

B.7 Fine mode fraction of AOD (Type 2 aerosols) as a function of RH for dry size distributions specified by the parameters R_1=0.05μm, R_2=1.5μm, lnσ_1=0.4,lnσ_2=0.72,$V_{t1}/(V_{t1}+V_{t2})$=1, 0.8, 0.6, 0.4, 0.2, 0.0 86

B.8 Fine mode fraction of AOD (Type 2 aerosols) as a function of RH for dry size distributions specified by the parameters R_1=0.05μm, R_2=2.0μm, lnσ_1=0.4,lnσ_2=0.72,$V_{t1}/(V_{t1}+V_{t2})$=1, 0.8, 0.6, 0.4, 0.2, 0.0 87

B.9 Fine mode fraction of AOD (Type 2 aerosols) as a function of RH for dry size distributions specified by the parameters R_1=0.05μm, R_2=2.5μm, lnσ_1=0.4,lnσ_2=0.72,$V_{t1}/(V_{t1}+V_{t2})$=1, 0.8, 0.6, 0.4, 0.2, 0.0 87

B.10 Fine mode fraction of AOD (Type 2 aerosols) as a function of RH for dry size distributions specified by the parameters R_1=0.05μm, R_2=3.0μm, lnσ_1=0.4,lnσ_2=0.72,$V_{t1}/(V_{t1}+V_{t2})$=1, 0.8, 0.6, 0.4, 0.2, 0.0 88
B.11 Fine mode fraction of AOD (Type 2 aerosols) as a function of RH for dry size distributions specified by the parameters R_1=0.05μm, R_2=1.5μm, lnσ_1=0.2,lnσ_2=0.2,$V_{t1}/(V_{t1}+V_{t2})$=1, 0.8, 0.6, 0.4, 0.2, 0.0 88
B.12 Fine mode fraction of AOD (Type 2 aerosols) as a function of RH for dry size distributions specified by the parameters R_1=0.05μm, R_2=1.5μm, lnσ_1=0.2,lnσ_2=0.4,$V_{t1}/(V_{t1}+V_{t2})$=1, 0.8, 0.6, 0.4, 0.2, 0.0 89
B.13 Fine mode fraction of AOD (Type 2 aerosols) as a function of RH for dry size distributions specified by the parameters R_1=0.05μm, R_2=1.5μm, lnσ_1=0.2,lnσ_2=0.6,$V_{t1}/(V_{t1}+V_{t2})$=1, 0.8, 0.6, 0.4, 0.2, 0.0 89
B.14 Fine mode fraction of AOD (Type 2 aerosols) as a function of RH for dry size distributions specified by the parameters R_1=0.05μm, R_2=1.5μm, lnσ_1=0.2,lnσ_2=0.8,$V_{t1}/(V_{t1}+V_{t2})$=1, 0.8, 0.6, 0.4, 0.2, 0.0 90
B.15 Fine mode fraction of AOD (Type 2 aerosols) as a function of RH for dry size distributions specified by the parameters R_1=0.05μm, R_2=1.5μm, lnσ_1=0.4,lnσ_2=0.2,$V_{t1}/(V_{t1}+V_{t2})$=1, 0.8, 0.6, 0.4, 0.2, 0.0 90
B.16 Fine mode fraction of AOD (Type 2 aerosols) as a function of RH for dry size distributions specified by the parameters R_1=0.05μm, R_2=1.5μm, lnσ_1=0.4,lnσ_2=0.4,$V_{t1}/(V_{t1}+V_{t2})$=1, 0.8, 0.6, 0.4, 0.2, 0.0 91
B.17 Fine mode fraction of AOD (Type 2 aerosols) as a function of RH for dry size distributions specified by the parameters R_1=0.05μm, R_2=1.5μm, lnσ_1=0.4,lnσ_2=0.6,$V_{t1}/(V_{t1}+V_{t2})$=1, 0.8, 0.6, 0.4, 0.2, 0.0 91
B.18 Fine mode fraction of AOD (Type 2 aerosols) as a function of RH for dry size distributions specified by the parameters R_1=0.05μm, R_2=1.5μm, lnσ_1=0.4,lnσ_2=0.8,$V_{t1}/(V_{t1}+V_{t2})$=1, 0.8, 0.6, 0.4, 0.2, 0.0 92
B.19 Fine mode fraction of AOD (Type 2 aerosols) as a function of RH for dry size distributions specified by the parameters R_1=0.05μm, R_2=1.5μm, lnσ_1=0.6,lnσ_2=0.2,$V_{t1}/(V_{t1}+V_{t2})$=1, 0.8, 0.6, 0.4, 0.2, 0.0 92
B.20 Fine mode fraction of AOD (Type 2 aerosols) as a function of RH for dry size distributions specified by the parameters R_1=0.05μm, R_2=1.5μm, lnσ_1=0.6,lnσ_2=0.4,$V_{t1}/(V_{t1}+V_{t2})$=1, 0.8, 0.6, 0.4, 0.2, 0.0 93

B.21 Fine mode fraction of AOD (Type 2 aerosols) as a function of RH for dry size distributions specified by the parameters R_1=0.05μm, R_2=1.5μm, lnσ_1=0.6,lnσ_2=0.6,$V_{t1}/(V_{t1}+V_{t2})$=1, 0.8, 0.6, 0.4, 0.2, 0.0 93
B.22 Fine mode fraction of AOD (Type 2 aerosols) as a function of RH for dry size distributions specified by the parameters R_1=0.05μm, R_2=1.5μm, lnσ_1=0.6,lnσ_2=0.8,$V_{t1}/(V_{t1}+V_{t2})$=1, 0.8, 0.6, 0.4, 0.2, 0.0 94
B.23 Fine mode fraction of AOD (Type 2 aerosols) as a function of RH for dry size distributions specified by the parameters R_1=0.05μm, R_2=1.5μm, lnσ_1=0.8,lnσ_2=0.2,$V_{t1}/(V_{t1}+V_{t2})$=1, 0.8, 0.6, 0.4, 0.2, 0.0 94
B.24 Fine mode fraction of AOD (Type 2 aerosols) as a function of RH for dry size distributions specified by the parameters R_1=0.05μm, R_2=1.5μm, lnσ_1=0.8,lnσ_2=0.4,$V_{t1}/(V_{t1}+V_{t2})$=1, 0.8, 0.6, 0.4, 0.2, 0.0 95
B.25 Fine mode fraction of AOD (Type 2 aerosols) as a function of RH for dry size distributions specified by the parameters R_1=0.05μm, R_2=1.5μm, lnσ_1=0.8,lnσ_2=0.6,$V_{t1}/(V_{t1}+V_{t2})$=1, 0.8, 0.6, 0.4, 0.2, 0.0 95
B.26 Fine mode fraction of AOD (Type 2 aerosols) as a function of RH for dry size distributions specified by the parameters R_1=0.05μm, R_2=1.5μm, lnσ_1=0.8,lnσ_2=0.8,$V_{t1}/(V_{t1}+V_{t2})$=1, 0.8, 0.6, 0.4, 0.2, 0.0 96

LIST OF ABBREVIATIONS

ACE	Aerosol Characterization Experiment
AE	Angstrom Exponent
AERONET	Aerosol Robotic Network
AOD	Aerosol Optical Depth
HSRL	High Spectral Resolution LIDAR
INDOEX	Indian Ocean Experiment
IPCC	Inter Governmental Panel on Climate Change
LIDAR	Light Detection and Ranging
MISR	Multi-angle Imaging SpectroRadiometer
MODIS	Moderate Resolution Imaging Spectroradiometer
PRD	Pearl River Delta
RH	Relative Humidity
SGP	Southern Great Plains
TOA	Top of Atmosphere
VOC	Volatile Organic Compounds

CHAPTER 1

INTRODUCTION

1.1 Atmospheric Aerosols

Atmospheric aerosols are solid or liquid particles that are suspended in the atmosphere. They range in size from a few nanometers (nm) to tens of micrometers (μm) in diameter. Aerosol particles occurring in the atmosphere may be either directly emitted into the atmosphere or formed there by oxidation of precursor gasses, such as sulfur dioxide, nitrogen oxides and volatile organic compounds (VOCs), where the resulting oxidation products nucleate to form new particles or condense on preexisting ones. Particles that are formed by following these two routes are referred to as primary and secondary particles respectively (Seinfeld & Pandis, 1998). The origin of atmospheric aerosols can be natural as well as anthropogenic. Natural sources include wind borne dust, sea spray, volcanic activities and biomass burning while aerosols attributable to human activities arise mainly from fuel combustion, industrial processes, nonindustrial fugitive sources (like construction work) and transportation sources (automobiles).

Atmospheric aerosols are classified into separate modes based on their size, formation process and lifetime in the atmosphere. The exact size ranges of these modes vary in the literature, but the definitions described in this section have been adopted from the book of Seinfeld and Pandis and will be used throughout this thesis (Seinfeld & Pandis, 1998). In accordance with the number, surface and volume distributions of aerosol particles shown in Figure 1.1 , three distinct groups of atmospheric particles can be defined. Particles having radius greater than 0.5 μm are identified as coarse mode. These particles mainly result from mechan-

Figure 1.1: Different modes present in aerosol size distribution (Seinfeld & Pandis, 1998)

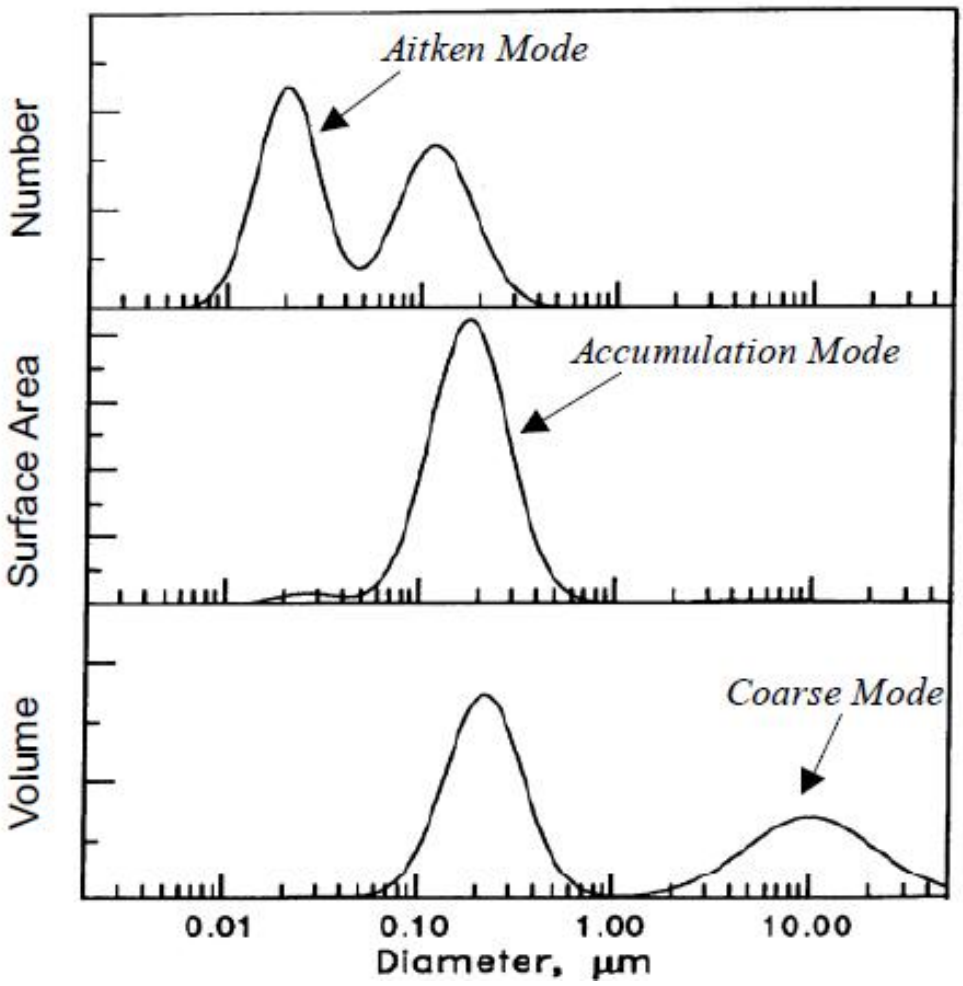

ical sources and are introduced directly into the atmosphere from both natural and anthropogenic sources. The most significant source is bursting of bubbles in the ocean creating coarse sea salt particles. Wind also picks up dust, soil and biological particles and suspends them in the atmosphere. Anthropogenic coarse particles are introduced in the atmosphere by means of abration of machinery on the surface of roads, and in industrial and agricultural processes. Particles with radius between 0.05 μm and 0.5 μm are considered as the accumulation mode representing a region of particle growth mainly due to coagulation of particles with radius less than 0.05 μm and from condensation of vapors onto existing particles, causing them to grow into this size range. They can also be introduced directly

into the atmosphere, mainly through incomplete combustion of wood, oil, coal, gasoline and other fuels. The accumulation mode has been so named because particle removal mechanisms are least efficient in this regime causing the particles to accumulate. The Aitken mode includes all particles having radius less than 0.05 μm. They are formed from ambient temperature gas to particle conversion as well as condensation of hot vapors during combustion processes. The Aitken and accumulation mode particles are collectively referred to as fine particles. These modes in general, originate separately, are transformed separately, are removed from the atmosphere by different mechanisms, have different lifetimes, have different chemical compositions and also differ in their optical properties. Hence distinction between the aitken, accumulation and coarse mode aerosol particles is of fundamental importance in any discussion of Physics, Chemistry, measurement or health effects of aerosols.

1.2 Significance of fine aerosol particles

The Aitken and accumulation mode particles are collectively referred to as fine particles. Anthropogenic emissions of fine atmospheric aerosols (radius $\leq 0.5\mu$m) and their precursors have increased dramatically over the past century and have been implicated in many areas ranging from human health to climate change (Seinfeld & Pandis, 1998; Finlayson-Pitts & Pitts, 2000). The degradation of visibility is perhaps the most visible aspect of urban and regional air pollution to the public. Fine aerosol particles in the size range of 0.05μm to 0.5μm in radius are major contributors to this phenomena because of their highly efficient light scattering properties (Horvath, 1995; Seinfeld & Pandis, 1998; Cheng & Tsai, 2000). In addition to visibility, the effects of fine atmospheric aerosols on human health have also been increasingly recognized. Air quality standards for particulate matter in countries such as united states were expressed some years ago in terms of total suspended particulate matter (TSP). The standard was then changed to mass of suspended particulate matter less than 10μm in size,

commonly called PM10, and more recently was modified to include particulate matter less than 2.5μm in diameter (PM2.5). The rationale for basing air quality standards on fine particles relied on the fact that they can penetrate deeper into the lungs and hence their potential adverse health effect is much greater (Phalen, 1984). Several epidemiological studies have associated fine particulate pollution with lung cancer and cardiopulmonary mortality (Dockery et al., 1993; Pope et al., 1995; Schwartz et al., 1996; Pope et al., 2002). On the other hand coarse particle fraction and total mass of suspended particles were found not to be consistently associated with mortality rates (Pope et al., 2002).

In their most recent report the inter governmental panel on climate change (IPCC) concluded that emissions of greenhouse gasses and aerosols due to human activities continue to alter the atmosphere in ways that are expected to effect the climate. The aerosols that are released into the atmosphere as a consequence of anthropogenic activities are mainly dominated by fine aerosol particles like the ones generated from industrial pollution and biomass burning (Kaufman et al., 2002; Kaufman et al., 2005b; Kaufman et al., 2005a; Kleidman et al., 2005). For a while it looked simple: greenhouse gasses warm the earth and the fine sulfate particles arising from anthropogenic sources cool it down (Charlson et al., 1992). Because aerosol particles in the atmosphere scatter sunlight back into space, they reduce the amount of energy that the planet absorbs, keeping it cooler. But this simplistic view ignored the fact that aerosol particles in the real world may also lead to heating of the lower atmosphere if they contain light absorbers such as elemental carbon (Andreae & Merlet, 2001). Scattering and absorbing of the solar radiation is known as the direct effect of aerosols on the global climate, which can lead to either cooling or warming of the atmosphere depending on the proportion of light scattered to that absorbed. There have been certain observations indicating that fine aerosol particles emitted from forest fires and urban pollution can suppress rain and snow fall (Rosenfeld, 1999; Rosenfeld, 2000). According to some arguments it might be a consequence of indirect effect of aerosols (Twomey, 1974; Twomey, 1977). As aerosol concentration increases within a cloud, the water in

the cloud gets spread over many more droplets, each of which is correspondingly smaller. This has three consequences: clouds with smaller drops reflect more sunlight, last longer and precipitate less. Hence it is evident that changing the concentration of fine aerosol particles in the atmosphere might affect the frequency of cloud occurrence, cloud thickness, cloud albido and rainfall amounts.

From the discussion above it appears that fine particle fraction of atmospheric aerosols have significant local and global impacts, whether they arise from anthropogenic sources (vehicular emissions, industrial processes, crop waste burning) or natural (forest fires). Local impacts include possible adverse health effects and degradation of visibility while global impacts imply their effect on earth's climate. Since we have little control over the natural sources of fine aerosol particles, there is an urgent need to monitor the emission of fine aerosol particles of anthropogenic origin, globally.

1.3 Monitoring the emission of fine aerosol particles of anthropogenic origin

One of the parameters that is widely used to monitor the increases and decreases in the anthropogenic emission of fine aerosol particles is fine mode fraction of aerosol optical depth as retrieved by several ground and satellite based instruments (Kaufman et al., 2002; Kaufman et al., 2005a; Kleidman et al., 2005; Dey & Di Girolamo, 2010; Kim et al., 2010). This parameter essentially gives an estimate of the fraction of the total aerosol optical depth that can be attributed to fine particles. MISR (Multi-angle Imaging Spectro Radiometer), onboard the NASA earth observing Terra spacecraft is one such instrument that performs retrieval of small(radius $< 0.35\mu$m), medium (0.35μm $\leq$ radius $\leq 0.7\mu$m) and large(radius $> 0.7\mu$m)particle fractions of total aerosol optical depth. The Aerosol Robotic Network (AERONET), which is a ground based network of sun/sky radiometers also retrieves the fine mode fraction. Since AERONET retrieves the fine mode fraction from optical measurements of spectral variations of aerosol opti-

cal depths assuming negligible spectral dependence of the coarse mode (ONeill et al., 2003) and does not consider any microphysical cut off radius, the MISR retrieved small particle fraction of AOD is somewhat different from the fine mode optical depth fraction reported by AERONET. Weak but statistically significant correlation between MISR retrieved small plus medium particle fraction of AOD (fs+fm) and AERONET retrieved fine mode fraction of AOD (AODfine/AOD) have been reported (Dey & Di Girolamo, 2010). MODIS (Moderate Resolution Imaging Spectroradiometer), one of the key instruments aboard NASA's Terra and Aqua spacecrafts also retrieves aerosol fine mode fraction. But in comparison to AERONET measurements, MODIS slightly overestimates fine mode fraction for dust dominated aerosols and underestimates in smoke and pollution dominated aerosol conditions (Kleidman et al., 2005). Although different instruments employ different algorithms, in a broader sense there is consistency between them in determining the contribution of fine mode aerosols to the total AOD over ocean surfaces.

Increase in fine mode fraction of AOD over a particular region, during a particular period of time (as documented by remote sensing studies)is often interpreted as increase in the emission of fine aerosol particles from manmade sources while decrease in the fine mode fraction is attributed to enhanced influence of coarse mode aerosols like dust and sea salt (Dey & Di Girolamo, 2010; Chu et al., 2003; Kim et al., 2010). In other words fine mode fraction of AOD has been used in the past as an indicator of the emission scenario of fine aerosol particles of anthropogenic origin.

1.4 Goal of this research

The goal of this research is to demonstrate that, depending on the parameters used to analytically specify the aerosol size distribution, positive changes in relative humidity alone is sufficient to explain large increases and decreases in the fine mode fraction of AOD without any change in the emission scenario of the

fine particles. Hence changes in the fine mode fraction of AOD as derived from AERONET/satellite based studies is not always an indication of increase or decrease in the emission of fine anthropogenic pollution particles.

The fine mode fraction of AOD is defined in this study as the contribution of particles having radius less than and equal to 0.7 μm to the total AOD. 0.7μm has been selected as the cut off radius because the small and medium particle fraction of the AOD, as defined by MISR, taken together (radius $\leq$ 0.7μm)is correlated to the AERONET fine mode fraction of AOD (Dey & Di Girolamo, 2010).The fine mode fraction of AOD is calculated for a variety of different aerosol size distributions (generated by varying the parameters of an analytical size distribution function) as a function of relative humidity ranging from 55% to 95%. During the calculations, the total number of aerosol particles is kept constant so that there is no emission of new particles. Increases and decreases in the fine mode fraction of AOD of significant magnitude for positive changes in relative humidity is documented for various aerosol size distributions corresponding to two different types of chemical composition.

The concern and question that is raised in this thesis can also be stated as follows: although fine mode fraction of AOD can definitely change if the emission scenario of fine particles changes (for example if there is increased crop waste burning, sudden wild fire or a surge of wind blown dust from elsewhere), is it only the increase or decrease in the emission of fine aerosol particles that can explain changes in remotely sensed fine mode fraction? According to the work presented in this thesis, increase in relative humidity can solely explain large changes in fine mode fraction of AOD depending on the size distribution of the aerosol particles. Hence prior to attributing increases and decreases in fine mode fraction of AOD to changes in emission of anthropogenic pollution, the role of relative humidity and the prevalent particle size distribution in the region must be accounted for.

CHAPTER 2

RELEVANT STUDIES

2.1 Impact of Relative Humidity on Aerosol Optical properties: Observation and model based studies

Water soluble aerosols when exposed to regions of enhanced relative humidity (RH), grow in size (Köhler, 1936) as well as undergo changes in refractive index and density (Tang & Munkelwitz, 1994). This growth is referred to as hygroscopic growth of aerosols and hygroscopic growth can lead to significat changes in aerosol optical properties.

One of the pioneering works to model the growth of hrygroscopic aerosols as a function of RH was by Hanel, who had proposed simple models based on theoretical considerations and observational evidence (Hänel, 1976). He had observed that the increase in particle size due to humidification is a complicated function of RH and the dry particle size. From his experiments Hanel had concluded that below a certain RH, the hygroscopic growth factor is independent of the dry size of the aerosols. Also for moderate and large RH values, the growth factor is smaller for those particles with smaller sizes in their dry state. The simple model that Hanel had proposed describing the aerosol growth as a function of RH is as follows:

$$\frac{r}{r_0} \approx (1 + (\frac{\rho_0}{\rho_w}) * \mu * (\frac{RH}{(1 - RH)}))^{\frac{1}{3}} \tag{2.1.1}$$

where, the growth factor $\frac{r}{r_0}$ is the ratio of the size of the particle over its dry size, ρ_0 and ρ_w are the densities of dry aerosol and pure water and μ is defined as the linear mass increase coefficient of the particle.

The curiosity of the scientific community on how the aerosol optical properties can get modified under the influence of enhanced RH conditions is not new. Twomey was one of the early researchers in this field who had calculated the change in the back-scattering coefficient of a model aerosol population as a function of RH. Other than stating that the back-scatter coefficient increased smoothly and steadily as the RH was increased from 80% ro 99.5%, Twomey also pointed out the importance of wavelength and aerosol size distribution under consideration in determining the change in the optical properties with hygroscopic growth of the aerosols (Twomey, 1977). Following Twomey, Fitzgerald (1984), also reemphasized the fact that the change in magnitude of the back-scatter coefficient due to increased RH has a strong dependence on wavelength. Fitzgerald had observed from his calculations that for a change of RH from 0 to 99%, the back-scattering coefficient at 0.694 μm increased by a factor of 5.7 for external mixture and 15.6 for an internal mixture scenario. However, for 10.6 μm radiation, the increase in back-scatter coefficient ranged from a factor of 2.1 to about 2.8 (Fitzgerald, 1984).

Given the strong impact that hygroscopic growth exudes on aerosol optical properties many more observation and model based studies have been devoted to this subject in the recent years. Su et. al. (2008) had calculated the back-scatter coefficient at 532 nm for an equilibrium mixture of Ammonium Sulfate and water in the accumulation mode and sea salt in the coarse mode. They found that the back-scatter coefficient had increased by over an order of magnitude as the RH was increased from 55% to 99% (Su et al., 2008). For an aerosol size distribution that had modelled based on aircraft and in-situ observations during the INDOEX field campaign, Twohy et. al. (2009) reported that the aerosol scattering cross section increased by about 600% as the RH was varied from 70% to 99%.

There have also been some studies that have modelled the impact of hygroscopic growth on aerosol optical properties using in-situ obervations. For example Liu et. al. (2008) had developed an empirical relation to calculate aerosol hygroscopic growth factor (defined as the ratio of the scattering coefficient at RH greater than 40% to the scattering coefficient at RH of 40%) at any ambient RH. This

empirical formula was based on in-situ measurements of aerosol physical, chemical and optical properties in the Guangzhou city of China recorded as a part of the Pearl River Delta campaign. The relation is given by:

$$f(RH) = 1 + a(\frac{RH}{100})b \tag{2.1.2}$$

where, a and b are the fitting parameters based on classification of air-mass type (urban, mixed, marine) during the campaign (Liu et al., 2008). Instead of trying to model the influence of RH on the scattering coefficient like Liu et. al., Veselouskii et. al. (2009) had applied an inversion algorithm on the ambient aerosol back-scattering coefficient and extinction coefficient as quantified by a multi-wavelength Mie-Raman Lidar to calculate aerosol parameters like AE, effective radius and specifications of the particle size distribution under varying RH conditions in the planetary boundary layer.

There have been quite a number of studies regarding the influence of RH on aerosol scattering coefficient but only a very few studies have explored the effect of RH on the absorption coefficient of aerosols. Nessler et. al. (2005), in a numerical study had investigated the role of RH in altering the absorption coefficient of aerosols that have been modelled to be representative of the Jungfraujoch which is a site located in the Swiss alps. Absorption coefficient enhancement factors as a function of RH were calculated for 10 different wavelengths in the range of 370 to 950 nm for summer and winter conditions. The enhancement factors varied from 0.94 to 1.78 in summer and from 0.84 to 1.53 in winter for a range of RH between 0% to 99% (Nessler et al., 2005). From their results it was concluded that although increase in absorption coefficient under high RH conditions is significant, it contributes only about 0.2% of the increase in extinction coefficient for wavelengths in the range of 450 to 700 nm.

So far, it has been stressed that the optical properties of the aerosols have a strong dependence on RH. But this dependence is to some extent determined by the chemical composition of the aerosols under consideration. Wulfmeyer et.

al. (2000), had applied a ground based water vapor differential absorption Lidar (DIAL) to investigate aerosol properties in the convective marine boundary layer. They observed that the back-scattering coefficient of aerosols as a function of RH was sensitive to variations in mass fractions of the soluble material present in the internally mixed aerosol (Wulfmeyer & Feingold, 2000). Re-enforcing the findings of Wulfmeyer et. al. (2000), Liu et. al. (2008) reported the impact of high RH on the optical properties of marine aerosols was greater than the urban aerosols, probably because of the higher mass fraciton of the soluble constituents present in the marine aerosols. In order to investigate the influence of water uptake on scattering properties of aerosols with different chemical compositions, Day and Malm (2001) made observations at 3 different rural national parks (Great Smokey Mountains, Grand Canyon, Big Bend) in the US. It was found that at any particular RH the maximum increase in the scattering coefficient corresponded to higher mass fractions of inorganic salts present (Day & Malm, 2001). The conclusions of Day and Malm (2001) go hand in hand with the conclusions of Kotchenruther et. al. (1999), which states that the higher fractions of carbon present in the aerosols correspond to lower value of the growth factor of scattering coefficient with increase in RH while higher mass fractions of inorganic salts correspond to higher value of growth factor.

The next question that arises is about the significance of the detailed chemical composition of the organic and inorganic components present in the aerosol in determining the influence of RH on the optical properties. Garland et. al. (2007), observed that the increase in extinction coefficient as a function of RH at 532 nm was not much affected by the detailed composition of the soluble organic components that were internally mixed with Ammonium Sulfate in tne laboratory generated aerosols as long as the water soluble fraction was similar. Regarding the detailed chemical composition of the soluble inorganic components, Tang (1996) found that per unit dry salt mass, the light scattered by the aerosol particles at any ambient RH, is only weakly dependent on the detailed chemical constituents of the hygroscopic sulfate and nitrate aerosols provided that the dry size distribution

remained unchanged.

Hence it can be concluded that the amount of light scattered and absorbed by aerosol particles is strongly dependent on the ambient RH. However, the importance of the dry particle size distribution, wavelength of the radiation and chemical compostion of the aerosols in determining the change in the optical properties with hygroscopic growth should always be kept in mind.

2.2 Studies that have focused on sensitivity of aerosol radiative forcing to changes in relative humidity

Other than affecting human health, aerosols are now widely known for influencing the Earths energy budget either directly by absorbing and scattering solar radiation or indirectly by changing the microphysical properties of clouds (reduction in cloud droplet size and increase in cloud droplet concentration) and thus impacting cloud albedo and lifetime. In other words aerosols present in the atmosphere perturbs the intensity of solar radiation that reaches the surface, the radiation that gets absorbed in the atmosphere and that which gets scattered back to space. This perturbation is referred to as aerosol radiative forcing.

There are huge uncertainties associated with the radiative forcing of atmospheric aerosols due to immense spatial and temporal heterogeneity of aerosol sources, the composition of the aerosols, their microphysical properties and meteorological parameters like relative humidity that strongly influence the optical properties of the aerosols. In order to reduce the uncertainty in aerosol radiative forcing, a key step is to concentrate on the factors that influence the optical properties of the aerosols and hence thereby influence the climate forcing. One such factor is relative humidity and there have been many studies regarding the sensitivity of aerosol radiative forcing to changes in relative humidity.

Bian et. al. (2009), observed using a global model that the worldwide average aerosol optical thickness calculated using relative humidity at a 1°x1.25° horizontal resolution was 11% higher than when the relative humidity was con-

sidered at a coarser resolution of 2°x2.5°. The direct radiative forcing at the top of the atmosphere was also 8 to 9% more negative when the relative humidity was considered at the finer resolution. According to the authors this increase in aerosol optical thickness and aerosol cooling with increase in spatial resolution of relative humidity was due to the highly non linear relationship between relative humidity and aerosol mass extinction efficiency at relative humidity levels greater than 80%. Cheng et. al. (2008) had also investigated the role of relative humidity in controlling aerosol optical properties and direct radiative forcing. They used a numerical model that was based on observations of aerosol physical and chemical properties as well as growth factors recorded during the Pearl River Delta campaign at Xinken, China. It was found that the aerosol radiative forcing in the surface boundary layer had strong dependence on relative humidity and the elemental carbon mixing state occurring in that region. For internal as well as coated mixture of elemental carbon, the direct radiative forcing at the surface boundary layer for relative humidity less than 60% was not very pronounced. However there was a cooling effect when the relative humidity was greater than 60% (Cheng & Tsai, 2000). In a similar study using in situ as well as aircraft measurements of aerosol properties at Gosan , South Korea; Yoon and KIm (2006), tried to quantify the changes in aerosol direct radiative forcing at the TOA, surface and the atmosphere with variations in relative humidity. As the relative humidity increased from 50% to 95%, the diurnal averaged direct forcing at the surface changed from -4.34W/m^2 to -9.63W/m^2. The forcing at the TOA changed from -2.72W/m^2 to -7.25W/m^2 and the forcing in the atmosphere changed from 1.62W/m^2 to 2.38W/m^2. However the diurnal averaged radiative forcing efficiency which is defined as the radiative forcing per unit aerosol optical depth at the surface, TOA and atmosphere was observed to decrease with increase in relative humidity. Markowicz (2003), had also reported similar dependence of aerosol forcing efficiency on relative humidity. They had found that decreasing the relative humidity to 55% from the ambient value enhanced the aerosol radiative forcing efficiency by as much as 6 to 10W/m^2 while studying aerosols over the sea

of Japan during the ACE-Asia experiment (March to April 2001).

From all these studies it can be inferred that hygroscopic growth of aerosols in the troposphere under the influence of humid tropical and subtropical air masses can significantly alter the magnitude of aerosol direct radiative forcing at the surface, TOA and the atmosphere. Hence humidity is a critical factor in determining the impact of aerosol forcing on the climate system and its importance has been recognized in the past as well as in the recent years.

2.3 Studies regarding role of relative humidity in influencing aerosol optical properties near cloud boundaries

In recent times many satellite based observational studies have tried to validate the aerosol indirect effect by establishing positive correlations between aerosol optical depth and cloud fraction. In other words some scientists believe that the positive correlation between aerosol optical depth and cloud fraction imply that in regions where there is comparatively more aerosol loading, the cloud droplet size gets reduced resulting in increased cloud lifetime and thus greater cloud fraction. For example Kaufman et. al. (2005), using MODIS data over the Atlantic Ocean observed that as the optical depth increased from 0.03 to 0.5, the cloud fraction persistently increased from 0.2 to 0.4. This was also accompanied by a 10 to 30% decrease in cloud droplet effective radius. There is some probability that these positive correlations might result from influence of aerosols on cloud properties, and hence verifies the aerosol indirect effect. But on the other hand retrieval artifacts like 3D- radiative cloud adjacency effects and cloud contamination can also explain such correlations between aerosol optical depth and cloud fraction. Another possible explanation can be the hygroscopic growth of aerosols near cloud boundaries where the relative humidity values are significantly high.

Regions surrounding clouds have comparatively higher values of relative humid-

ity than ambient values and several observational studies have confirmed this fact (Radke & Hobbs, 1991; Lu et al., 2003; Twohy et al., 2009).When detrained cloud droplets near the cloud edge evaporate on getting mixed with the surrounding dry air, the humidity of the air adjacent to the cloud boundary increases. According to the work of Laird (2005), these regions of enhanced humidity can sometimes extend to distances as far as four times the radius of the cloud. Twohy et. al. (2009), observed that in the vicinity of marine clouds (INDOEX) the relative humidity increased by 4 to 6% when comparing 1Km to 100m distance from the cloud boundary. They hypothesized that the hygroscopic growth of aerosols in the nearest 100 m of marine clouds was responsible for increased concentration of particles with diameters in the range 0.3 to 20μm and decrease in concentration of particles with diameters in the range 0.1 to 3.0μm in that region. This hypothesis is in alliance with the findings of Koren et. al. (2007). Using AERONET aerosol optical depth estimates as clouds advected over 15 stations worldwide, they found, after averaging 3 to 5 years worth of data that the optical depth increases by about 13 % at a wavelength of 440nm and nearly 22% at a wavelength of 870nm as the cloud edge is approached while the Angstrom exponent systematically decreases. The decrease in the Angstrom exponent suggests that larger sized aerosol particles are dominant closer to the cloud boundary as was later validated by Twohy et. al. (2009) in the case of marine cumulus clouds. Koren et. al. (2007) had also reached the same conclusion that hygroscopic growth of aerosols close to cloud boundary is responsible for the increase in aerosol optical depth as the cloud edge is approached.

Since LIDAR observations are more reliable than passive remote sensing (due to better cloud detection and essentially no cloud adjacency effect when operated at night), it is worth mentioning a few LIDAR based studies of aerosol optical properties in high relative humidity environment near the cloud edges. One of the pioneering studies in this regard was by Platt and Gambling (1972). They noticed enhancement in aerosol backscatter coefficient at a wavelength of 694nm as the visible edges of small continental cumulus clouds approached. From the vertical

profile of the backscatter coefficient it was evident that the maximum increase was near the cloud base. They hypothesized that this pronounced increase in the backscatter coefficient near cloud base was due to hygroscopic growth of aerosols in the moist air advected up from below the cloud base. More recently Su et. al. (2008) used the aircraft based HSRL data to study the aerosol backscatter coefficient as a function of distance from cloud edge at visible and near infrared wavelengths for several different clouds over a period of 3 days. Their observations reveal that at a wavelength of 532nm the backscatter coefficient and the optical depth increased by 26 to 30% and 8 to 17% respectively when approaching the cloud edge from a distance of 4.5Km to a distance of 0.1Km. Su et. al. (2008) have attributed this increase in aerosol optical depth and backscatter to aerosol swelling in regions of high relative humidity near cloud boundaries and have stated that to some extent in cloud aerosol processing might also be responsible.

However Tackett and Di Girolamo(2009) demonstrated that hygroscopic growth of aerosols alone is not enough to explain such increases in backscatter coefficient as cloud edges are approached. Instead of using aircraft based LIDAR data like Su et. al. (2008), they have used satellite based LIDAR observations to investigate the aerosol optical properties in the vicinity of boundary layer clouds over the western tropical Atlantic. They observed that the layer integrated median backscatter at wavelengths of 532nm and 1064nm increased by about 31% and 42% respectively when comparing 2.99Km to 0.33Km from the cloud boundary. Unlike Platt and Gambling (1971) who found that the maximum increase in the backscatter coefficient was adjacent to cloud base, the work of Tackett and Di Girolamo (2009) reveal that the magnitude of enhancement of the backscatter coefficient is greatest near the cloud top as well as the cloud base. The authors have reached the conclusion that multiple processes are responsible for modifying the aerosol size distribution near the cloud edges and thus hygroscopic growth of aerosols cannot be completely responsible for the enhanced backscatter in the vicinity of clouds although it might be an important contributor.

It is evident that hygroscopic growth can immensely influence aerosol optical

properties in regions of enhanced humidity like in the neighborhood of clouds and it is a very important process that must be taken into consideration when performing radiative transfer calculations in near cloud environment.

CHAPTER 3

METHODOLOGY

The goal of this research is to demonstrate that the contribution of particles of radius less than and equal to 0.7 μm to the total aerosol optical depth (defined in this study as fine mode fraction of AOD) can either increase or decrease with enhancement in relative humidity (depending on the parameters used to specify the aerosol size distribution) even when the emission scenario remain unchanged. The fraction of AOD that can be attributed to small (radius $\leq$ 0.35 μm) and medium (radius $\leq$ 0.7 μm) sized particles as defined by MISR, which is also in turn correlated to the AERONET fine mode fraction of AOD (Dey & Di Girolamo, 2010) is often thought to be representative of anthropogenic aerosol loading. Hence it is often assumed that the increase in fine mode fraction of AOD, as derived from ground and satellite based radiometer, is related to increase in pollution of anthropogenic origin while the decrease in fine mode fraction is associated with enhanced dust activity or influence of larger marine aerosols (Kaufman et al., 2005b; Kleidman et al., 2005; Dey & Di Girolamo, 2010). Although changes in emission patterns of aerosols of both natural and athropogenic origin can be responsible for changes in fine mode fraction of AOD, the purpose of this research is to imply that for certain size distributions relative humidity alone is sufficient to explain large increases or decreases in the fine mode fraction. Hence it is important to consider the role of relative humidity and the prevelant particle size distribution in a region prior to attributing increases or decreases in fine mode fraction of AOD to changing emission scenarios.

In order to demonstrate the influence of relative humidity on the contribution of fine mode particles (radius $\leq$ 0.7 μm) to AOD, it was required to generate various

different aerosol size distributions and then model the hygroscopic growth of these different aerosol populations in accordance with their chemical composition. The role of relative humidity in modifying the refractive index of the aerosol particles has also been considered in this study. Finally, using Mie theory for homogeneous spheres the fraction of AOD due to particles of radius ≤ 0.7 μm has been calculated as a function of relative humidity for a variety of different aerosol size distributions.

3.1 Analytical Size Distribution Function

There are significant concentrations of aerosol particles in the atmosphere, sometimes as high as 10^7 to 10^8 cm^{-3} whether in urban or remote regions. The dimensions of these particles can range from a few nanometers to about 100 μm, spanning over several orders of magnitude. Partciles generated from combustion such as those from autombiles, power generation and wood burning can be as small as few nanometers and as large as 1 μm. Aerosols of natural origin like wind blown dust, pollens, plant fragments and sea salt are generally larger than 1 μm. Aerosols that are produced by photochemical processes in the atmosphere are typically less than 1 μm in size. The size of these particles not only affects their lifetime in the atmosphere but also the way they interact with radiation. Hence mathematically characterizing aerosol size distributions is essential.

A measured aerosol size distribution can be reported as a table of distribution values for dozens of diameters. But for many applications carrying around hundreds and thousands of distribution values can be cumbersome. Hence in these cases it is often convenient to use a relatively simple analytical function describing the atmospheric aerosol distribution. Of the various mathematical functions that have been porposed, the lognormal distribution provides a good fit to the observed shapes of the ambient aerosol disrtibutions and is thus commonly used in atmospheric applications. An aerosol population is said to be lognormally distributed

if

$$N(lnr_p) = \frac{\mathrm{d}N}{\mathrm{d}lnr_p} = \frac{N_t}{\sqrt{2\pi} ln\sigma_g} exp(\frac{-(lnr_p - ln\bar{r}_{pg})^2}{2ln^2\sigma_g}) \tag{3.1.1}$$

where,

r_p =particle radius

$N(lnr_p)\mathrm{d}lnr_p = \mathrm{d}N$ = Number of particles per unit volume of air having radii in the range lnr_p and $(lnr_p + \mathrm{d}lnr_p)$

$N_t = \int_{-\infty}^{\infty} N(lnr_p)\mathrm{d}lnr_p$= Total aerosol number concentration per unit volume of air

$\bar{r}_{pg}$ = Median radius

σ_g = Geometric standard deviation

N($\ln r_p$) is known as the aerosol number distribution function, where the independent variable is the natural log of the particle radius. Several aerosol properties are more sensitive to surface area and volume distribution function rather than the number distribution function.

The surface area distribution function is represented as S($\ln r_p$) such that:

$S(lnr_p)\mathrm{d}lnr_p$ = Surface area of particles per unit volume of air having radii in the range $\ln r_p$ and $(lnr_p + \mathrm{d}lnr_p)$.

The volume distribution function is represented as $V(lnr_p)$ such that:

$V(lnr_P)\mathrm{d}lnr_p$ = Volume of aerosol particles per unit volume of air having radii in the range lnr_p and $(lnr_p + \mathrm{d}lnr_p)$.

Just like the number distribution function, aerosol surface area and volume distribution can also be represented by lognormal function. As as result of particle emission, in-situ formation and a variety of other subsequent processes, the atmospheric aerosol distribution is characterised by a number of modes, as depicted in figure 1.1. The volume distribution in most areas is dominated by two modes; the accumulation mode (radius $\leq 0.5\mu$m) and the coarse mode (radius $> 0.5\mu$m). The accumulation mode particles are a consequence of primary emissions, condensation of secondary sulfates, nitrates and organics from the gas phase and coagulation of smaller particles. On the other hand particles in the coarse mode

are generally produced by mechanical processes such as wind or erosion (dust, sea salt, pollens). Most of the material in the coarse mode is primary, but there are some secondary sulfates and nitrates. As a result atmospheric aerosol volume distributions are often described as the sum of two lognormal distritbutions as shown below:

$$V(lnr_p) = \frac{\mathrm{d}V}{\mathrm{d}lnr_p} = \sum_{i=1}^{2} \frac{V_{ti}}{\sqrt{2\pi} ln\sigma_i} exp(\frac{-(lnr_p - lnR_i)^2}{2ln^2\sigma_i}) \tag{3.1.2}$$

where,

V_{ti} = Modal Volume concentration (accumulation/coarse)

R_i = median radius of the accumulation/coarse mode

$\ln\sigma_i$ = variance of accumulation/coarse mode.

Table 3.1: Table listing different combinations of fractional volume concentration in the accumulation and coarse modes

No	Accumulation Mode Fraction $\frac{V_{t1}}{V_{t1}+V_{t2}}$	Coarse Mode Fraction $\frac{V_{t2}}{V_{t1}+V_{t2}}$
1	1.0	0.0
2	0.8	0.2
3	0.6	0.4
4	0.4	0.6
5	0.2	0.8
6	0.0	1.0

In order to theoretically investigate the influence of relative humidity on the fine mode fraction of AOD, bimodal lognormal volume distribution function (given by equation 3.1.2) has been used in this study to represent ambient aerosol populations. Loeb and Schuster (2008) had used bimodal lognormal volume distribution function to represent ambient aerosol population while investigating the influence of increasing RH on Angstrom Exponent of aerosol particles. Due to the similarity of their work with this study, volume distribution function has been chosen over number and surface area distribution functions in this thesis. As it was required

Table 3.2: Different combinations of the parameter values (R_1, R_2, $Ln\sigma_1$, $Ln\sigma_2$) that have been used in the lognormal volume distribution function to generate a variety of different dry aerosol size distributions

No	$\ln\sigma_1$	$\ln\sigma_2$	$R_1(\mu m)$	$R_2(\mu m)$
1	0.4	0.72	0.005	1.0
2	0.4	0.72	0.005	1.5
3	0.4	0.72	0.005	2.0
4	0.4	0.72	0.005	2.5
5	0.4	0.72	0.005	3.0
6	0.4	0.72	0.05	1.0
7	0.4	0.72	0.05	1.5
8	0.4	0.72	0.05	2.0
9	0.4	0.72	0.05	2.5
10	0.4	0.72	0.05	3.0
11	0.2	0.2	0.05	1.5
12	0.2	0.4	0.05	1.5
13	0.2	0.6	0.05	1.5
14	0.2	0.8	0.05	1.5
15	0.4	0.2	0.05	1.5
16	0.4	0.4	0.05	1.5
17	0.4	0.6	0.05	1.5
18	0.4	0.8	0.05	1.5
19	0.6	0.2	0.05	1.5
20	0.6	0.4	0.05	1.5
21	0.6	0.6	0.05	1.5
22	0.6	0.8	0.05	1.5
23	0.8	0.2	0.05	1.5
24	0.8	0.4	0.05	1.5
25	0.8	0.6	0.05	1.5
26	0.8	0.8	0.05	1.5

to consider a variety of different aerosol size distributions; the values of the parameters V_{ti}, R_i and $ln\sigma_i$ in equation 3.1.2 were varied sequentially. The Tables 3.1 and 3.2 displays the different sets of parameter values that have been used in equation 3.1.2 in order to generate an ensemble of size distributions. For each of the 26 different combinations of the parameters $\ln\sigma_1, ln\sigma_2, R_1 and R_2$ displayed in Table 3.2, the volume fraction of the accumulation mode ($\frac{V_{t1}}{V_{t1}+V_{t2}}$) has been varied from 0 to 1 in steps of 0.2 (Table 3.1) to generate a total of 156 different size distributions. Although this is a theoretical study, the values of the parameters

specifying the dry aerosol populations have been chosen to be representative of realistic scenarios.

3.2 Aerosol Particle Model and Chemical Composition

Aerosol particles in the atmosphere can either occur as an external mixture where the individual particles are made up of a single substance or as an internal mixture, where several substances in different proportions constitutes the aerosol particles. In this study the aerosol particles have been assumed to occur in internal mixture form. In accordance to the work of Nilsson (1979), the particles are considered to be partly made up of water soluble fraction (E) and partly of water insoluble fraction (1-E) in the dry state. As the value of critical relative humidity (deliquescent relative humidity at which the salt begins to dissolve in the absorbed water) is different for different electrolytes present in the water soluble component of the aerosols, the composite water soluble part dissolves gradually when the relative humidity(RH) increases. At any particular relative humidity, a fraction of E is assumed to have been dissolved (salts whose critical RH have been exceeded) and for very high relative humidity values (RH $> 95\%$) the entire water soluble fraction gets dissolved leaving behind an insoluble nucleus surrounded by a more or less diluted electrolyte. The Figure 3.1 demonstrates the aerosol particle model.

The water soluble fraction of aerosols primarily consists of ions like SO_4^{--}, NO_3^-, Cl^-, OH^-, H^+, NH_4^+, Na^+, K^+, Mg^{++} and Ca^{++} (Brosset, 1976). For the purpose of this study, the chemical composition of the water soluble fraction present in the aerosol has been adopted from Nilsson (1979). Table 3.3 lists the assumed mass fractions and the critical relative humidities of the electrolytes that supposedly constitute the water soluble fraction in the aerosol particle model.

In order to investigate the importance of aerosol chemical composition while studying the effects of relative humidity on aerosol optical properties, the amount

Table 3.3: Mass fraction and critical relative humidities of the salts constituting the soluble part of the aerosol particles

Electrolyte	RH(%)	Mass Fraction(%)
LiCl	13	2.5
$CaCl_2$	18	2.5
$MgCl_2$	33	2.5
$Zn(NO_3)_2$	45	2.5
NH_4NO_3	62	5
$NaNO_3$	74	5
NaCl	76	5
NH_4Cl	77	5
$(NH_4)_2SO_4$	80	50
KCl	85	5
Na_2SO_4	86	5
$MgSO_4$	91	5
KNO_3	92	5

Table 3.4: Parameter values specifying the chemical composition of the aerosol particles in accordance to Nilsson (1979). δ_s is the mass fraction of water soluble components, δ_i is the mass fraction of water insoluble components, δ_{soot} is the mass fraction of soot and ρ represents the densities of the respective components.

Type 1							
	E = δ_s	δ_i	δ_{soot}	ρ_s gm/cm^3	ρ_i gm/cm^3	ρ_{soot}	ρ_0 gm/cm^3
Accumulation Mode	0.8	0.2	0.0	2.0	3.67	2.0	2.2
Coarse Mode	0.4	0.6	0.0	2.0	3.38	2.0	2.65
Type 2							
	E = δ_s	δ_i	δ_{soot}	ρ_s gm/cm^3	ρ_i gm/cm^3	ρ_{soot}	ρ_0 gm/cm^3
Accumulation Mode	0.6	0.1	0.3	2.0	3.67	2.0	2.1
Coarse Mode	0.4	0.6	0.0	2.0	3.38	2.0	2.65

Figure 3.1: Aerosol particle model adopted from Nilsson (1979)

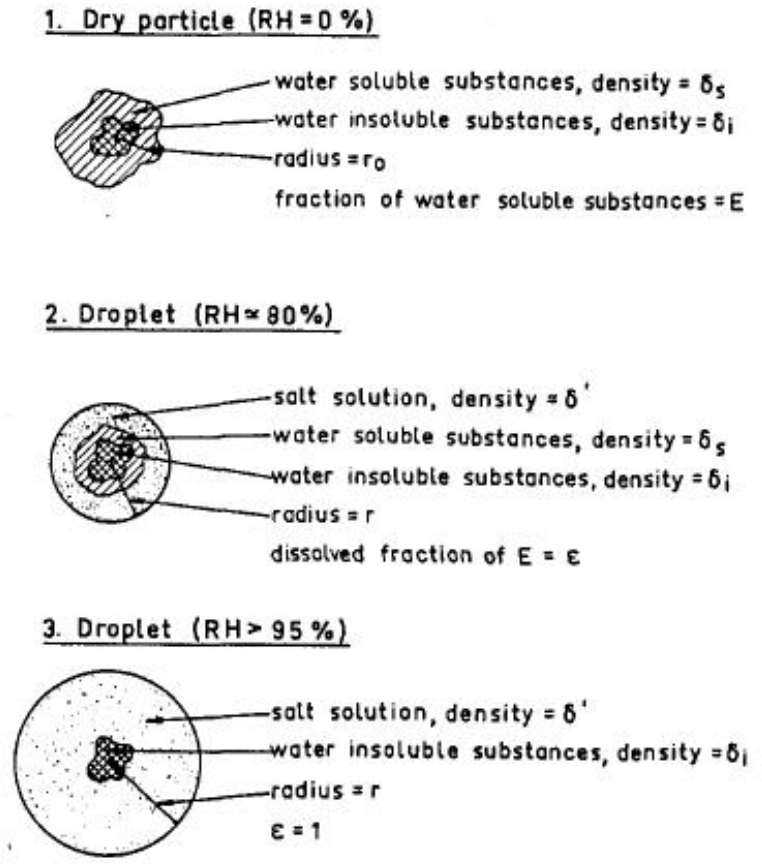

of soot present has been varied to create aerosols of two different types. The values of the parameters that have been used to specify the chemical composition of the aerosol particles (mass fraction of water soluble components, mass fraction of water insoluble components, mass fraction of soot, density of water soluble components, density of water insoluble components, density of soot, average density of the dry aerosol particles) are in accordance with (Nilsson, 1979) and have been summarized in Table 3.4. In the Table 3.4 accumulation mode refers to particles having radius $\leq 0.5\ \mu m$ and the coarse mode includes particles having radius $> 0.5 \mu m$.

3.3 Complex Index of Refraction of the Aerosol particles and its dependence on relative humidity

The complex refractive index of aerosol particles (n=n' + ik) depends on the chemical composition of the aerosol, the wavelength of radiation under consideration and also on the ambient relative humidity. In this study the complex refractive index of the dry aerosol particles (RH=0%) has been calculated using the formula:

$$n_0 = (n_1\frac{\delta_1}{\rho_1} + n_2\frac{\delta_2}{\rho_2} + ... + n_x\frac{\delta_x}{\rho_x}) * (\frac{\delta_1}{\rho_1} + \frac{\delta_2}{\rho_2} + ... + \frac{\delta_x}{\rho_x})^{-1} \tag{3.3.1}$$

where,

n_0 = Complex refractive index of dry aerosol particle

n_x = Complex refractive index of component 'x' present in the aerosol

δ_x = Mass fraction of component 'x'

ρ_x = Density of component 'x'.

Hänel (1976), one of the pioneers to study the optical properties of hygroscopic aerosols under enhanced RH conditions had calculated the real and imaginary parts of the complex refractive index of aerosols separately by mixing the refractive index values of the included components in volume proportions. Hence in this study the complex refractive index of the dry aerosol particles has been calculated in the simplest possible way by direct mixing of the complex refractive indices of the included components in accordance to their volume fractions. The complex refractive index of the aerosols under enhanced RH conditions is then calculated by mixing the refractive index of the dry particles and the refractive index of water in volume fractions as shown in equation 3.3.2.

$$n_f = n_0 \left(\frac{r}{r_0}\right)_f^{-3} + n_w \left[1 - \left(\frac{r}{r_0}\right)_f^{-3}\right] \tag{3.3.2}$$

where,

n_f = Complex refractive index of the aerosol particles at RH=f

n_0 = Complex refractive index of the dry aerosol particle

n_w = Complex refractive index of water

$\left(\frac{r}{r_0}\right)_f$ = Particle growth factor at RH = f (r_0 is the radius of the dry particle and r is the radius of the particle at RH = f)

Table 3.5: Complex refractive indices (n=n' + ik)

Wavelength	Water Soluble Fraction		Water Insoluble Fraction		Soot		Water	
	n'	k	n'	k	n'	k	n'	k
0.55	1.53	0.005	1.53	0.008	1.57	0.5	1.333	0.0

Both the formulae have been adopted from Nilsson (1979) and incorporates the dependence of complex index of refraction of the aerosol particles on detailed chemical composition as well as relative humidity. However, the use of the formulae require the knowledge of refractive index of the individual components present in the aerosol as well as the refractive index of water at the desired wavelength. As discussed in Section (1.2) the aerosols in this study have been considered to be composed of various proportions of water soluble components, water insoluble components and soot. Since the wavelength of interest in this study is 550 nm; the complex refractive indices of the soluble components, insoluble components, soot and water at 550 nm have been specified in Table 3.5 as listed by Nilsson (1979).

MISR retrieves small, medium and large particle fraction of AOD at four spectral bands. The center wavelengths of these bands are 446 nm, 558 nm, 672 nm and 867 nm. MODIS also retrieves fine mode fraction of AOD but only at 550 nm wavelength. Therefore, as the mid visible spectral band is common to both MISR and MODIS, 550 nm has been selected as the wavelength of interest in this study.

3.4 Aerosol Particle Growth Factor as a Function of Relative Humidity

The growth factor ($\frac{r}{r_0}$) of an aerosol particle, which is a function of relative humidity, is defined as the ratio of radius of the particle at any particular RH to the dry radius. It is a parameter of great importance as it represents the change in the dimension of an aerosol particle with changes in relative humidity. In this study, the growth factor is the parameter which modifies both the size disitribution and refractive index and thus accounts for the influence of humidity on the optical properties of the aerosols.

According to fundamental work of Köhler (1936)), it is known that the size of a droplet of water and salt solution is determined by the equilibrium between condensation and evaporation at the surface of the droplet. The equilibrium saturation ratio (S), which is the ratio of saturation vapor pressure over the surface of the solution droplet to the saturation vapor pressure over a plane surface of pure water can be expressed as

$$S = \frac{e'(r)}{e(\infty)} = exp(\frac{2\sigma' M'}{r\rho' RT}) * (1 + i\frac{M_w m_s}{M_s m_w})^{-1} \tag{3.4.1}$$

where,

$e'(r)$ = Saturation vapor pressure over solution droplet

$e(\infty)$ = Saturation vapor pressure over plane surface of pure water

σ' = Surface tension of solution

M' = Molecular weight of solution

r = Radius of the droplet

ρ' = Density of the solution

R = Universal gas constant

T = Temperature of droplet

i = Van't Hoff factor, which is determined empirically and indicates the degree of dissociation of the salt solution

M_w = Molecular weight of water

M_s = Molecular weight of salt

m_s = Mass of salt in the solution

m_w = Mass of water

When the solution droplet is in thermodynamic equilibrium with the surrounding air in that case

$$S = \frac{RH(\%)}{100} \tag{3.4.2}$$

In order to calculate the growth factor of an aerosol particle of given chemical composition and dry radius corresponding to various relative humidity values, it is essential to express the parameters σ', M′, ρ' and $\frac{m_s}{m_w}$ of equation 3.4.1 in terms of parameters of the aerosol particle model that has been adopted in this study as shown in Figure 3.1.

3.4.1 Parameters in the Equilibrium equation 3.4.1 expressed as paramters of the aerosol particle model

- Mass of the dry particle:

$$m_0 = \frac{4}{3}\pi r_0^3 \rho_0 \tag{3.4.3}$$

where, r_0 = Radius of the dry particle

ρ_0 = Average density of the dry particle

$$\rho_0 = \left(\frac{\delta_s}{\rho_s} + \frac{\delta_i}{\rho_i} + \frac{\delta_{soot}}{\rho_{soot}}\right)^{-1}$$

δ_s = E = Mass fraction of water soluble component

δ_i = Mass fraction of water insoluble component

δ_{soot} = Mass fraction of soot

ρ_s = Density of water soluble fraction

ρ_i = Density of water insoluble fraction

ρ_{soot} = Density of soot.

- Mass of the water soluble fraction:

$$m_{ds} = Em_0 = \frac{4}{3}\pi E r_0^3 \rho_0 \tag{3.4.4}$$

- Mass of the dissolved matter:

$$m_s = \epsilon m_{ds} = \frac{4}{3}\pi \epsilon E r_o^3 \rho_0 \tag{3.4.5}$$

where, ϵ = Fraction of E that gets dissolved to form a solution.

- Mass of water:

$$m_w = \frac{4}{3}\pi (r^3 - r_0^3)\rho_w \tag{3.4.6}$$

where, r = Radius of the droplet

ρ_w = Density of water

-

$$\frac{m_s}{m_w} = \frac{\epsilon E r_0^3 \rho_0}{(r^3 - r_0^3)\rho_w} \tag{3.4.7}$$

- Density of salt solution

$$\rho' = \frac{m_s + m_w}{\frac{m_s}{\rho_s} + \frac{m_w}{\rho_w}} = \frac{[r^3\rho_w + (\epsilon E\rho_0 - \rho_w)r_0^3]\rho_s}{r^3\rho_s + (\epsilon E\rho_0 - \rho_s)r_0^3} \tag{3.4.8}$$

- Molecular weight of salt solution:

$$M' = \frac{m_s + m_w}{\frac{m_s}{M_s} + \frac{m_w}{M_w}} = \frac{M_s M_w [r^3\rho_w + (\epsilon E\rho_0 - \rho_w)r_0^3]}{M_s r^3 \rho_w + (M_w \epsilon E\rho_0 - M_s\rho_w)r_0^3} \tag{3.4.9}$$

- Surface tension of the droplet:

$$\sigma' = \sigma_w(T) + b\left(\frac{m_s}{m_w}\right) \tag{3.4.10}$$

where,

$\sigma_w(T)$ = Surface tension of water at temperature T(K)

b = Constant, depending on the salt solution. E.g. b=27.6 for NaCl and 16.4 for $(NH_4)_2SO_4$ (Hänel, 1976)

Substituting the expressions for σ', M′, ρ' and $\frac{m_s}{m_w}$ in equation 3.4.1, we finally get

$$
\begin{aligned}
S &= \frac{RH(\%)}{100} \\
&= exp\left(\frac{2\left[\sigma_w(T) + b\frac{\epsilon E\rho_0}{\left(\frac{r^3}{{r_0}^3}-1\right)\rho_w}\right]\left[\frac{M_sM_w\left[\left(\frac{r^3}{{r_0}^3}-1\right)\rho_w+\epsilon E\rho_0\right]}{M_s\rho_w\left(\frac{r^3}{{r_0}^3}-1\right)+M_w\epsilon\rho_0}\right]}{r_0\left(\frac{r}{r_0}\right)\frac{\left[\left(\frac{r^3}{{r_0}^3}-1\right)\rho_w+\epsilon E\rho_0\right]\rho_sRT}{\left(\frac{r^3}{{r_0}^3}-1\right)\rho_s+\epsilon E\rho_0}} \right) \\
&\times \left(1 + i\frac{M_w}{M_s}\frac{\epsilon E\rho_0}{\left(\frac{r^3}{{r_0}^3}-1\right)\rho_w}\right)^{-1} \qquad (3.4.11)
\end{aligned}
$$

To be able to calculate the growth factor (r/r_0) from equation 3.4.11, numerical values of the parameters E, ϵ, ρ_0, ρ_s, b, M_s, i, σ_w, M_w, R and T are needed. The temperature of the droplet has been kept fixed at 288°K. The surface tension of water (σ_w(T)) at 288° K is 73 dyne cm^{-1}. Molecular weight of water (M_w) is 18 gm $mole^{-1}$ and the universal gas constant (R) is 8.314 x10^7 erg $K^{-1}mole^{-1}$. The value of the parameters E, ρ_s, ρ_0, M_s and b are dependent on the dry size of the aerosol particles as well as on the composition. Table 3.6 summarizes the values of these parameters that have been used in this study in accordance to the chemical composition and mode as specified in Nilsson (1979). In Table 3.6, δ_s is the mass fraction of the soluble components, δ_i is the mass fraction of the insoluble components and δ_{soot} is the mass fraction of soot, while ρ_s is the density of the soluble components, ρ_0 is the average density of the aerosol particle, M_s is the molecular weight of the soluble components and b is a constant for the salt

Table 3.6: Mass fractions and parameter values corresponding to Type 1 and Type 2 aerosol compositions for calculating the growth factor

		Mass Fraction			Parameter Values				
Aerosol Type	Mode	δ_s(=E)	δ_i	δ_{soot}	E	ρ_s (gm/ cm^3)	ρ_0 (gm/ cm^3)	M_s	b
Type 1	Accumulation	0.8	0.2	0.0	0.8	2.0	2.2	100	20
	Coarse	0.4	0.6	0.0	0.4	2.0	2.65	100	20
Type 2	Accumuation	0.6	0.1	0.3	0.6	2.0	2.1	100	20
	Coarse	0.4	0.6	0.0	0.4	2.0	2.65	100	20

solution.

The Van't Hoff dissociation factor (i) and the dissolved fraction of E(ϵ) is dependent on the relative humidity and the Table 3.7 lists the values of these two parameters as a function of relative humidity in accordance to Nilsson (1979).

Due to the transcendental nature of equation 3.4.11, the formula cannot be restructured to calculate $\left(\frac{r}{r_0}\right)$ directly. Hence the growth factor $\left(\frac{r}{r_0}\right)$ from equation 3.4.11 for a particular RH and dry particle radius r_0 has been solved iteratively by successive adaptation of guess growth factor values. The Figures 3.2 and 3.3 show the calculated growth factor as a function of RH for Type 1 and Type 2 aerosols corresponding to dry radius of 0.05 μm.

3.5 Calculation of fine mode fraction of aerosol optical depth

Aerosol optical depth (AOD) is a measure of the degree to which aerosols prevent the transmission of light. It is also sometimes referred to as aerosol optical thickness (τ), and is defined as the integrated volume extinction coefficient over a vertical column of unit cross-section. The volume extinction coefficient (β_e) is the fractional depletion of radiance per unit path length.

$$AOD = \tau = \int_{z_1}^{z_2} \beta_e \mathrm{d}z \tag{3.5.1}$$

Figure 3.2: The growth factor $\left(\frac{r}{r_0}\right)$ as a function of RH for Type 1 aerosols corresponding to dry radius of 0.05 μm.

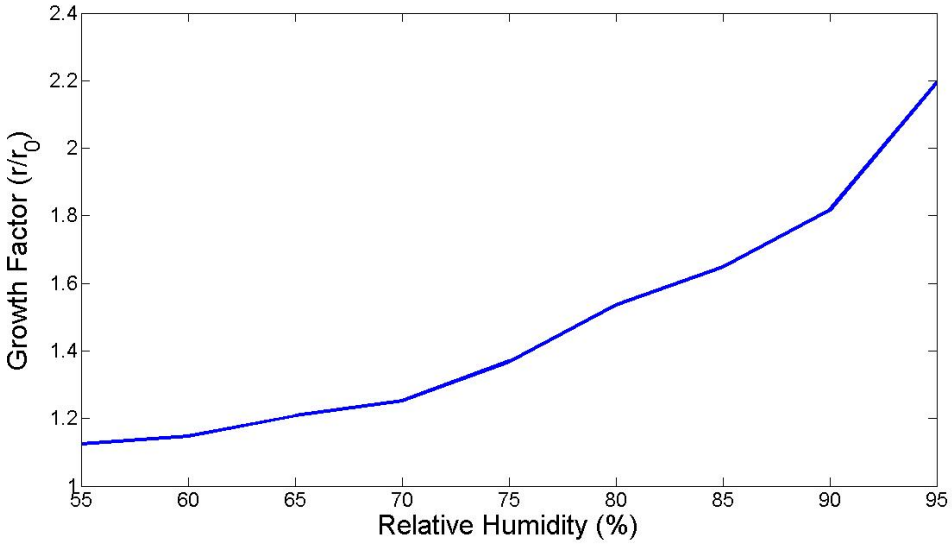

Figure 3.3: The growth factor $\left(\frac{r}{r_0}\right)$ as a function of RH for Type 2 aerosols corresponding to dry radius of 0.05 μm.

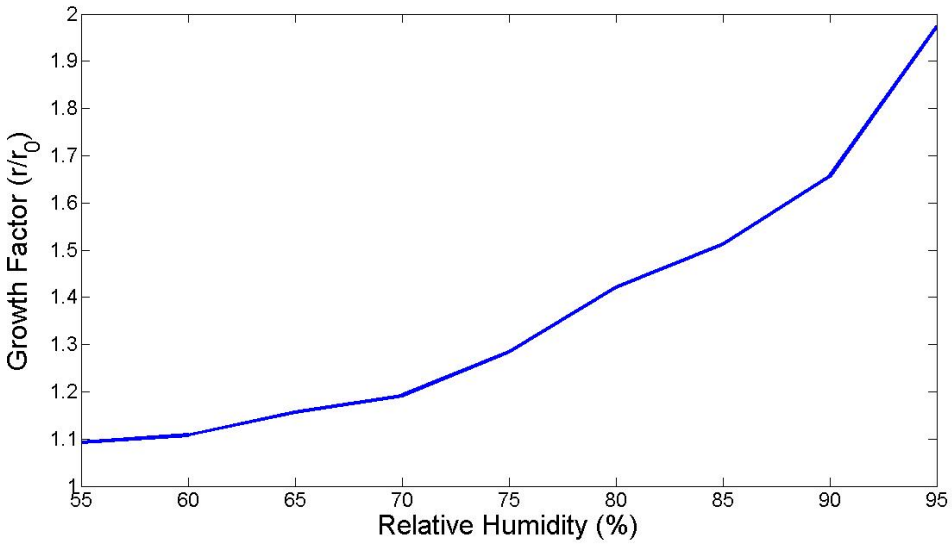

Table 3.7: Van't Hoff factor i and the dissolved fraction ϵ of the water soluble components at different relative humidities. The value of i and ϵ corresponding to RH of 76% was not listed in the source (Nilsson, 1979)

RH(%)	i	ϵ
20	16.85	0.02
30	14.45	0.05
40	12.00	0.07
50	9.55	0.10
60	7.10	0.16
70	4.7	0.3
75	3.6	0.5
76	-	-
80	2.85	0.8
85	2.40	0.90
90	2.10	0.96
95	1.94	1.0
96	1.93	1.0
97	1.97	1.0
98	1.96	1.0
99	2.03	1.0
99.5	2.10	1.0
99.8	2.40	1.0
100	2.63	1.0

and

$$\beta_e = \int_0^\infty Q_{ext}(r)\pi r^2 N(r)\mathrm{d}r \tag{3.5.2}$$

where,

Q_{ext} is the extinction efficiency,

πr^2 is the geometric cross-section of the aerosols (assuming spherical particles)

N(r) is the particle number size distribution function.

So, the final expression for aerosol optical thickness turns out to be

$$\tau = \int_{z_1}^{z_2}\int_0^\infty Q_{ext}(r)\pi r^2 N(r)\mathrm{d}r\mathrm{d}z \tag{3.5.3}$$

In this study, the fine mode fraction of AOD has been defined as the fraction of AOD that can be attributed to particles of radius ≤ 0.7 μm. In other words,

it is the ratio of the AOD due to particles of radius ≤ 0.7 μm to the total AOD.

$$Fine\ Mode\ Fraction\ of\ AOD = \frac{\tau_{fine}}{\tau_{total}} = \frac{\int_{z_1}^{z_2}\int_0^{0.7\mu m} Q_{ext}(r)\pi r^2 N(r)\mathrm{d}r\mathrm{d}z}{\int_{z_1}^{z_2}\int_0^{\infty} Q_{ext}(r)\pi r^2 N(r)\mathrm{d}r\mathrm{d}z} \tag{3.5.4}$$

For the purpose of calculating the AOD and the fine mode fraction of AOD numerically at various relative humidity levels (55,60,65,70,75,80,85,90,95), it was necessary to discretize the expression for τ:

$$\tau = [\Sigma_{i=1}^{n}(Q_{ext})_i \pi r_i^2 conc_i]\mathrm{d}z \tag{3.5.5}$$

It has been assumed that the aerosol particles span in radius from 0.0005 μm to 10 μm and this range has been divided into 10,000 equally spaced intervals (n). The mid-point of each interval (r_i) represents the radius of the particles lying in that interval. The number of aerosol particles corresponding to each interval ($conc_i$) depends on the size distribution function that has been used to represent the aerosol population. The extinction efficiency for the particles in each interval ($(Q_{ext})_i$) has been calculated using Mie theory (Wiscombe, 1980) based on BHMIE.M MATLAB code originally developed by (Bohren & Huffman, 1983). Finally, the aerosols have been considered to be distributed uniformly throughout the vertical layer under consideration and thus the extinction coefficient has been multiplied with a vertical column height of 1 Km to yield the resulting total aerosol optical thickness. The fine mode fraction of AOD corresponding to any particular relative humidity level and size distribution is then calculated by considering the fractional contribution of all particles in the size bins whose right edge is less than 0.7 μm (at the relative humidity level under consideration) to the toal AOD. Fine mode fraction of AOD as defined in this thesis is also equivalent to fine mode fraction of the volume extinction coefficient. This is because since the aerosols have been assumed to be distributed uniformly throughout the vertical layer of 1 Km, the AOD is just the product of the extinction coefficient and the vertical column height. Hence the fine mode fraction of AOD $\equiv \frac{\beta_{efine}}{\beta_{etotal}}$

CHAPTER 4

RESULTS AND DISCUSSION

This Chapter quantifies the increases and decreases in the fine mode fraction of aerosol optical depth (AOD) with positive changes in relative humidity for the various aerosol size distributions and chemical compositions that have been described in Chapter 3. It has been observed in this study that depending upon the size distribution and the chemical composition of the aerosols under consideration, fine mode fraction of AOD can either increase continuously, decrease continuously, remain constant or even exhibit mixed behavior as the relative humidity is gradually increased (in equal steps of 5%)from 55% to 95%. Mixed behavior implies that instead of continuously increasing or decreasing with rise in the value of relative humidity, the fine mode fraction of aerosol optical depth for certain size distributions first tend to increase, then decrease and then again increase as the value of relative humidity keeps on increasing.

4.1 Trends in the variation of fine mode fraction of AOD with positive changes in relative humidity

The fine mode fraction of AOD has been defined in this study as the fraction of total AOD that is contributed by aerosol particles having radius less than and equal to 0.7μm. When plotting fine mode fraction of AOD as a function of RH for the 156 different size distributions of the two composition types, it was observed that fine mode fraction can either increase continuously, decrease continuously, remain constant or even exhibit mixed behavior (decrease and then increase) as the RH was gradually increased from 55% to 95% depending on the dry size

distribution and the chemical composition of the aerosol particles.

Figure 4.1, 4.2, 4.3 and 4.4 demonstrates the above mentioned four different trends (continuous increase, continuous decrease, constant throughout and mixed) in the behavior of fine mode fraction of AOD with increase in relative humidity. These four different trends shown, correspond to four different dry aerosol size distributions (composition type 1: no soot case) characterized by the parameters R_1 , R_2 , $\mathrm{Ln}\sigma_1$, $\mathrm{Ln}\sigma_2$ and $V_{t1}/(V_{t1} + V_{t2})$ which stand for median radius of the accumulation mode, median radius of the coarse mode, width of the accumulation mode, width of the coarse mode and the volume fraction of the accumulation mode respectively. The values of these 5 parameters specifying the dry size distribution are labelled within Figure 4.1, 4.2, 4.3 and 4.4 for each of these four different trends. In these figures it can be noticed that the change in fine mode fraction can be substantial with increase in RH (55% to 95%), e.g. for the continuous increase scenario, the fine mode fraction increases from 22% to 52%, while for the continuous decrease scenario the fine mode fraction decreases from 66% to 51%.

To understand why these four different trends exist, we need to closely examine how the aerosol size distribution and the cumulative AOD for these four different scenarios change with increase in RH. Figure 4.5, 4.6, 4.7 and 4.8 show how the size distribution gets modified for four of the above mentioned dry aerosol populations and Figure 4.9, 4.10, 4.11 and 4.12 show how the cumulative aerosol optical depth gets modified as the relative humidity is increased from dry state to 55% to 75% to 95%. The discontinuity that can be observed in the cumulative aerosol optical depth curves (Figures 4.9 - 4.12) arises from the difference in compostion of the accumulation and the coarse mode of the Type 1 aerosol particles. From these curves we can see how the contribution of the fine mode particles to the total AOD changes with increase in RH for the dry size distributions corresponding to the four different trends.

With increase in relative humidity, the aerosol particles undergo hygroscopic growth. If the total number of aerosol particles remain constant (i.e. no new aerosol particles are emitted), then with positive changes in relative humidity

Figure 4.1: An example of continuous increase in the fine mode fraction of AOD with increase in RH

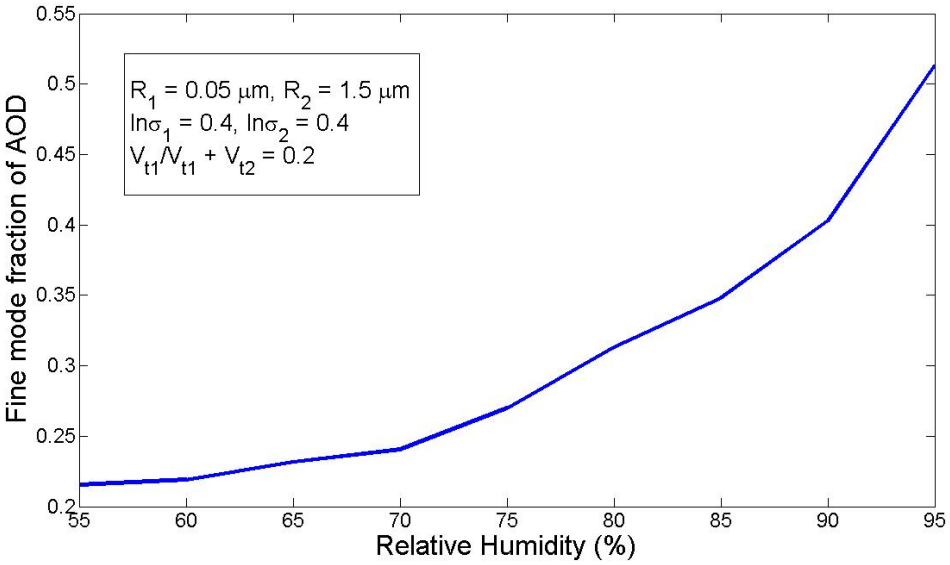

Figure 4.2: An example of continuous decrease in the fine mode fraction of AOD with increase in RH

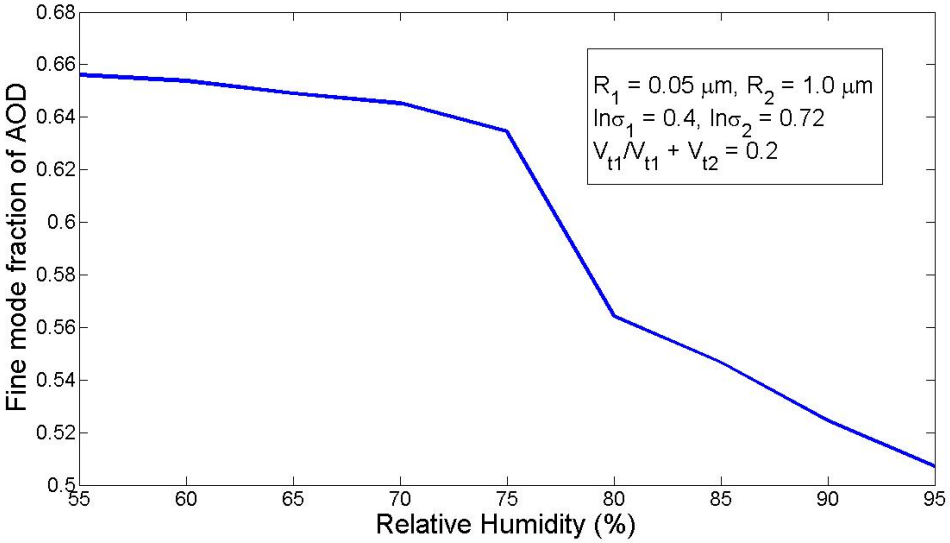

Figure 4.3: An example of Fine mode fraction of AOD remains constant with increase in RH

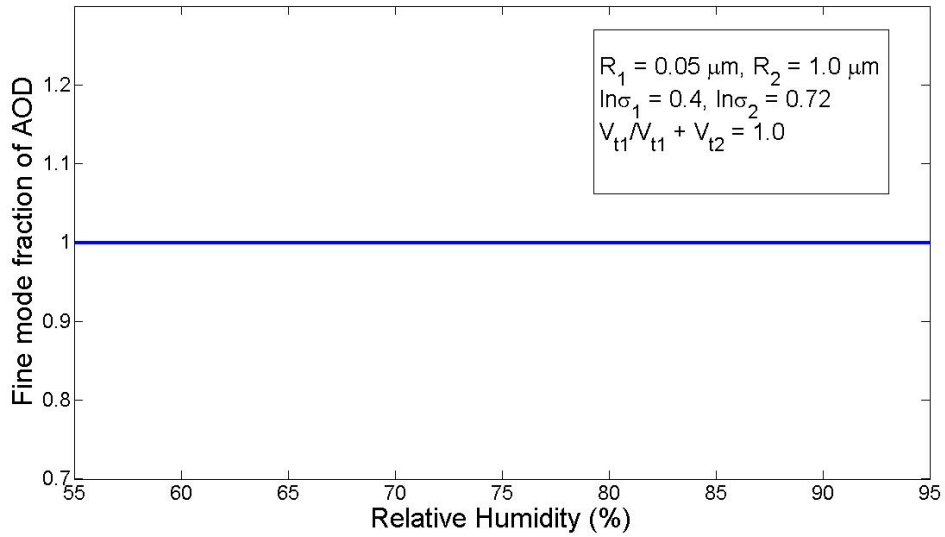

Figure 4.4: An example of Fine mode fraction of AOD exhibits mixed behavior with increase in RH

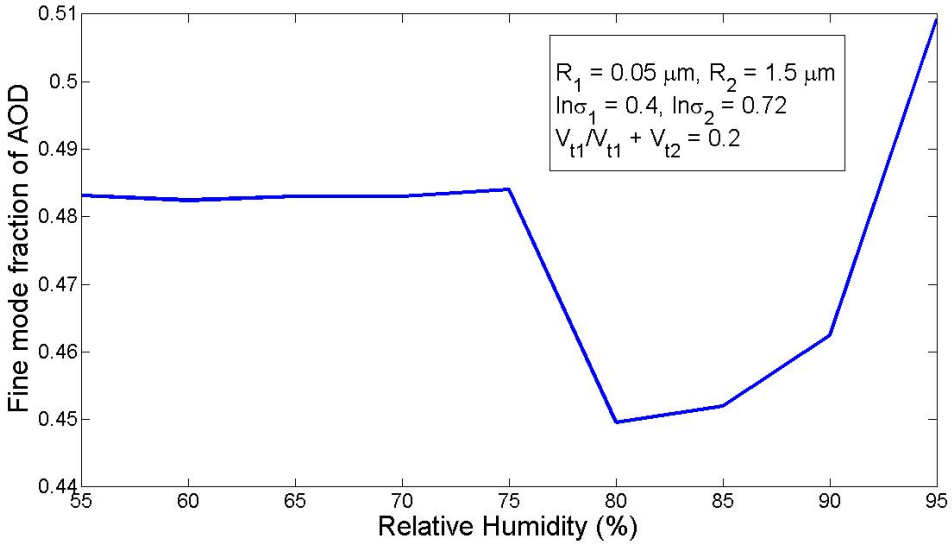

Figure 4.5: Changes in Aerosol Size Distribution with increase in RH for Type 1 aerosols: Dry size distribution corresponding to the continuous increase in fine mode fraction scenario

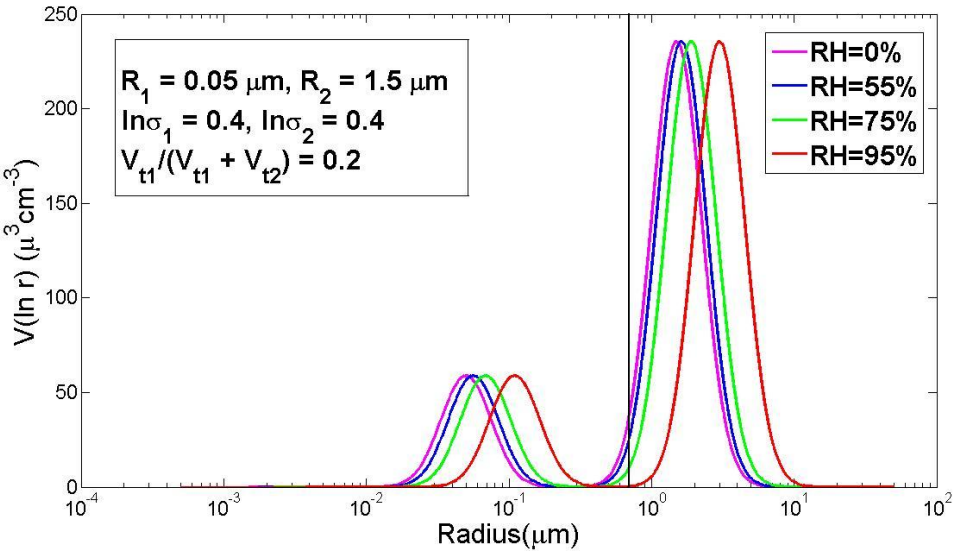

Figure 4.6: Changes in Aerosol Size Distribution with increase in RH for Type 1 aerosols: Dry size distribution corresponding to the continuous decrease in fine mode fraction scenario

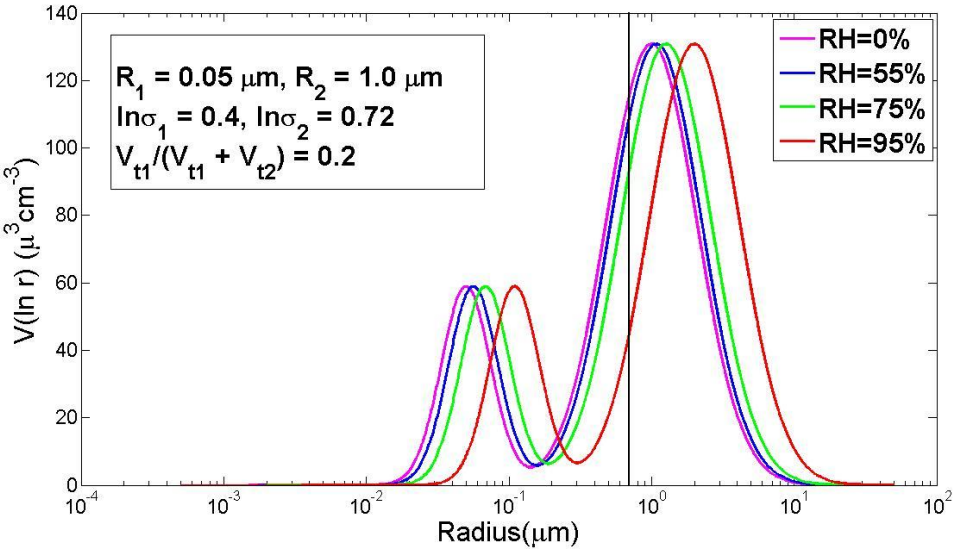

Figure 4.7: Changes in Aerosol Size Distribution with increase in RH for Type 1 aerosols: Dry size distribution corresponding to the constant fine mode fraction scenario

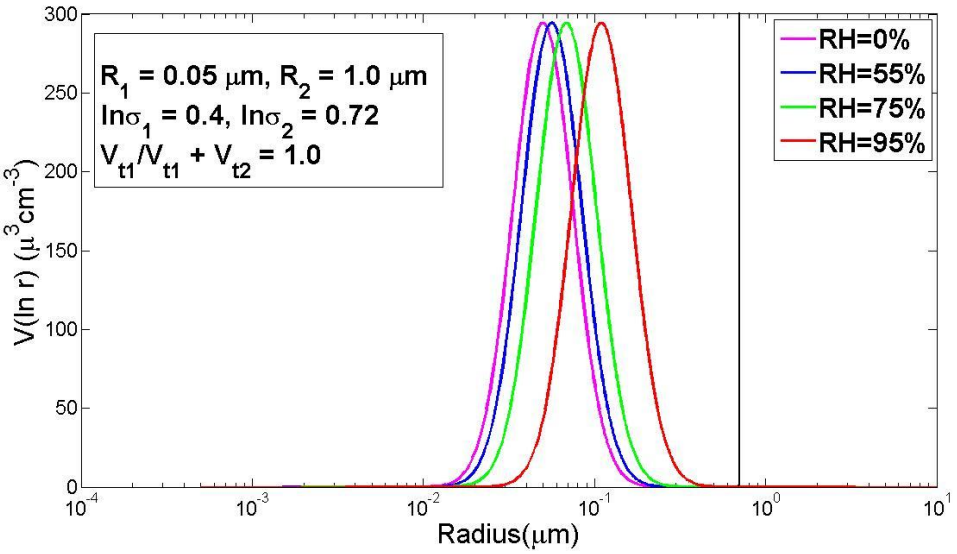

Figure 4.8: Changes in Aerosol Size Distribution with increase in RH for Type 1 aerosols: Dry size distribution corresponding to the mixed behavior in fine mode fraction scenario

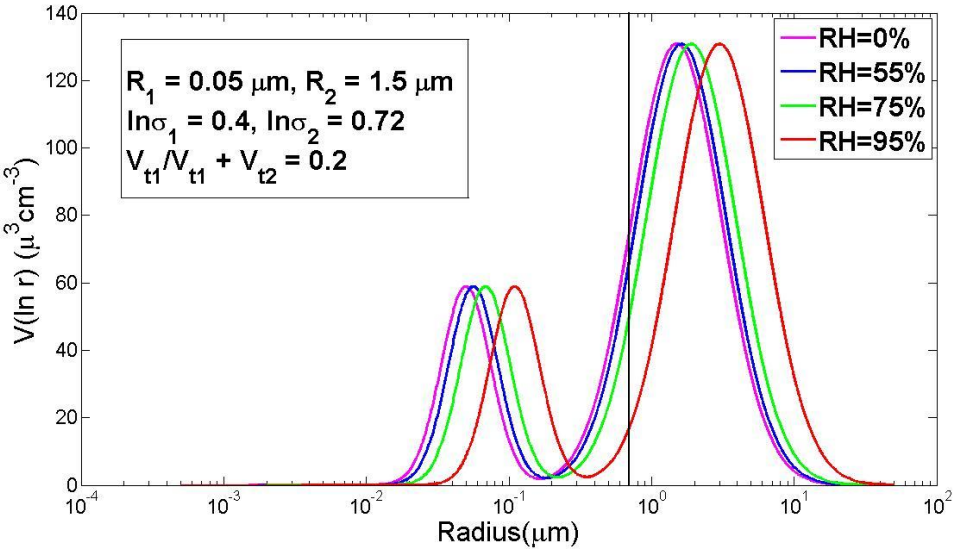

Figure 4.9: Normalized Cumulative Aerosol Optical Depth for RH = 55%, 75%, 95% (Composition: Type 1 aerosols). Dry size distribution corresponding to continuous increase in fine mode fraction scenario.

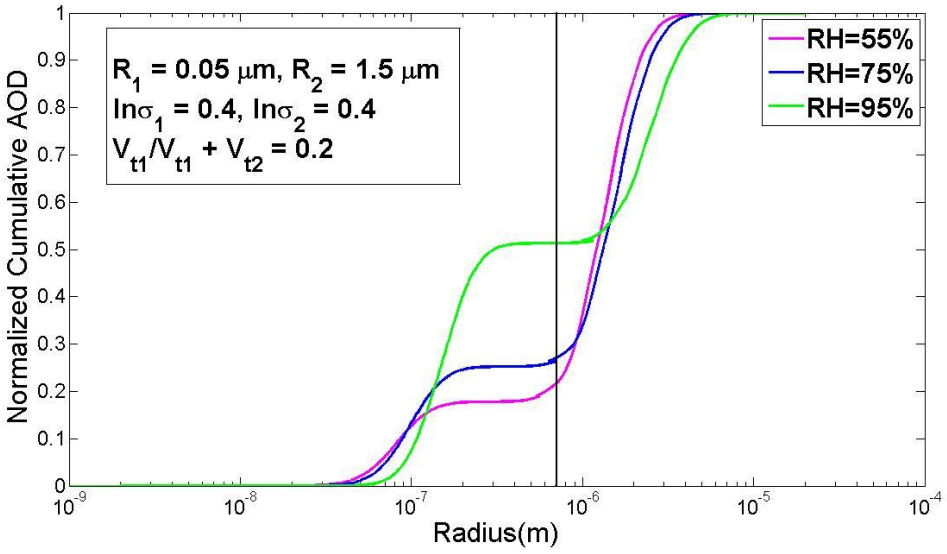

Figure 4.10: Normalized Cumulative Aerosol Optical Depth for RH = 55%, 75%, 95% (Composition: Type 1 aerosols). Dry size distribution corresponding to continuous decrease in fine mode fraction scenario.

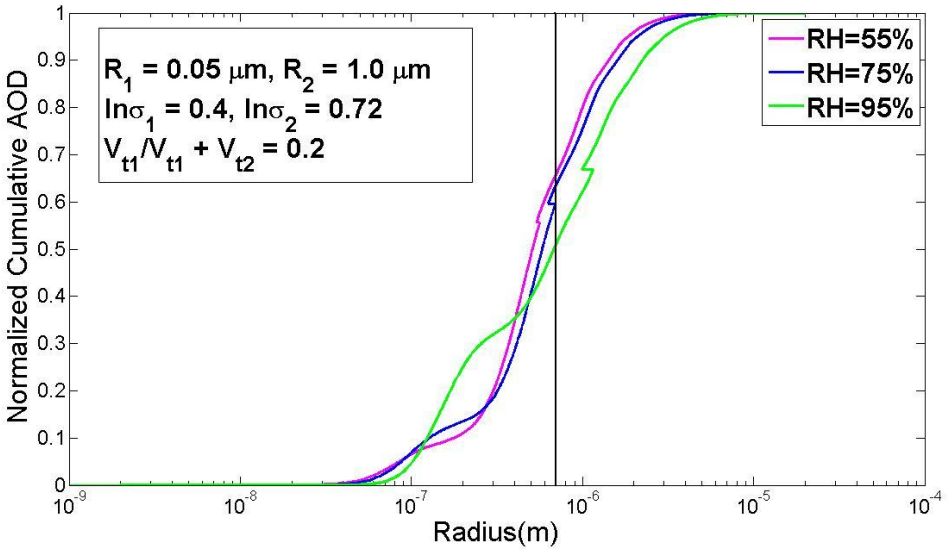

Figure 4.11: Normalized Cumulative Aerosol Optical Depth for RH = 55%, 75%, 95% (Composition: Type 1 aerosols). Dry size distribution corresponding to constant fine mode fraction scenario.

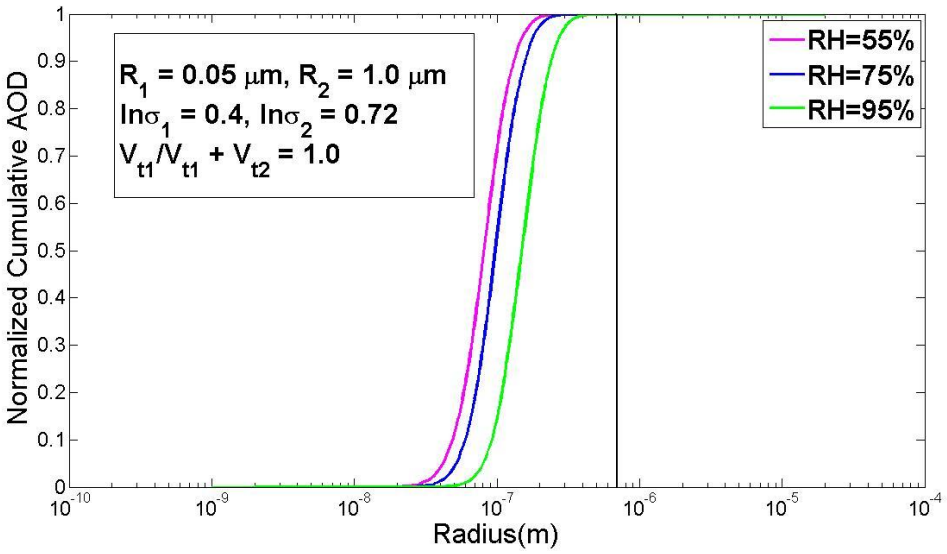

Figure 4.12: Normalized Cumulative Aerosol Optical Depth for RH = 55%, 75%, 95% (Composition: Type 1 aerosols). Dry size distribution corresponding to mixed behavior in fine mode fraction scenario.

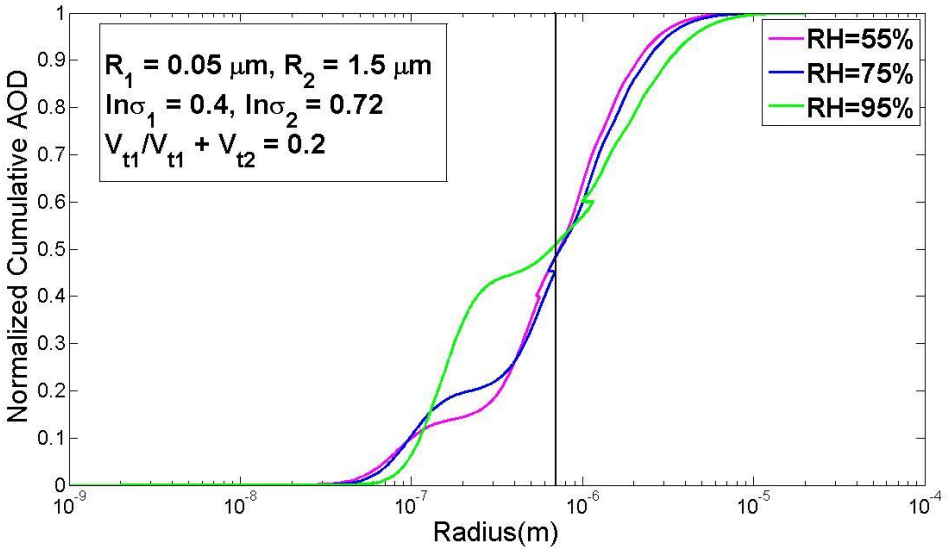

the number of aerosol particles having radius $\leq 0.7\mu$m should decrease as a consequence of particles growing out of the 0.7μm boundary. Thus instinctively it appears that fine mode fraction of AOD should decrease with increase in relative humidity. But that is not always the case. With increase in relative humidity the size distribution of the aerosol particles get modified and the number of aerosol particles within each size interval changes. As can be noticed from the plot of extinction coefficient as a function of particle radius for Type 1 aerosols, Figure 4.13, the already large aerosol particles might swell to larger sizes, but that would not increase their extinction efficiency much. This is because for larger sized aerosol particles, the extinction efficiency tend to stagnate at a value ≈ 2. But for the very small sized aerosol particles the story is different. For these particles, even slight increase in the radius can increase their extinction efficiency to a great extent thus significantly increasing their contribution to the total AOD.

As a consequence the aerosol particles that had radius$\ll 0.7\mu$m in the dry state and contributed negligibly to the extinction due to their small size, might grow to sizes where they start contributing significantly to the total AOD while still remaining below the 0.7μm cut off. Apparently this should increase the contribution of particles having radius $\leq 0.7\mu$m to the total AOD (fine mode fraction).But it is to be kept in mind that as a result of hygroscopic growth some of the aerosol particles grow out of the 0.7μm boundary and thus tend to decrease the fine mode fraction of AOD. Also, the first hump in the extinction efficiency curve (Figure 4.13) when plotted as a function of dry particle radius implies that for a very small range of radius just below 0.7 μm, slight increase in radius due to hygroscopic growth can result in decrease in extinction efficiency of the aerosol particles lying in that range. This might as well lead to decrease in fine mode fraction of AOD due to particles growing into this narrow radius range with increasing RH while still remaining below the 0.7 μm cut-off. However from Figure 4.14 it seems that the contribution of this hump in reducing the fine mode fraction of AOD with hygroscopic growth is negligible. Another factor that might be responsible for change in fine mode fraction with increase in RH is the change in refractive

Figure 4.13: Extinction efficiency ($\lambda = 550$ nm) as a function of particle radius for Type 1 aerosols and water, using Mie theory for spherical particles

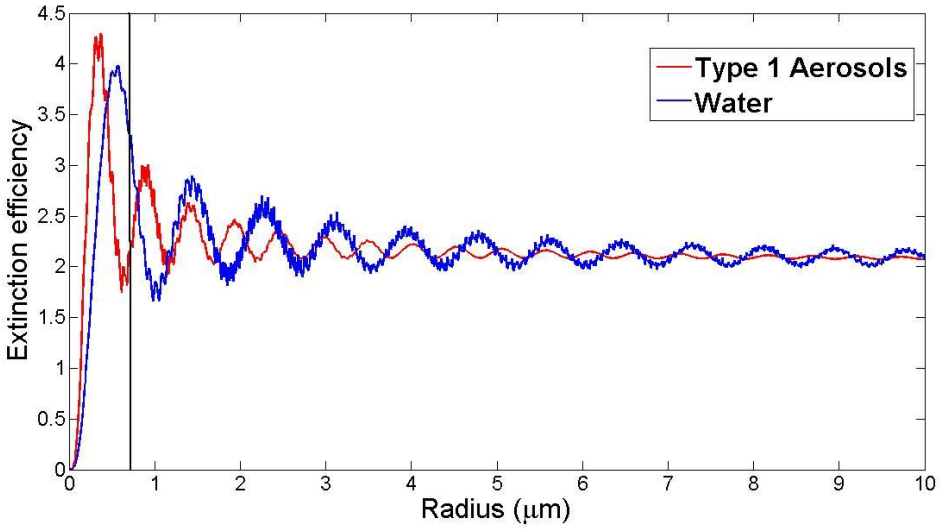

Figure 4.14: Product of extinction efficiency ($\lambda = 550$ nm) and square of particle radius as a function of particle radius for Type 1 aerosols and water

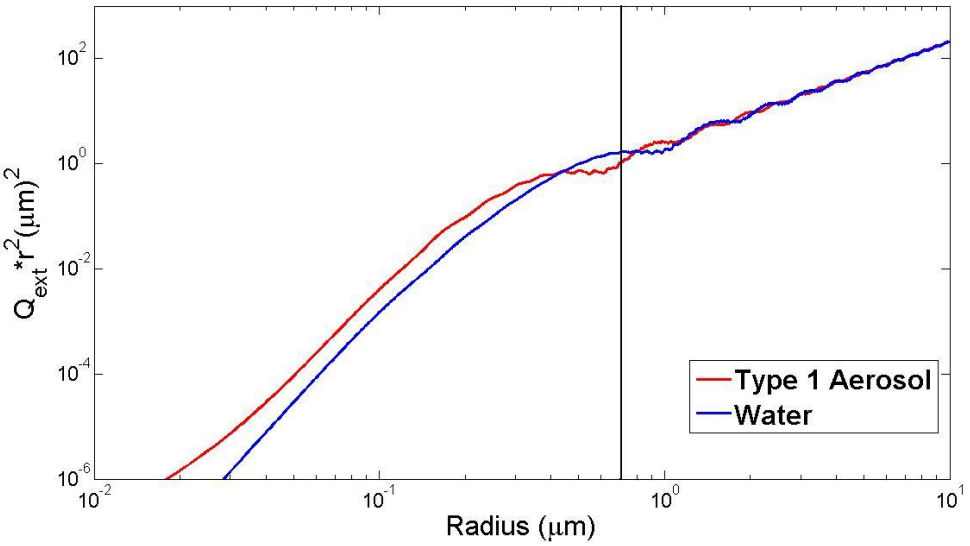

index of the aerosol particles as they get humidified. This results in change in the extinction efficiency of a hygroscopically grown aerosol particle in comparison to a dry aerosol particle of the same size (Figure 4.13 and Figure 4.14). As a single particle grows with increasing RH, it's index of refraction decreases. This in effect would slow down its contribution to AOD with increasing RH relative to a particle whose index of refraction remains constant. Hence there are several factors that might be responsible for increase or decrease in fine mode fraction with increase in RH. The two most important factors are the dry size distribution of the aerosol particles and how the size distribution gets modified with increase in relative humidity (which in turn depends on the chemical compostion of the aerosols).

From Figure 4.1 it can be noticed that for that particular dry size distribution, the fine mode fraction increases from a value of 0.2 to a value of 0.5 as the RH increases from 55% to 95% and the increase in the fine mode fraction takes place in a continuous fashion with the rise in relative humidity. In other words, at a relative humidity of 55%, 20% of the total aerosol optical depth is contributed by particles having radius less than and equal to 0.7μm. But as the RH increases, the value of fine mode fraction of AOD continues to increase until at RH equal to 95% when all most 50% of the total aerosol optical depth can be attributed to particles having radius $\leq$ 0.7μm. This continuous increase in the fine mode fraction of AOD with increase in the value of relative humidity takes place because for this particular dry size distribution and composition, each time the RH increases by 5%, the contribution of the particles that move out of the 0.7μm boundary to the total AOD is less than the increase in contribution of the smaller particles that remain within the 0.7μm range (Figure 4.5). However, as can be seen from Figure 4.2, for the same aerosol composition, if the dry size distribution of the aerosol particles is such that the contribution of the particles that grow out of the 0.7μm boundary to the total aerosol optical depth dominates each time the relative humidity increases by 5% (Figure 4.6)then in that case the fine mode fraction of AOD decreases in a continuous manner as the relative humidity increases from

55% to 95%. For certain dry size distributions, the fine mode fraction of AOD might also remain constant with increase in relative humidity as demonstrated in Figure 4.3. Figure 4.3 corresponds to a dry size distribution in which all the particles lie in the accumulation mode $[V_{t1}/(V_{t1} + V_{t2}) = 1.0]$ and there are no particles in the coarse mode. Hence irrespective of the value of relative humidity the fine mode fraction of AOD is always equal to unity because in the dry state nearly all of the particles lie within the 0.7μm cut off and as the relative humidity increases, the contribution of the particles that grow out of the 0.7μm boundary to the total aerosol optical depth is negligible (Figure 4.7). Interestingly the fine mode fraction of AOD might also exhibit mixed behavior with increase in relative humidity as demonstrated in Figure 4.4. Mixed behavior implies that for some dry aerosol size distributions, instead of increasing or decreasing in a continuous manner with positive changes in relative humidity, the fine mode fraction of AOD might decrease initially and then continue to increase with further increase in relative humidity or vice versa. The reason for this mixed trend in fine mode fraction of AOD is quite simple. Each time the relative humidity increases by 5%, there is a competition between two terms. One of them tends to decrease the fine mode fraction of AOD due to some particles moving out of the 0.7μm cut off radius and the other tend to increase the fine mode fraction due to increase in contribution of some of the smaller aerosol particles to the AOD that still remain within the 0.7μm boundary (Figure 4.8). It is not necessary that each time the relative humidity increases by 5%, the first term or the second term continue to dominate throughout resulting in continuous decrease or continuous increase respectively. Thus depending upon the dry size distribution of the aerosol particles, this mixed behavior of the fine mode fraction of AOD is quite probable.

4.2 Quantification of the increases and decreases in fine mode fraction of AOD

The objective of this thesis was to demonstrate that, depending upon the values of the parameters used in the analytical size distribution function of the aerosols, fine mode fraction of AOD can increase or decrease significantly due to positive changes in relative humidity even when the emission scenario of fine particles remain unchanged. The fine mode fraction of AOD has been calculated in this study for 156 different aerosol size distributions (generated by sequential variation of the values of the parameters in the analytical size distribution function) of two different chemical compositions types at values of relative humidity ranging from 55% to 95% .Variation in the fine mode fraction of AOD as a function of relative humidity for these 156 different aerosol size distributions are presented in Appendix A and B.

Figures 4.15− 4.20 illustrate the magnitude of the increases and decreases in fine mode fraction of AOD for several aerosol size distributions corresponding to two different types of chemical composition, due to increase in relative humidity. The two different colors of the bar graphs stand for the two different composition types. Type 1 aerosols have no soot in their composition while Type 2 aerosols consists of 30% soot. The values of the parameters specifying the analytical size distribution function corresponding to each of the bars, are indicated in the Figures. R_1 and R_2 stand for the median radius of the accumulation and coarse mode respectively. Lnσ_1 and Lnσ_2 represent the width of the accumulation and coarse mode respectively while the arrows indicate the value of the volume fraction of the accumulation mode. In case of the size distributions in which, the fine mode fraction of AOD increases or decreases in a continuous fashion with rise in the value of relative humidity; the change in fine mode fraction has been calculated by subtracting the fine mode fraction at RH equal to 55% from the fine mode fraction at RH equal to 95%. Hence negative values of change in fine mode fraction indicates decrease in the fine mode fraction with increase in relative humidity while

Figure 4.15: Change in fine mode fraction of AOD with increase in RH for dry size distribution characterized by parameters R_1=0.005μm; Lnσ_1=0.4; Lnσ_2=0.72. The value of R_2 increases steadily from 1 μm to 3 μm along the horizontal axis. Arrows indicate the accumulation mode fraction

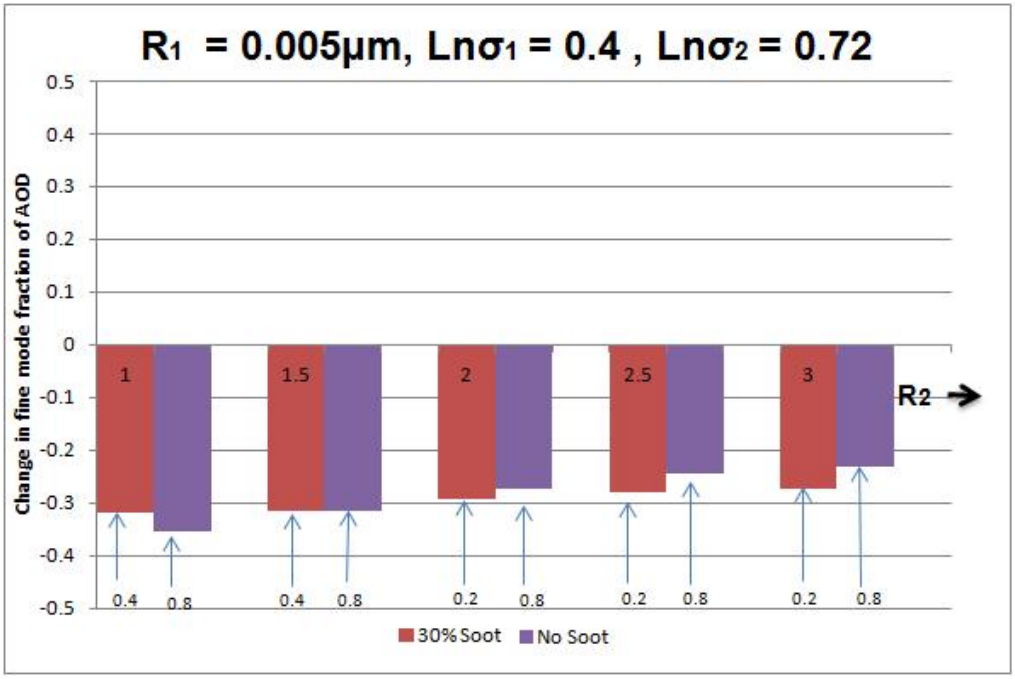

Figure 4.16: Change in fine mode fraction of AOD with increase in RH for dry size distribution characterized by parameters R_1=0.05μm; Lnσ_1=0.4; Lnσ_2=0.72. The value of R_2 increases steadily from 1 μm to 3 μm along the horizontal axis. Arrows indicate the accumulation mode fraction

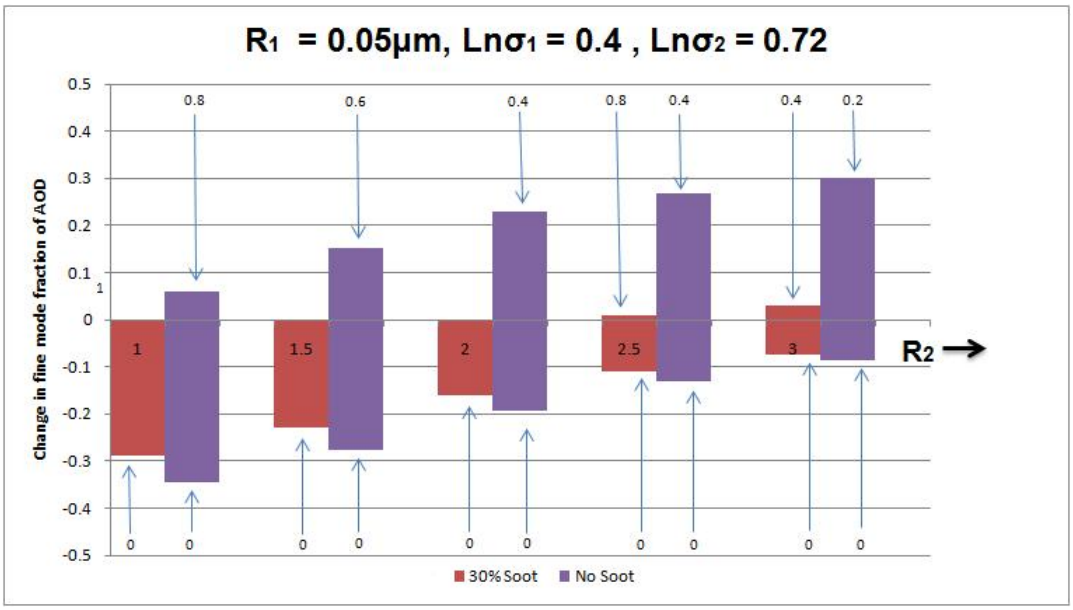

Figure 4.17: Change in fine mode fraction of AOD with increase in RH for dry size distribution characterized by parameters R_1=0.05μm; R_2=1.5μm; Lnσ_1=0.2. The value of Lnσ_2 increases steadily from 0.2 to 0.8 along the horizontal axis. Arrows indicate the accumulation mode fraction

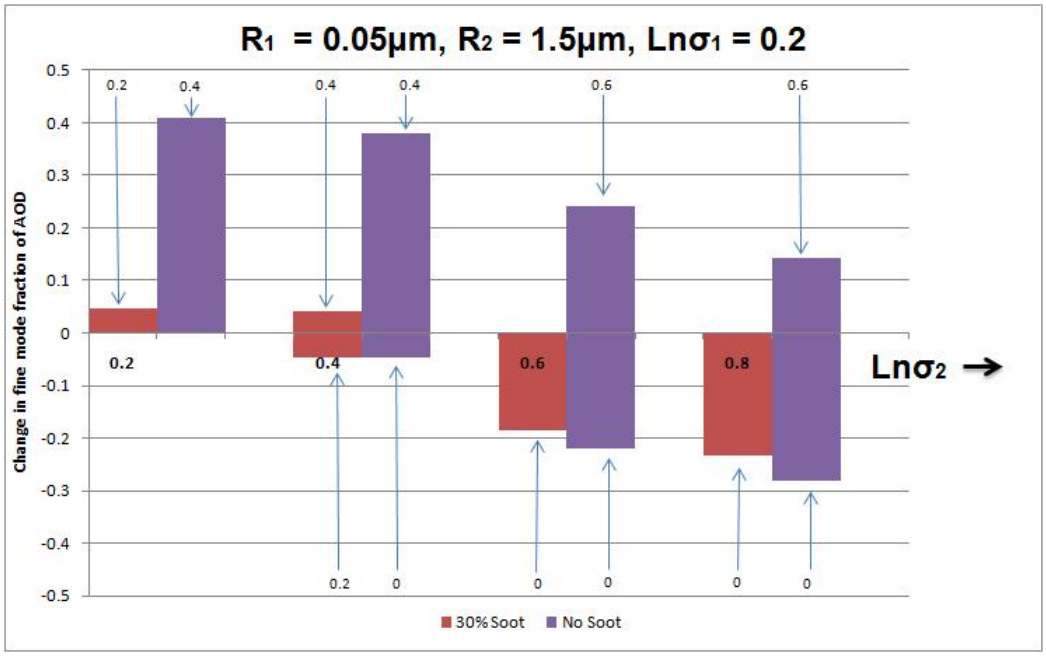

Figure 4.18: Change in fine mode fraction of AOD with increase in RH for dry size distribution characterized by parameters R_1=0.05μm; R_2=1.5μm; Lnσ_1=0.4. The value of Lnσ_2 increases steadily from 0.2 to 0.8 along the horizontal axis. Arrows indicate the accumulation mode fraction

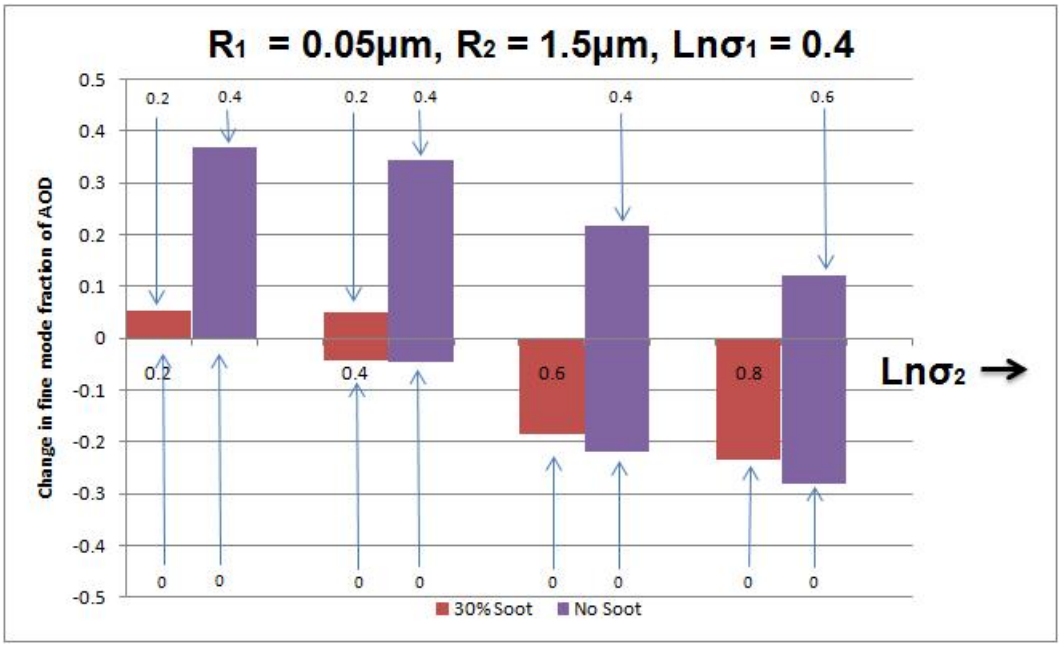

Figure 4.19: Change in fine mode fraction of AOD with increase in RH for dry size distribution characterized by parameters R_1=0.05μm; R_2=1.5μm; Lnσ_1=0.6. The value of Lnσ_2 increases steadily from 0.2 to 0.8 along the horizontal axis. Arrows indicate the accumulation mode fraction

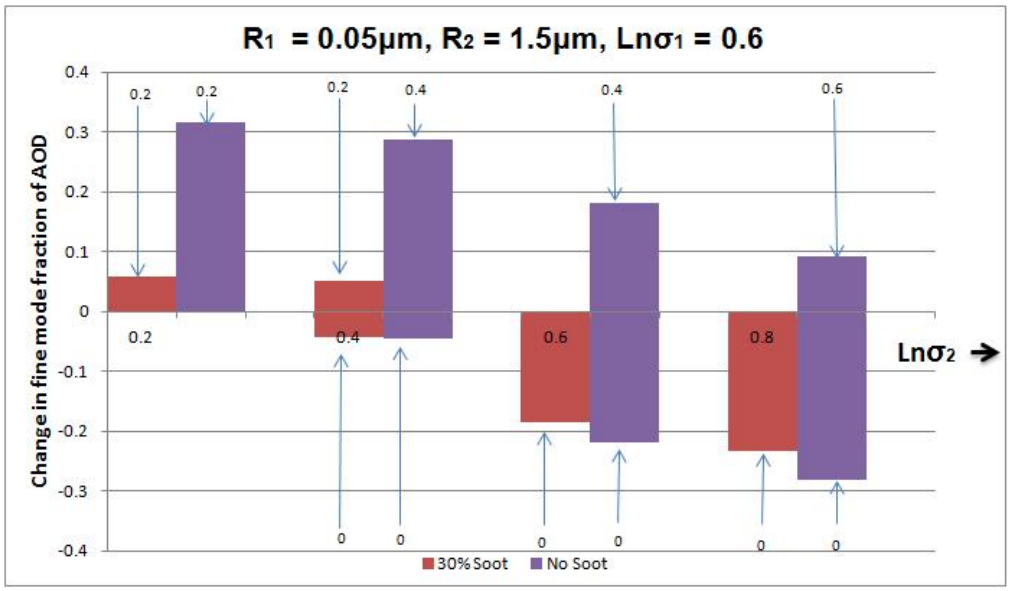

Figure 4.20: Change in fine mode fraction of AOD with increase in RH for dry size distribution characterized by parameters R_1=0.05μm; R_2=1.5μm; Lnσ_1=0.8. The value of Lnσ_2 increases steadily from 0.2 to 0.8 along the horizontal axis. Arrows indicate the accumulation mode fraction

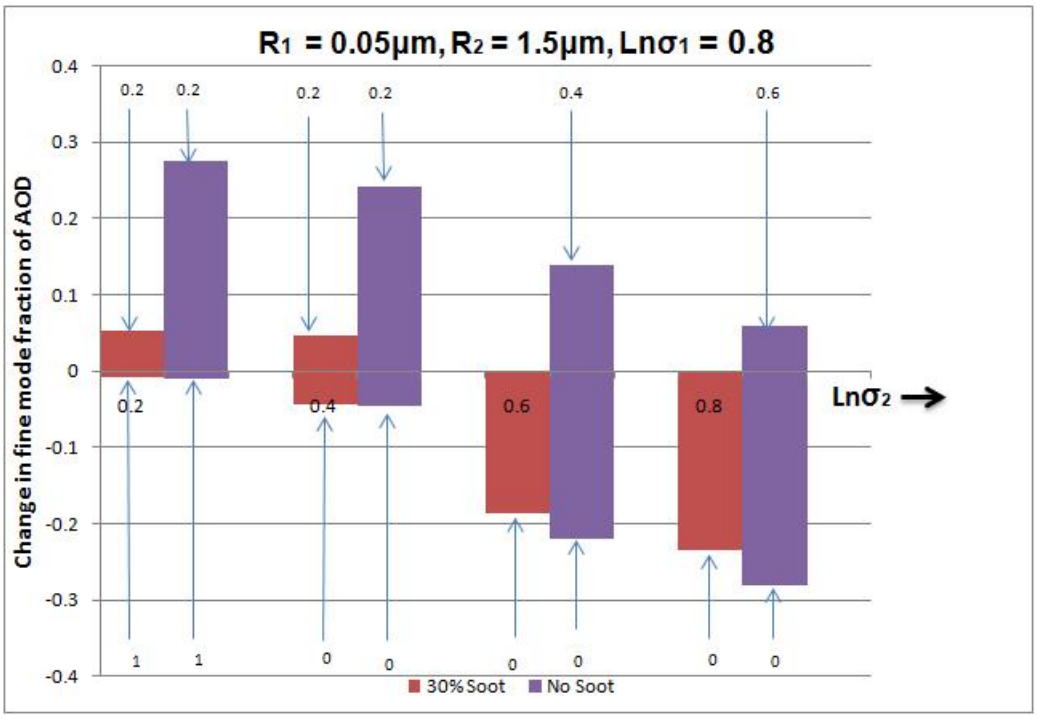

positive values indicate increase in the fine mode fraction with increase in relative humidity. However in case of the size distributions corresponding to which the fine mode fraction exhibits mixed behavior with increase in relative humidity, the minimum and the maximum values of the fine mode fraction of AOD are located for the entire range of relative humidity (55% to 95%)and then the minimum is subtracted from the maximum to calculate the magnitude of the change in fine mode fraction. If the maximum corresponds to a higher value of relative humidity than the minimum, in that case the change in the fine mode fraction is positive while if the maximum corresponds to a lower value of relative humidity in comparison of the minimum, then the change in the fine mode fraction is negative.

4.3 Discussion of the results

From Figures 4.15− 4.20 it is to be noticed that there is atleast one and in some cases two values of the volume fraction of the accumulation mode corresponding to each of the 26 diffferent combinations of the values of the parameters R_1, R_2, $\text{Ln}\sigma_1$ and $\text{Ln}\sigma_2$ (that specify the dry size distribution) for which change in fine mode fraction of AOD has been plotted. In this study the volume fraction of the accumulation mode has been varied from 0-1 in steps of 0.2 for each combination of the values of the parameters R_1, R_2, $\text{Ln}\sigma_1$ and $\text{Ln}\sigma_2$, generating an ensemble of size distributions. Hence corresponding to each set of values of these parameters, the value of the accumulation mode fraction for which the change in fine mode fraction of AOD with positive changes in RH is maximum (either in the positive or negative direction) has been identified. Then for that particular dry size distribution, the change in fine mode fraction of AOD with increase in RH has been plotted.

It can be seen from Figure 4.15 that the change in fine mode fraction is always negative for the set of dry sized distributions in which the median radius of the accumulation mode (R_1) is equal to 0.005 μm. This is true for both the composition types that have been studies in this thesis. However, if the value of R_1 is kept fixed at 0.005 μm and the median radius of the coarse mode (R_2) is gradually

increased from 1 μm to 3 μm in equal steps of 0.5 μm, then the magnitude of the change in fine mode fraction gradually decreases. Negative change in fine mode fraction implies decrease in fine mode fraction of AOD as the RH is increased from 55% to 95%. In the case of the dry size distributions that are characterised by value of R_1 equal to 0.005 μm, most of the particles in the accumulation mode are so small that they contribute negligibly to the total AOD in the dry state as well as at elevated levels of RH. Hence depending upon the value of R_2 as well as the other parameters specifying the size distribution, the contribution of the particles that move out of the 0.7 μm cut-off range with increase in RH is greater than the increase in contribution of the smaller particles to the total AOD, that remain within the 0.7 μm range. Thus change in fine mode fraction with positive change in RH is always negative for the size disitributions characterized by R_1 equal to 0.005 μm. However, if the median radius of the coarse mode is increased in the dry sized distributions then lesser and lesser particles are concentrated in and around 0.7 μm boundary in the dry state. So as the RH increases,the contribution to the total AOD of the particles that outgrow 0.7 μm cut-off also decreases and so decreases the magnitude of fine mode fraction.

However, the story is different when the median radius of the accumulation mode for the dry size distributions is equal to 0.05 μm. In that case, depending upon the volume fraction of the accumulation mode ($V_{t1}/V_{t1} + V_{t2}$) as well as the other parameters specifying the size distribution, change in fine mode fraction can be both positive and negative with increase in RH. This is because the sum of the accumulation mode particles are large enough in the dry state. So, with increase in RH they can grow to sizes such that they can contribute significantly to the total AOD while still remaining within the 0.7 μm cut-off radius. It can be noticed from Figure 4.16 that when R_1 is kept fixed at 0.05 μm and R_2 is increased steadily in steps of 0.5 μm, the magnitude of the change in fine mode fraction in the negative direction steadily decreases while it steadily increases in the positive direction. The reason being that as R_2 increases (the other parameters of the size distribution being fixed), the dry size distribution gets more biased with coarser

particles and fewer particles are concentrated in and around 0.7 μm. Hence, with increase in median radius of the coarse mode, the contribution of the particles that grow out of the 0.7 μm boundary to the total AOD decreases.

From figures 4.17- 4.20 it can be noticed that when the values of the parameters R_1, R_2 and $Ln\sigma_1$ specifying the dry size distribution is kept fixed and the value of $Ln\sigma_2$ is steadily increased from 0.2 to 0.8 in equal steps of 0.2, they magnitude of the change in fine mode fraction steadily decreases in the positive direction and increases in the negative direction. $Ln\sigma_2$ denotes the width of the coarse mode. Hence, higher value of $Ln\sigma_2$ implies that the coarse mode particles are more spread out and lower value denotes that the coarse mode particles are densely packed in and around R_2. The values of the parameters R_1, R_2 and $Ln\sigma_1$ being fixed, the more spread out the coarse mode particles are (higher the value of $Ln\sigma_2$), greater are the number of particles located near the 0.7 μm range in the dry state. Thus the contribution of particles outgrowing the 0.7 μm radius to the total AOD will be greater for the dry size distributions characterized by higher value of $Ln\sigma_2$ with increase in RH.

Another interesting fact that can be observed in Figures 4.15- 4.20 is that for Type 2 aerosols, which has 30% soot in its composition, the change in fine mode fraction of AOD is mostly negative with increase in RH. In other words, for majority of the dry size distributions that has been used in this study, the fnie mode fraction of AOD for Type 2 aerosols decreases with increase in RH. A possible explanation can be that due to the presence of soot in its composition, Type 2 aerosols have lesser amount of soluble salts in comparison to Type 1 aerosols of the same size. Hence Type 2 aerosols cannot grow as much as Type 1 aerosols with increase in RH. Now, an increase in fine mode fraction of AOD with a rise in RH takes place mainly due to an increase in contribution of the aerosol particles that are very small in the dry state, but with a rise in RH can grow to sizes such that they can contribute significantly to the toal AOD while still remaining within the 0.7 μm radius. Therefore these very small aerosol particles must undergo enough hygroscopic growth so as to increase the fine mode fraction

of AOD. But for Type 2 aerosols with 30% soot in its composition, it is a difficult goal. So for Type 2 aerosols the change in fine mode fraction of AOD is mostly negative as the contribution of the particles that move out of the 0.7 μm range due to increase in RH in most cases is greater than the increase in contribution of the smaller particles to the total AOD.

CHAPTER 5

CONCLUSION

5.1 Applicability of the results to other definitions of fine mode fraction

Fine mode fraction of AOD has been defined in this thesis as the fraction of the total AOD that can be attributed to particles of radius less than and equal to 0.7 μm. The reason for choosing 0.7 μm as the cut-off radius is that MISR defined small (r $<$ 0.35 μm) and medium (0.35 μm $\leq$ r $\leq$ 0.7 μm) particle fraction of AOD taken together is correlated to the AERONET fine mode fraction, although it is defined and calculated differently from MISR (Dey & Di Girolamo, 2010).

Other than MISR, fine mode fraction of AOD is also retrieved by AERONET (which is a ground based network of sunphotometers) as well as by MODIS (which is key instrument aboard NASA's TERRA and AQUA satellites). It would be really interesting to know whether the increases and decreases in fine mode fraction of AOD as defined in this thesis is also applicable to the AERONET and MODIS definitions of fine mode fraction. AERONET defines fine mode fraction as the fraction of the total volume of the aerosol particles that is contributed by the submicron sized aerosols (r $<$ 0.5 μm) (Kleidman et al., 2005). The Figures 5.1 - 5.4 represent the change in fine mode fraction as defined by AERONET with increase in RH, for the dry size distribution presented in 4.1 corresponding to the continuous increase, continuous decrease, constant and mized behavior scenario of fine mode fraction of AOD (as defined in this thesis).

It can be noticed from the Figures 5.1 - 5.4 that the behavior of fine mode fraction as defined by AERONET does not exactly match the behavior of fine mode

Figure 5.1: Fine mode fraction of AOD as defined by AERONET as a function of RH (R_1=0.05 μm, R_2=1.5 μm, Lnσ_1 = 0.4, Lnσ_2=0.4, $V_{t1}/V_{t1} + V_{t2} = 0.2$)

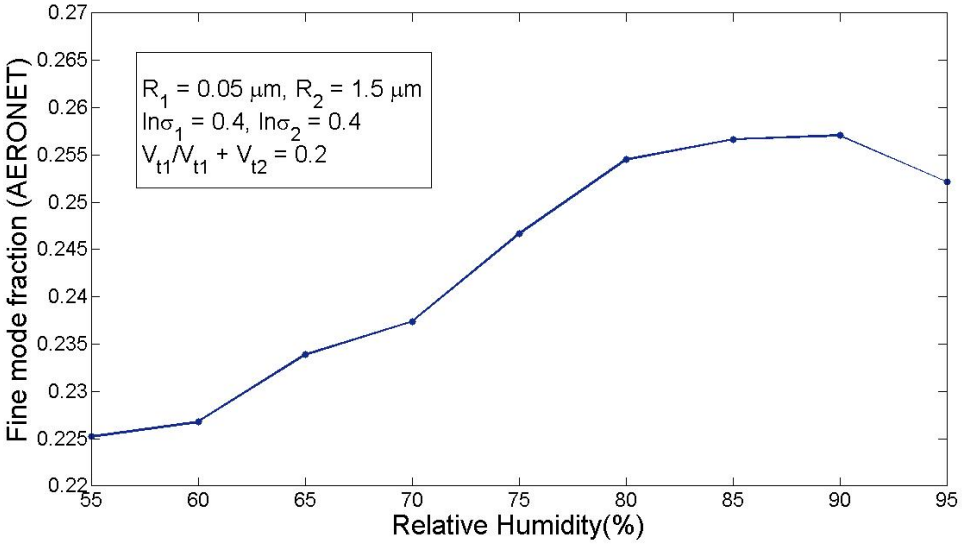

Figure 5.2: Fine mode fraction of AOD as defined by AERONET as a function of RH (R_1=0.05 μm, R_2=1 μm, Lnσ_1 = 0.4, Lnσ_2=0.72, $V_{t1}/V_{t1} + V_{t2} = 0.2$)

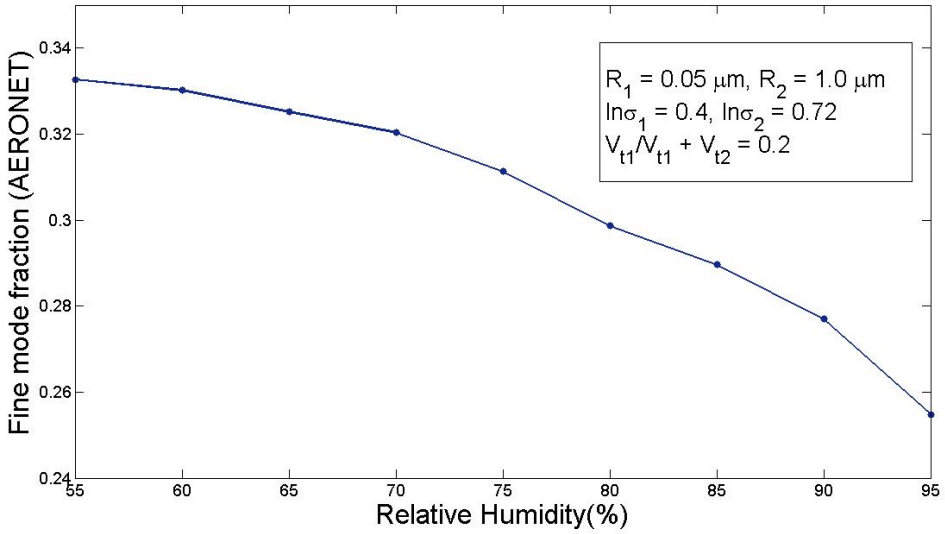

Figure 5.3: Fine mode fraction of AOD as defined by AERONET as a function of RH (R_1=0.05 μm, R_2=1 μm, Lnσ_1 = 0.4, Lnσ_2=0.72, $V_{t1}/V_{t1} + V_{t2} = 1$)

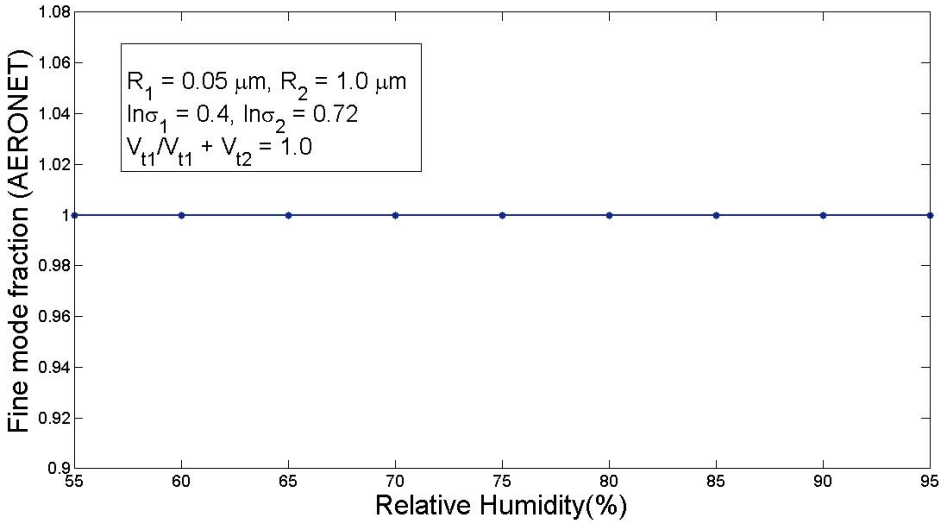

Figure 5.4: Fine mode fraction of AOD as defined by AERONET as a function of RH (R_1=0.05 μm, R_2=1.5 μm, Lnσ_1 = 0.4, Lnσ_2=0.72, $V_{t1}/V_{t1} + V_{t2} = 0.2$)

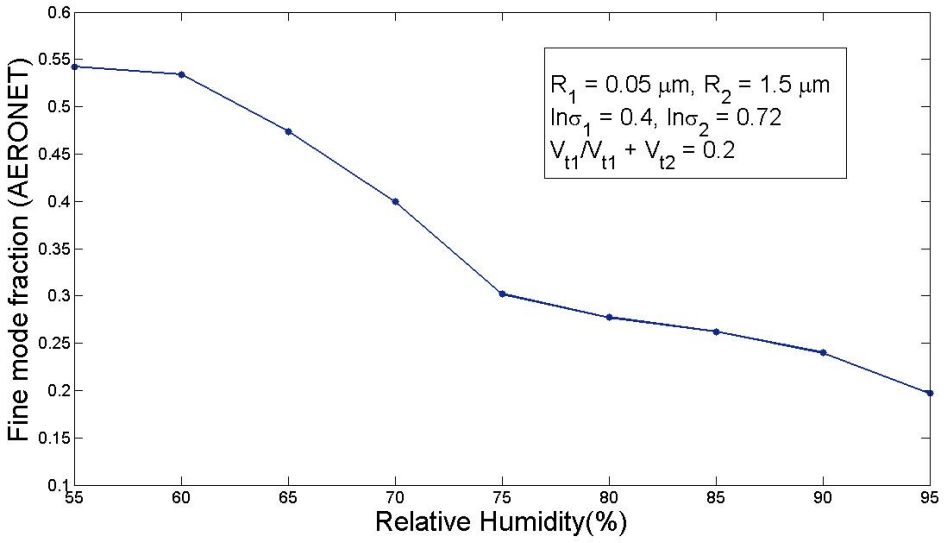

Figure 5.5: Fine mode fraction of AOD as defined by MODIS as a function of RH (R_1=0.05 μm, R_2=1.5 μm, Lnσ_1 = 0.4, Lnσ_2=0.4, $V_{t1}/V_{t1} + V_{t2} = 0.2$)

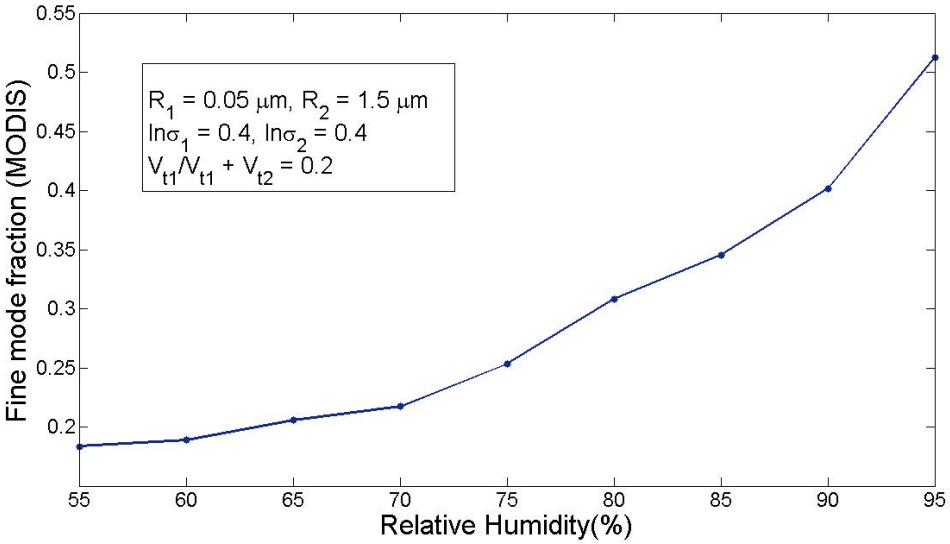

Figure 5.6: Fine mode fraction of AOD as defined by MODIS as a function of RH (R_1=0.05 μm, R_2=1 μm, Lnσ_1 = 0.4, Lnσ_2=0.72, $V_{t1}/V_{t1} + V_{t2} = 0.2$)

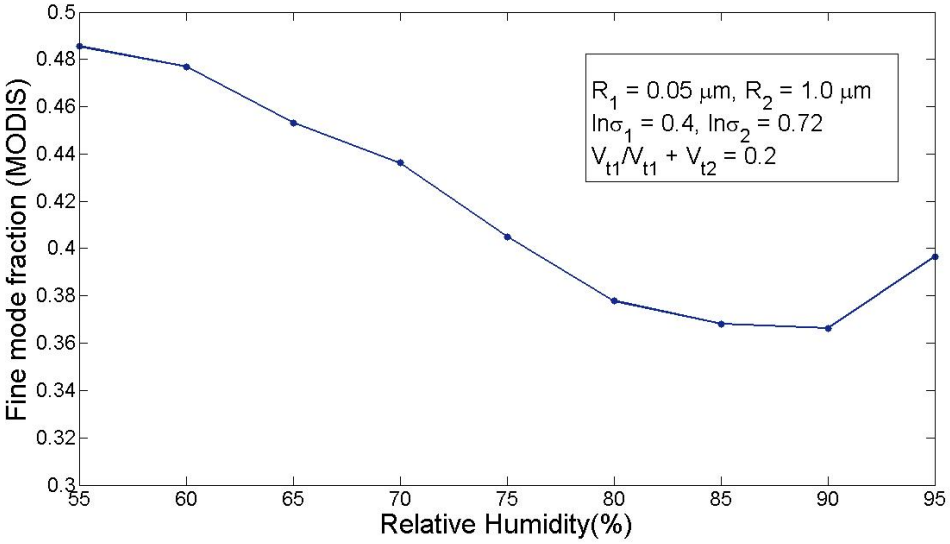

Figure 5.7: Fine mode fraction of AOD as defined by MODIS as a function of RH (R_1=0.05 μm, R_2=1 μm, Lnσ_1 = 0.4, Lnσ_2=0.72, $V_{t1}/V_{t1} + V_{t2} = 1$)

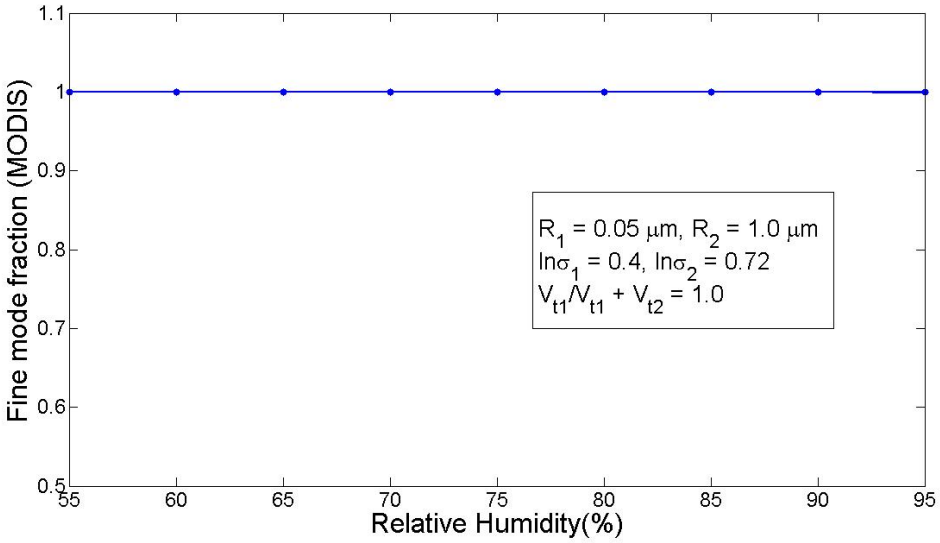

Figure 5.8: Fine mode fraction of AOD as defined by MODIS as a function of RH (R_1=0.05 μm, R_2=1.5 μm, Lnσ_1 = 0.4, Lnσ_2=0.72, $V_{t1}/V_{t1} + V_{t2} = 0.2$)

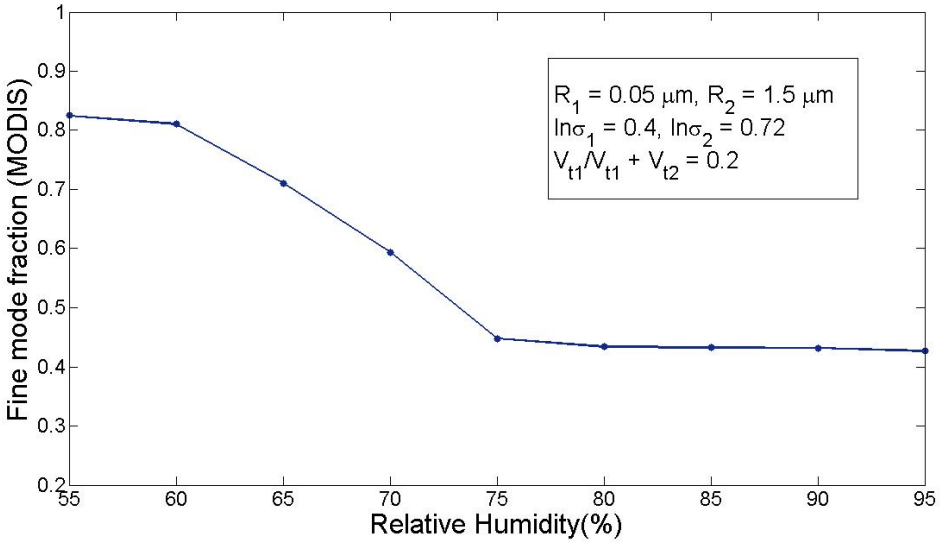

fraction of AOD as defined in this thesis, even though the dry size distribution and composition in both cases are the same.

Similar is the case for the MODIS defined fine mode fraction of AOD. Fine mode fraction of AOD as defined by MODIS is the fraction of the AOD at 550 nm that is contributed by particles of radius less than and equal to 0.5 μm (submicron sized particles) (Kleidman et al., 2005). The Figures 5.5 - 5.8 shows the MODIS defintion of fine mode fraction of 550 nm AOD as a function of RH for the dry sized distribution and compostion identical to the AERONET scenarios.

The reason for this mismatch in behavior is that the definition of fine mode fraction used by AERONET or MODIS is different from that used in this thesis. However, the goal of this thesis was to imply that for certain size distributions fine mode fraction of AOD can increase or decrease significantly with positive changes in RH. From the above Figures it is evident that even when fine mode fraction is defined in accordance to AERONET or MODIS, it does demonstrate significant increase or decreases as the RH is increased from 55% to 95%, although the emission scenario remains unchanged.

5.2 Assumptions

It has been assumed in this thesis that the aerosol particles become spherical upon deliquescence. Therefore Mie theory for spherical particles has been used to calculate the extinction efficiency of the aerosol particles under enhanced RH conditions. This assumption is very common among climate models that use Mie theory to calculate the scattering and absorption by the ambient aerosol particles (Bohren & Huffman, 1983; Bond & Bergstrom, 2006). But using transmission and scanning electron microscopes it has been found that aerosol particles collected from ambient air can display a wide variety of shapes (Adachi et al., 2011; Ebert et al., 2002; Pósfai & Buseck, 2010).

Hence the use of Mie theory to calculate the scattering and absorption by aerosol particles under ambient RH conditions might not be appropriate. Most recently

Adachi et. al. have reinforced this fact by using aerosol samples collected from Mexico City, Mexico (Adachi et al., 2011). These aerosols collected from Mexico City, Mexico, had sulfate particles embedded within weakly hygroscopic organic aerosols. Upon increasing the RH, only the sulfate parts of the aerosol deliquesced but the entire particle did not become spherical. When discrete dipole aproximation was used to calculate the light scattering by these observed non-sperical aerosol particles, it was found that for particles greater than 1 μm, the spherical shape assumption used in Mie theory under estimates the light scattering by about 50%. However this thesis deals with increases and decreases in fine mode fraction of AOD as defined in several satellite and ground based aerosol property retrieval algorithms (like in MISR, MODIS and AERONET), where ambient aerosol particles are assumed to be spherical in shape. Hence the use of spherical shape assumptions in this thesis is consistent with the remotely sensed data we aim to interprete.

In order to carry out the calculation of AOD and fine mode fraction of AOD for the ensemble of size distributions that has been cosnidered in this study, it has been assumed that aerosol particles span in radius from 0.0005 μm to 10 μm. This is because the extinction efficiency of aerosol particles having radius less than 0.0005 μm for 550 nm radiation is negligible. Also, it is a common tendency of these very small sized aerosol particles to grow in size by either coagulation or condensation of vapor on their surface, soon after they aref ormed or emitted in the atmosphere. Hence very few aerosol particles that are suspended in the atmosphere have radius less than 0.0005 μm. The assumption that the aerosol particles having radius greater than 10 μm do not contribute at all to the AOD for the aerosol size distribution used in this study, is justified in the folllowing section.

5.3 Error estimation

The analytical methodology that led to the results of this thesis involves two possible sources of error. An estimation of the magnitude of these possible errors is thus necessary before interpreting the results.

Fine mode fraction of AOD has been defined in this study as the fraction of the total AOD that is contributed by aerosol particles having radius less than and equal to 0.7μm. This fixed microphysical cut off radius of 0.7μm is the source of the first type of error. In this study it has been assumed that the aerosol particles span in radius from 0.0005μm to 10μm and this range has been divided into 10000 bins of equal width. The values of the parameters used in the analytical size distribution function, determines the number of aerosol particles lying in each bin corresponding to each of the size distributions. In order to numerically calculate the fine mode fraction of AOD it is necessary to identify the size bin whose upper limit is exactly equal to 0.7um and calculate the fraction of total optical depth that is contributed by particles lying in that bin as well as in bins that have their upper boundary less than 0.7μm. Since there is no such bin whose upper limit exactly matches 0.7μm, the bin whose right boundary is closest to 0.7μm at the relative humidity level under consideration is used instead. Hence the upper limit of that bin is very slightly greater than the 0.7μm cut off. In order to estimate the error arising from this fact, a size distribution for which majority of the particles are concentrated around 0.7μm radius in the dry state is selected from the ensemble of size distributions used in this study. The parameter values of the selected size distribution are as follows: R_1=0.05μm, R_2=1μm, Ln_1=0.4, Ln_2=0.72, $V_{t1}/(V_{t1}+V_{t2})$= 0.6; where R_1 is the median radius of the accumulation mode, R_2 is the median radius of the coarse mode, $\mathrm{Ln}\sigma_1$ indicates the width of the accumulation mode, $\mathrm{Ln}\sigma_2$ indicates the width of the coarse mode and $V_{t1}/(V_{t1}+V_{t2})$ is the volume fraction of the accumulation mode. The fraction of the total optical depth that is contributed by the bin that encloses the 0.7μm boundary is then calculated for each relative humidity level, for the

selected size distribution. Half of this fractional optical depth that is contributed by the last bin encapsulating the 0.7μm boundary has been used as an estimate of the maximum uncertainty that might arise from this cause for each of the aerosol composition types (Type 1 and Type 2) and relative humidity levels under consideration. Table 5.1 below lists the uncertainties so calculated, in estimating the fine mode fraction of AOD for each of the two aerosol composition types and nine relative humidity levels.

Table 5.1: Error estimate in fine mode fraction of AOD due to fixed microphysical cut-off radius of 0.7μm

Relative Humidity (%)	Composition: Type 1	Composition: Type 2
55	0.000161	0.0000862
60	0.000160	0.0000878
65	0.000165	0.00009723
70	0.000172	0.000105
75	0.000189	0.00013
80	0.000316	0.000192
85	0.000314	0.000213
90	0.000298	0.00023
95	0.000232	0.000225

Table 5.2: Error estimate in fine mode fraction of AOD from the assumption that particles larger than 10μm do not contribute to the aerosol optical depth for the size distributions under consideration

Relative Humidity (%)	Composition: Type 1	Composition: Type 2
55	1.3793e-13	7.1606e-14
60	1.3606e-13	7.2215e-14
65	1.3111e-13	7.4925e-14
70	1.2369e-13	7.4292e-14
75	1.1222e-13	7.6365e-14
80	9.6979e-14	7.6618e-14
85	8.7978e-14	7.6255e-14
90	7.6129e-14	7.4441e-14
95	5.6431e-14	6.7216e-14

In order to carry out the calculation of fine mode fraction of AOD, an assumption has been made that aerosol particles having radius greater than 10μm do

not contribute to the aerosol optical depth for the aerosol size distributions under consideration in this study. Hence an estimate of the maximum possible error that might arise from this assumption must be listed. For that purpose an extreme size distribution is selected from amongst the various size distributions used in this study, for which the concentration of aerosol particles is maximum in and around 10μm. The selected size distribution is characterized by the parameters R_1= 0.05μm, R_2=3.0μm, Lnσ_1=0.4, Lnσ_2=0.72, $V_{t1}/(V_{t1} + V_{t2})$=0.0. For this particular size distribution, since the volume fraction of the accumulation mode is zero, all the particles are concentrated in the coarse mode. The upper limit of the aerosol particle radius under consideration is extended from 10μm to 50μm, while the lower limit still being 0.0005μm. The fraction of the AOD that is contributed by aerosol particles having radius greater than 10μm is then calculated for this extreme size distribution, corresponding to each relative humidity level and composition types. This gives an estimate of the maximum possible uncertainty that might arise from the assumption that aerosol particles having radius greater than 10μm do not contribute significantly to the total AOD for the size distributions that have been considered in this thesis. Table 5.2 lists the uncertainties so calculated for each relative humidity level and composition types. Therefore, from Tables 5.1 and 5.2 we see that variation in fine mode AOD with RH of more than 0.000316 cannot be explained by errors in the numerics.

5.4 Impact of RH on Angstrom Exponent

Angstrom exponent is a parameter that is used to descibe the wavelength dependence of aerosol optical depth or the aerosol extinction coefficient. For measurements of optical thickness $\tau_{\lambda 1}$ and $\tau_{\lambda 2}$ taken at two different wavelengths $\lambda 1$ and $\lambda 2$ respectively, the angstrom exponent is given by

$$\alpha = -\frac{log\frac{\tau_{\lambda 1}}{\tau_{\lambda 2}}}{log\frac{\lambda 1}{\lambda 2}} \tag{5.4.1}$$

It is a common convention that Angstrom Exponent is inversely related to the size of the aerosol particles (Ångström, 1929; Schuster et al., 2006). In other words, smaller the aerosol particles, the larger the exponent. This is because the extinction efficiency of larger sized aerosol particles is more or less spectrally neutral. Hence Angstrom Exponent is a parameter that is widely used to gauge the particle size of atmospheric aerosols or clouds.

Instinctively it appears that the Angstrom Exponent of an aerosol population should always decrease with increase in RH, as the aerosol particles undergo hygroscopic growth. However, just like fine mode fraction of AOD defined in this thesis, Angstrom Exponent can also increase continuously, decrease continuously or even exhibit mixed bahavior (increase and then decrease) with positive changes in RH, depending on the parameters used to specify the size distribution of the aerosols. Loeb and Schuster theoretically investigated the effect of increasing RH on Angstrom Exponent for an Aerosol Population representative of marine environments (Loeb & Schuster, 2008). They assumed the dry bimodal size distribution to be composed of Ammonium Sulfate in mode 1 and sea salt in mode 2. Then the hygroscopic growth of these two modes where modelled for nine different accumulation mode fractions as shown in the Figure 5.9. The Figure indicates that the bimodal mixture of the two modes (accumulation and coarse) of an aerosol population can result in Angstrom Exponents that can either increase or decrease as the aerosols swell, depending upon the initial accumulation mode fraction and RH. In general it was observed that for the particular aerosol size distribution under consideration, dry accumulation mode fractions of less than 0.6 tend to produce an increase in the Angstrom Exponent as aerosols swell, while dry accumulation mode fractions greater than 0.8 tend to produce a decrease in angstrom exponent with hygroscopic growth of the aerosols.

Therefore as in the case of fine mode fraction of AOD, increase in RH can also result in significant increases and decreases in Angstrom Exponent depending upon the dry size distribution. Hence increase in Angstrom Exponent should not always be interpreted as increase in concentration of smaller aerosol particles

Figure 5.9: Change in Angstrom Exponent with RH for 9 different accumulation mode fracitons (dry). (Loeb & Schuster, 2008)

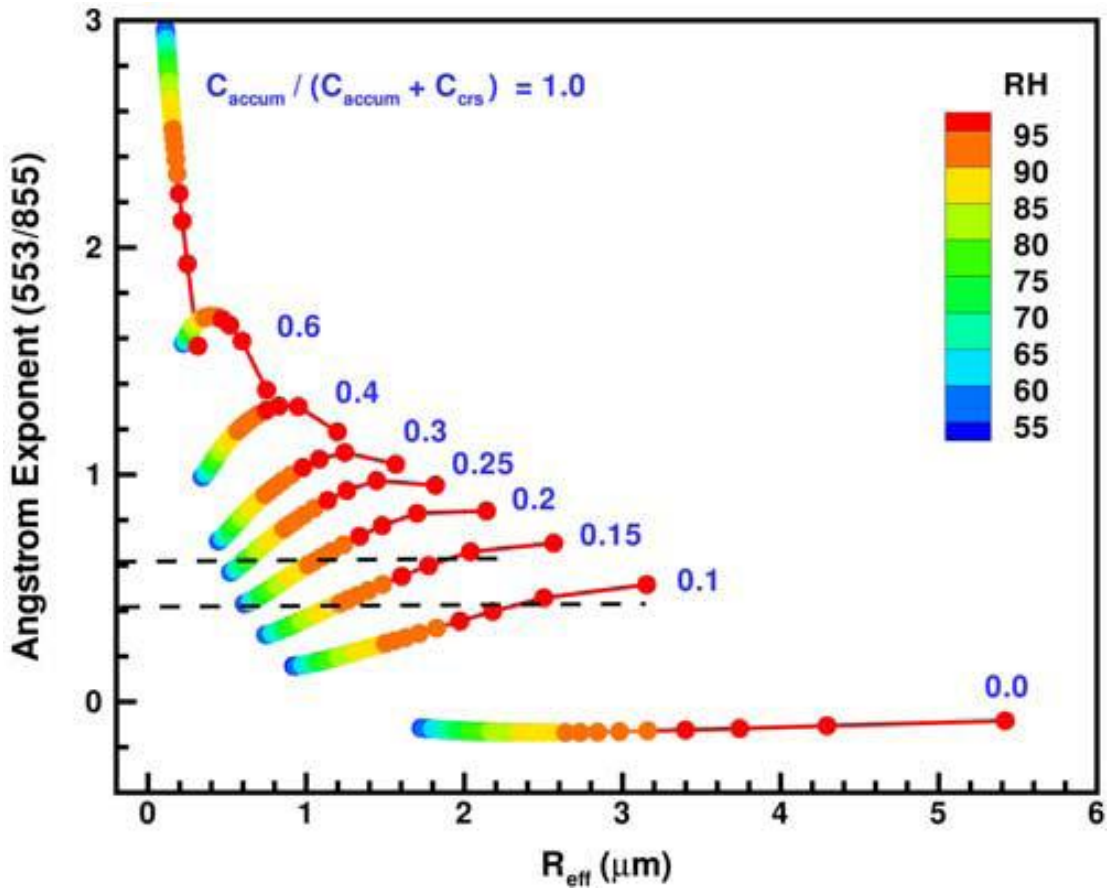

without investigating the role of RH.

5.5 Conclusion

From the results presented in this thesis, it is evident that depending upon the values of the parameters used in the analytical size distribution function and the chemical composition of the aerosols, fine mode fraction of AOD can increase as well as decrease significantly with increase in the value of relative humidity, even when the emission pattern of the fine aerosol particles remain unaltered. Hence the applicability of fine mode fraction of AOD, as retrieved by several ground and satellite based instruments, to serve as an indicator of the increases

and decreases in the emission of fine anthropogenic pollution particles becomes questionable. This is because, if proper investigations regarding the prevalent particle size distribution and relative humidity conditions are not made then the changes in the value of fine mode fraction of AOD that might be taking place due to changes in ambient relative humidity can be misinterpreted as increase or decrease in man made pollution.

APPENDIX A

VARIATION IN THE FINE MODE FRACTION OF AOD AS A FUNCTION OF RELATIVE HUMIDITY FOR TYPE 1 AEROSOLS

This Appendix presents the variation in the fine mode fraction of AOD with increasing RH for the 156 different dry aerosol size distributions of composition Type1.

Figure A.1: Fine mode fraction of AOD (Type 1 aerosols) as a function of RH for dry size distributions specified by the parameters R_1=0.005μm, R_2=1μm, lnσ_1=0.4,lnσ_2=0.72,$V_{t1}/(V_{t1} + V_{t2})$=1, 0.8, 0.6, 0.4, 0.2, 0.0

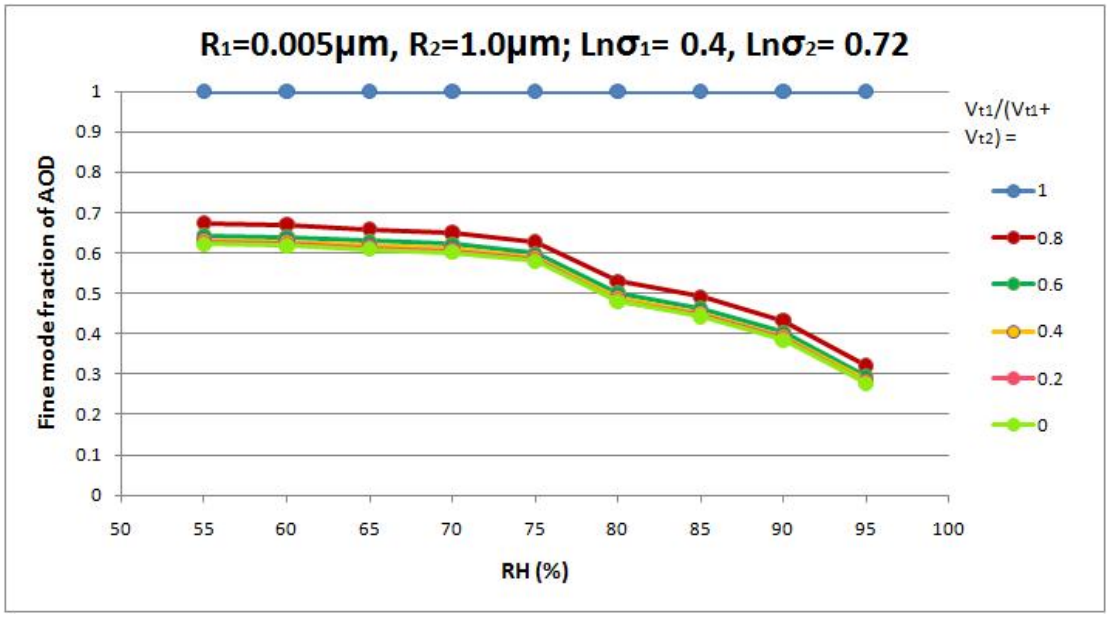

Figure A.2: Fine mode fraction of AOD (Type 1 aerosols) as a function of RH for dry size distributions specified by the parameters R_1=0.005μm, R_2=1.5μm, lnσ_1=0.4,lnσ_2=0.72,$V_{t1}/(V_{t1} + V_{t2})$=1, 0.8, 0.6, 0.4, 0.2, 0.0

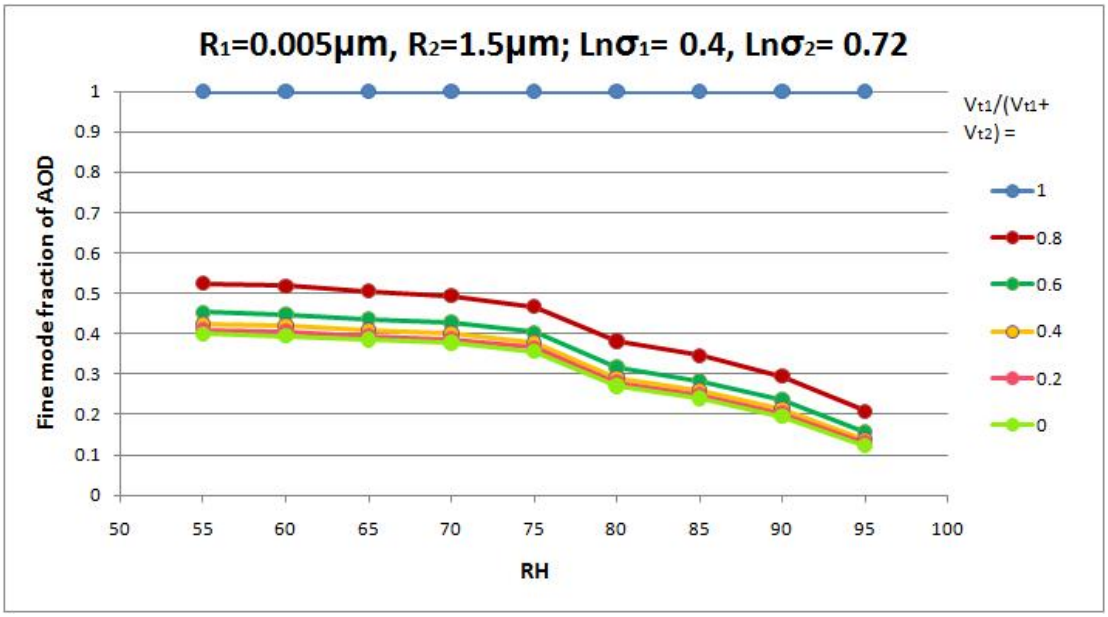

Figure A.3: Fine mode fraction of AOD (Type 1 aerosols) as a function of RH for dry size distributions specified by the parameters R_1=0.005μm, R_2=2.0, lnσ_1=0.4,lnσ_2=0.72,$V_{t1}/(V_{t1} + V_{t2})$=1, 0.8, 0.6, 0.4, 0.2, 0.0

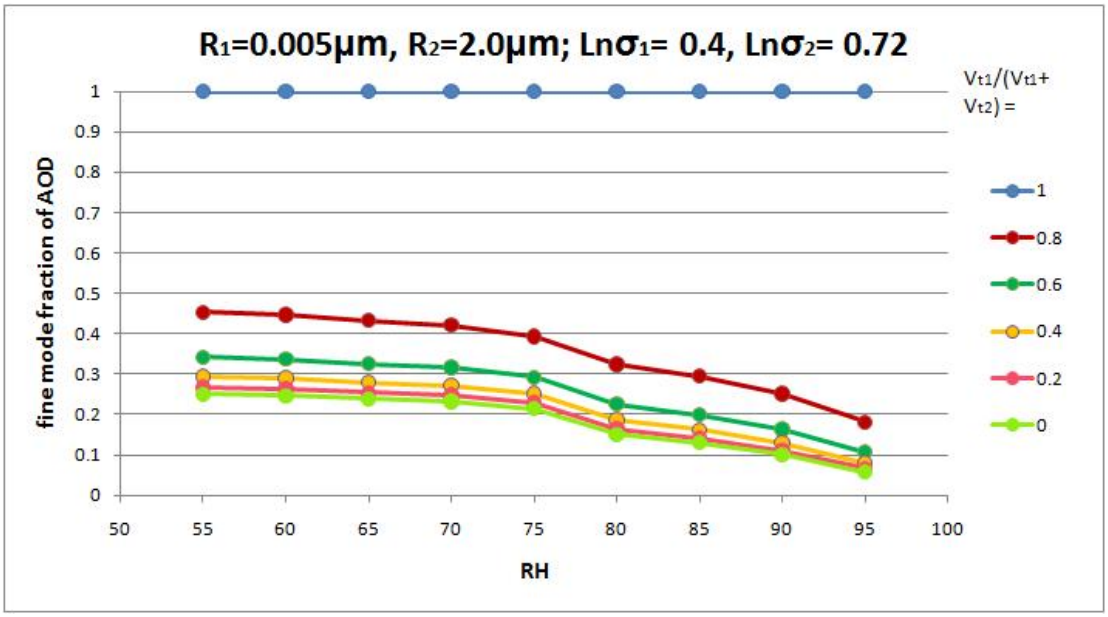

Figure A.4: Fine mode fraction of AOD (Type 1 aerosols) as a function of RH for dry size distributions specified by the parameters R_1=0.005μm, R_2=2.5μm, lnσ_1=0.4,lnσ_2=0.72,$V_{t1}/(V_{t1} + V_{t2})$=1, 0.8, 0.6, 0.4, 0.2, 0.0

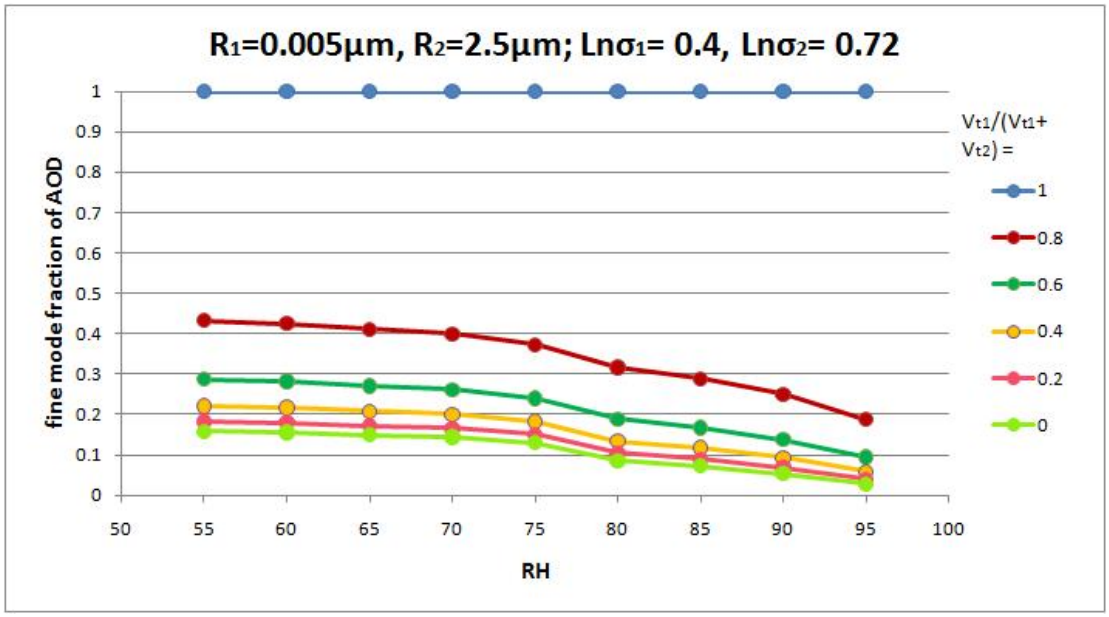

Figure A.5: Fine mode fraction of AOD (Type 1 aerosols) as a function of RH for dry size distributions specified by the parameters R_1=0.005μm, R_2=3μm, lnσ_1=0.4,lnσ_2=0.72,$V_{t1}/(V_{t1} + V_{t2})$=1, 0.8, 0.6, 0.4, 0.2, 0.0

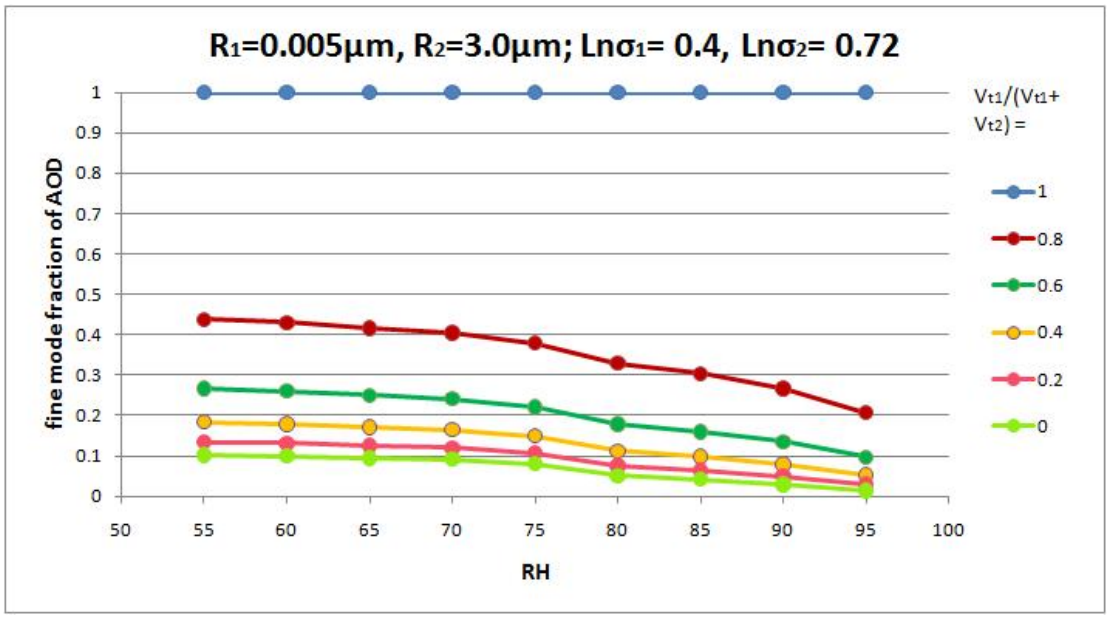

Figure A.6: Fine mode fraction of AOD (Type 1 aerosols) as a function of RH for dry size distributions specified by the parameters R_1=0.05μm, R_2=1μm, lnσ_1=0.4,lnσ_2=0.72,$V_{t1}/(V_{t1} + V_{t2})$=1, 0.8, 0.6, 0.4, 0.2, 0.0

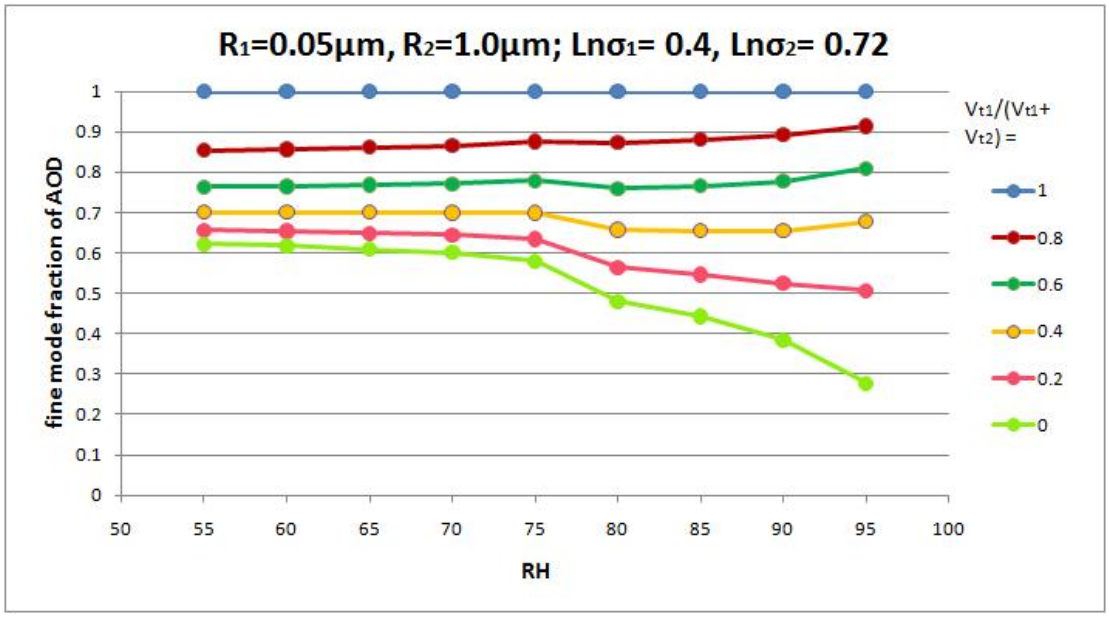

Figure A.7: Fine mode fraction of AOD (Type 1 aerosols) as a function of RH for dry size distributions specified by the parameters R_1=0.05μm, R_2=1.5μm, lnσ_1=0.4,lnσ_2=0.72,$V_{t1}/(V_{t1} + V_{t2})$=1, 0.8, 0.6, 0.4, 0.2, 0.0

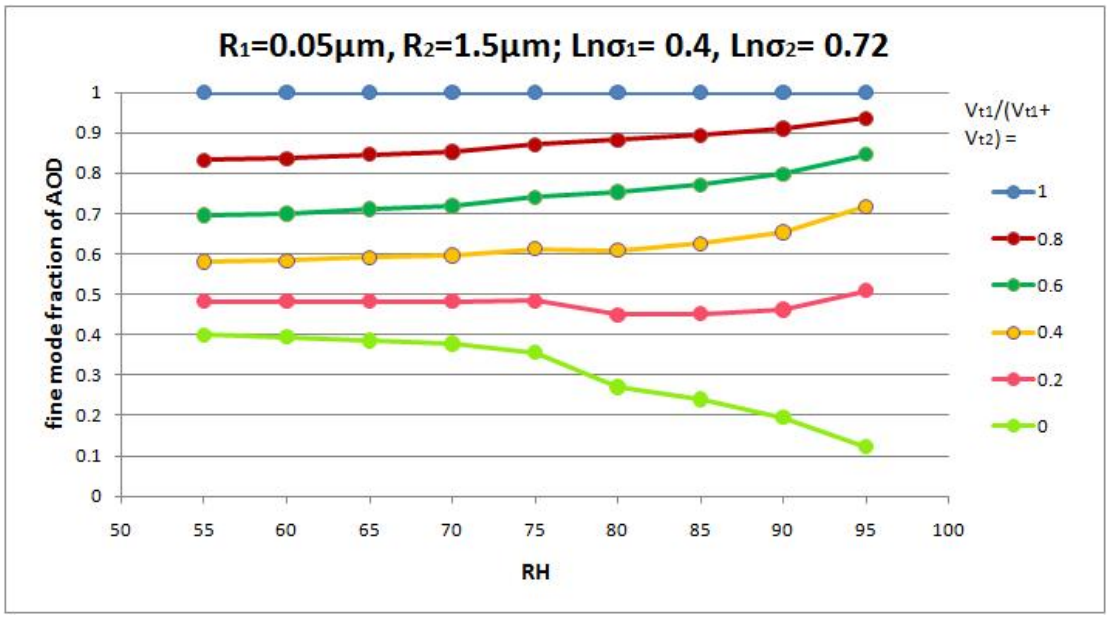

Figure A.8: Fine mode fraction of AOD (Type 1 aerosols) as a function of RH for dry size distributions specified by the parameters R_1=0.05μm, R_2=2μm, lnσ_1=0.4,lnσ_2=0.72,$V_{t1}/(V_{t1} + V_{t2})$=1, 0.8, 0.6, 0.4, 0.2, 0.0

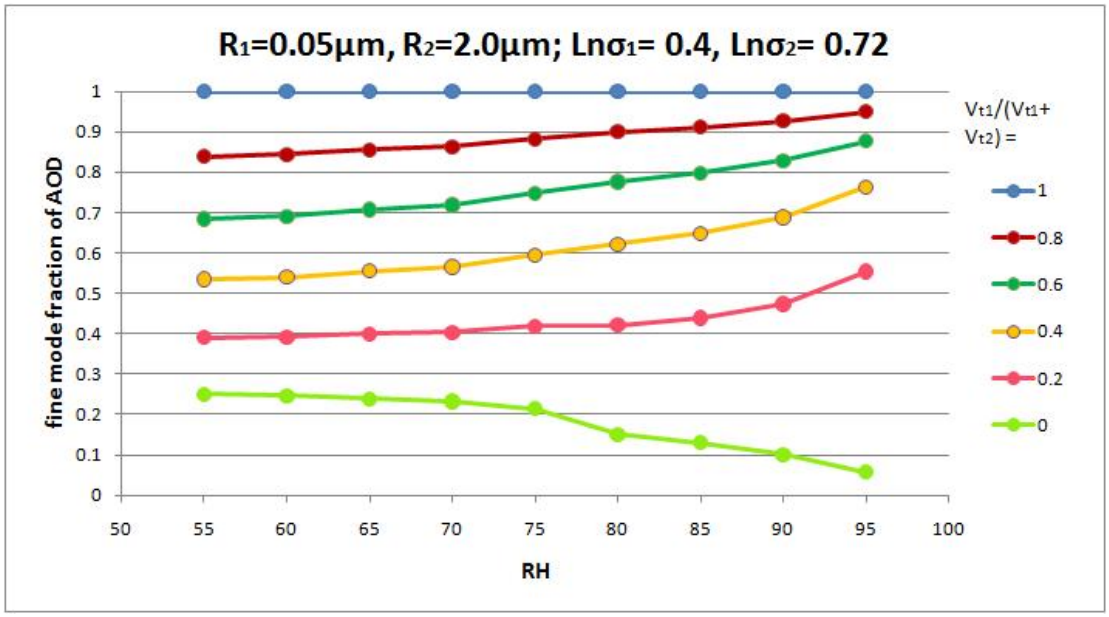

Figure A.9: Fine mode fraction of AOD (Type 1 aerosols) as a function of RH for dry size distributions specified by the parameters R_1=0.05, R_2=2.5μm, lnσ_1=0.4,lnσ_2=0.72,$V_{t1}/(V_{t1} + V_{t2})$=1, 0.8, 0.6, 0.4, 0.2, 0.0

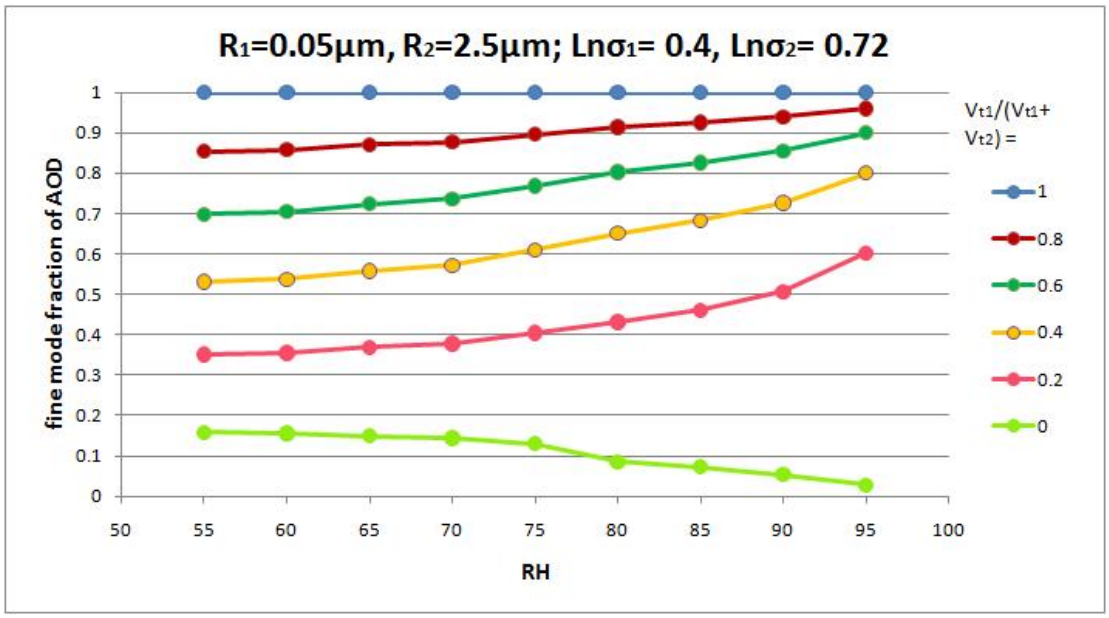

Figure A.10: Fine mode fraction of AOD (Type 1 aerosols) as a function of RH for dry size distributions specified by the parameters R_1=0.05μm, R_2=3μm, lnσ_1=0.4,lnσ_2=0.72,$V_{t1}/(V_{t1} + V_{t2})$=1, 0.8, 0.6, 0.4, 0.2, 0.0

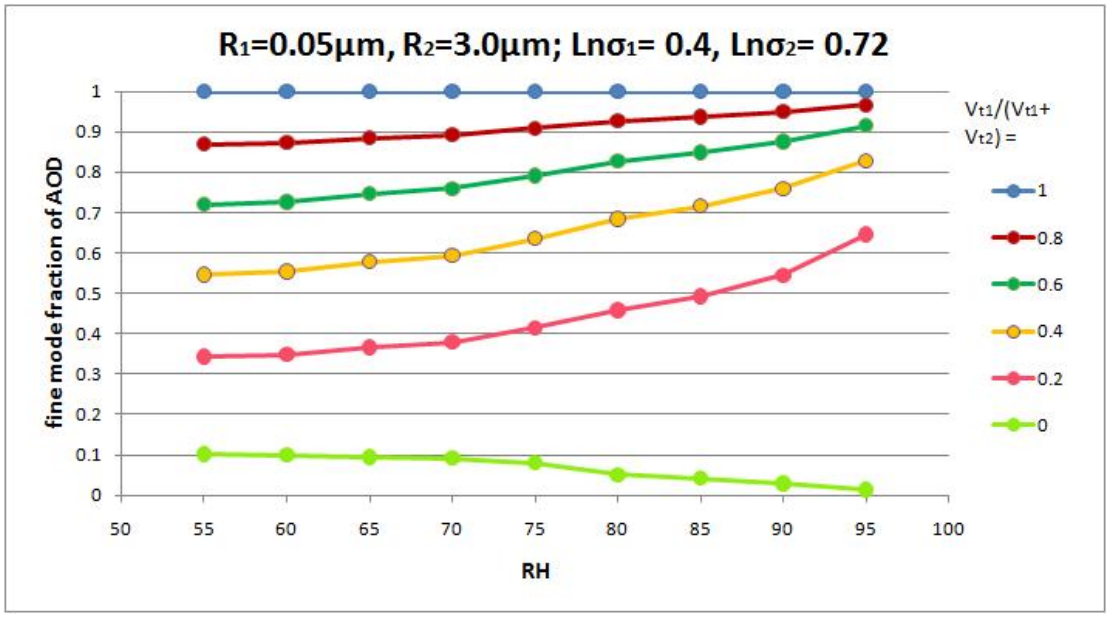

Figure A.11: Fine mode fraction of AOD (Type 1 aerosols) as a function of RH for dry size distributions specified by the parameters R_1=0.05μm, R_2=1.5μm, lnσ_1=0.2,lnσ_2=0.2,$V_{t1}/(V_{t1} + V_{t2})$=1, 0.8, 0.6, 0.4, 0.2, 0.0

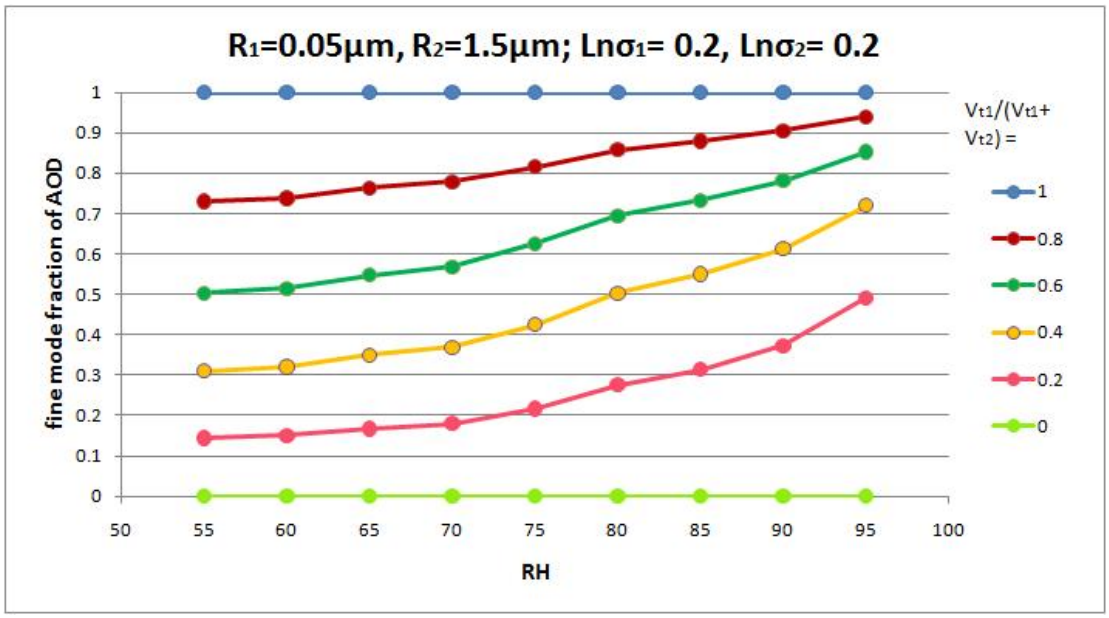

Figure A.12: Fine mode fraction of AOD (Type 1 aerosols) as a function of RH for dry size distributions specified by the parameters R_1=0.05μm, R_2=1.5μm, lnσ_1=0.2,lnσ_2=0.4,$V_{t1}/(V_{t1} + V_{t2})$=1, 0.8, 0.6, 0.4, 0.2, 0.0

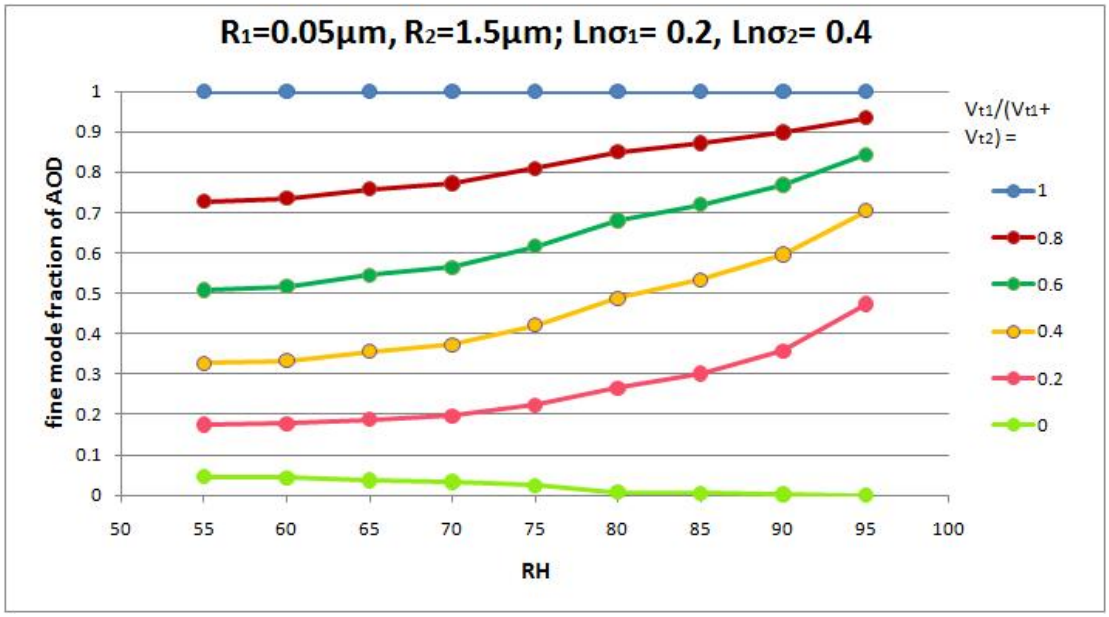

Figure A.13: Fine mode fraction of AOD (Type 1 aerosols) as a function of RH for dry size distributions specified by the parameters R_1=0.05μm, R_2=1.5μm, lnσ_1=0.2,lnσ_2=0.6,$V_{t1}/(V_{t1} + V_{t2})$=1, 0.8, 0.6, 0.4, 0.2, 0.0

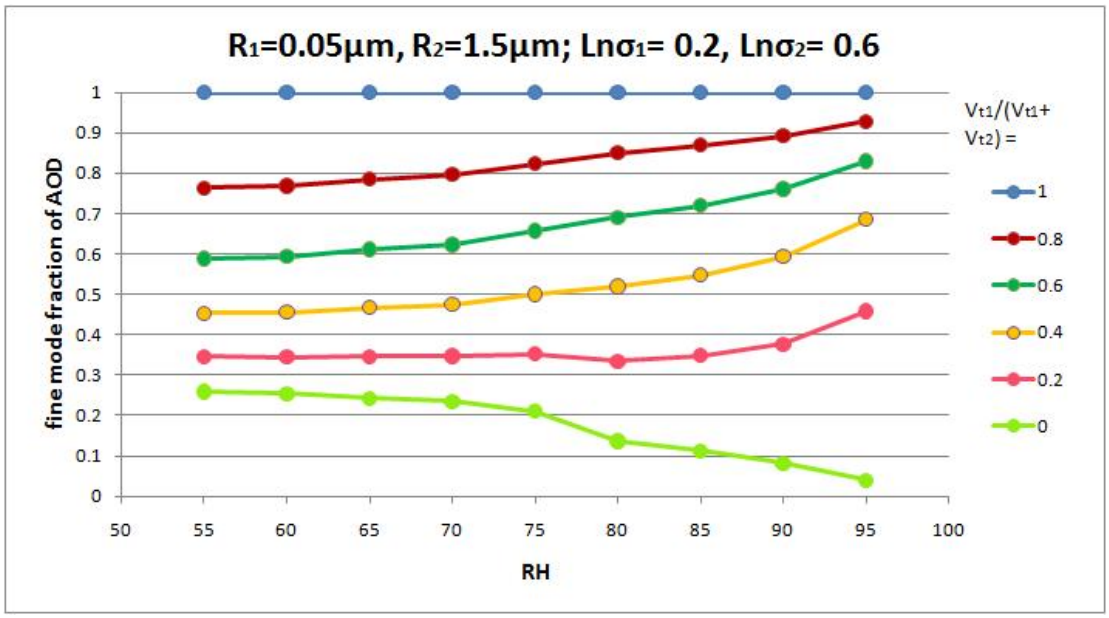

Figure A.14: Fine mode fraction of AOD (Type 1 aerosols) as a function of RH for dry size distributions specified by the parameters R_1=0.05μm, R_2=1.5μm, lnσ_1=0.2,lnσ_2=0.8,$V_{t1}/(V_{t1} + V_{t2})$=1, 0.8, 0.6, 0.4, 0.2, 0.0

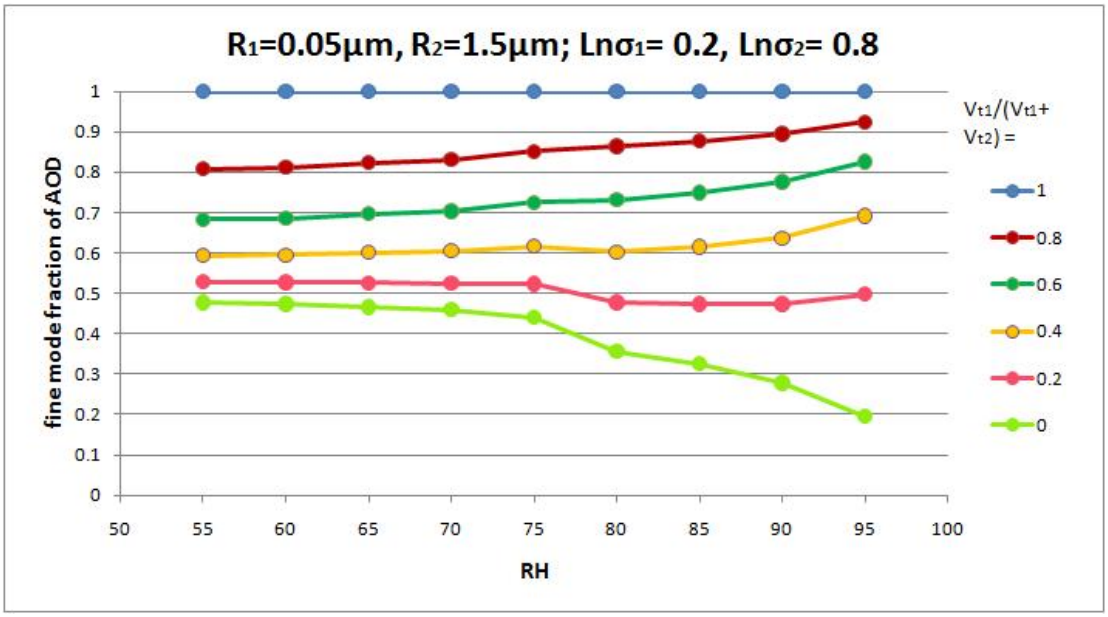

Figure A.15: Fine mode fraction of AOD (Type 1 aerosols) as a function of RH for dry size distributions specified by the parameters R_1=0.05μm, R_2=1.5μm, lnσ_1=0.4,lnσ_2=0.2,$V_{t1}/(V_{t1} + V_{t2})$=1, 0.8, 0.6, 0.4, 0.2, 0.0

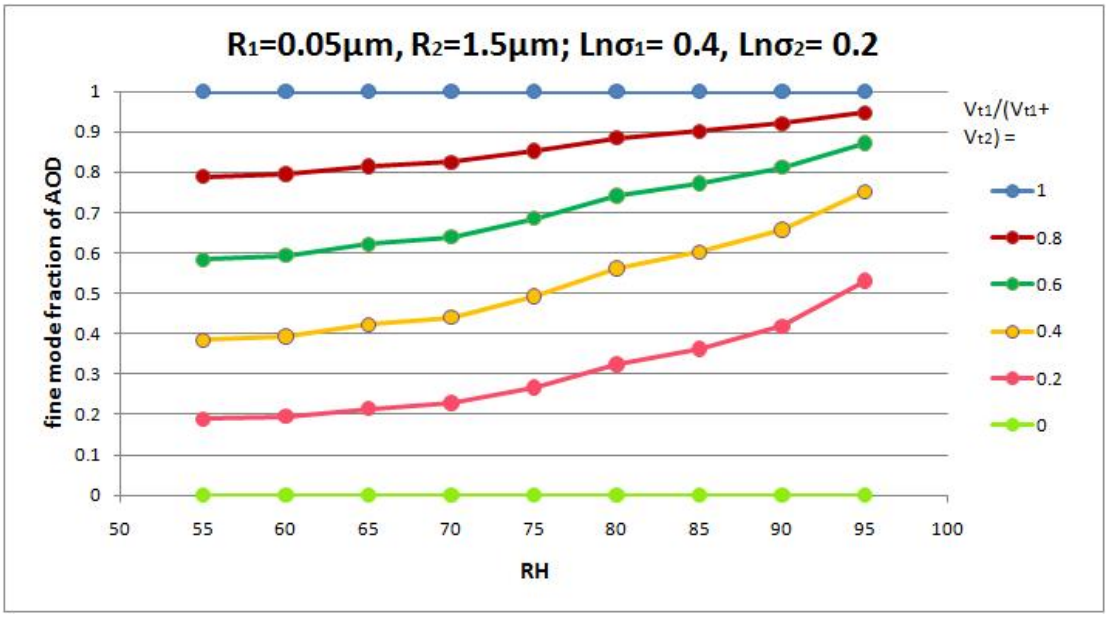

Figure A.16: Fine mode fraction of AOD (Type 1 aerosols) as a function of RH for dry size distributions specified by the parameters R_1=0.05μm, R_2=1.5μm, lnσ_1=0.4,lnσ_2=0.4,$V_{t1}/(V_{t1} + V_{t2})$=1, 0.8, 0.6, 0.4, 0.2, 0.0

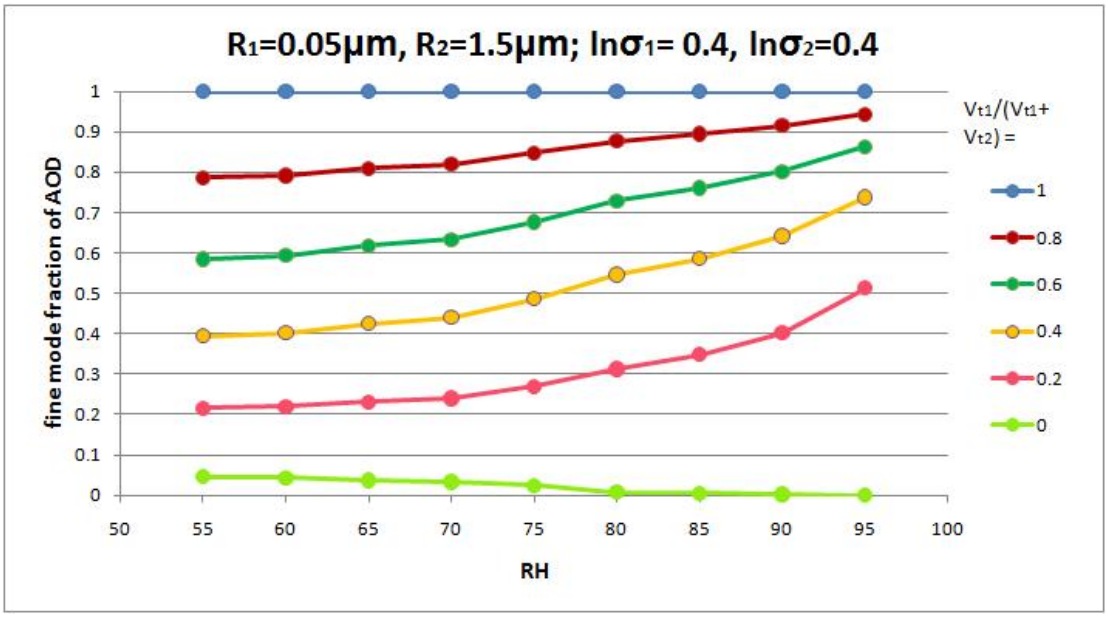

Figure A.17: Fine mode fraction of AOD (Type 1 aerosols) as a function of RH for dry size distributions specified by the parameters R_1=0.05μm, R_2=1.5μm, lnσ_1=0.4,lnσ_2=0.6,$V_{t1}/(V_{t1} + V_{t2})$=1, 0.8, 0.6, 0.4, 0.2, 0.0

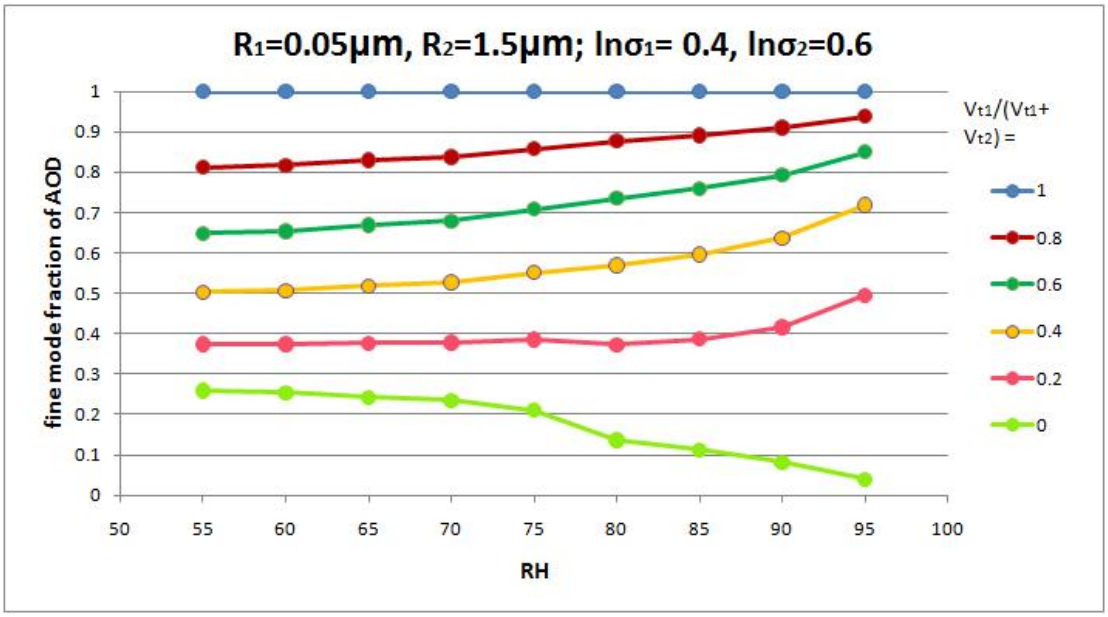

Figure A.18: Fine mode fraction of AOD (Type 1 aerosols) as a function of RH for dry size distributions specified by the parameters R_1=0.05μm, R_2=1.5μm, lnσ_1=0.4,lnσ_2=0.8,$V_{t1}/(V_{t1} + V_{t2})$=1, 0.8, 0.6, 0.4, 0.2, 0.0

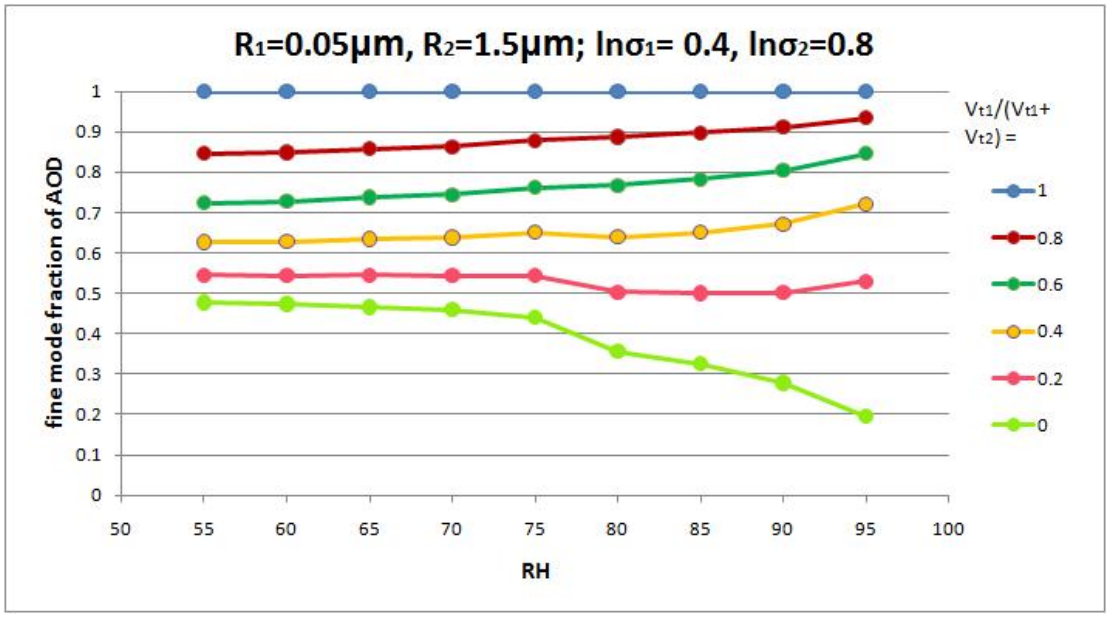

Figure A.19: Fine mode fraction of AOD (Type 1 aerosols) as a function of RH for dry size distributions specified by the parameters R_1=0.05μm, R_2=1.5μm, lnσ_1=0.6,lnσ_2=0.2,$V_{t1}/(V_{t1} + V_{t2})$=1, 0.8, 0.6, 0.4, 0.2, 0.0

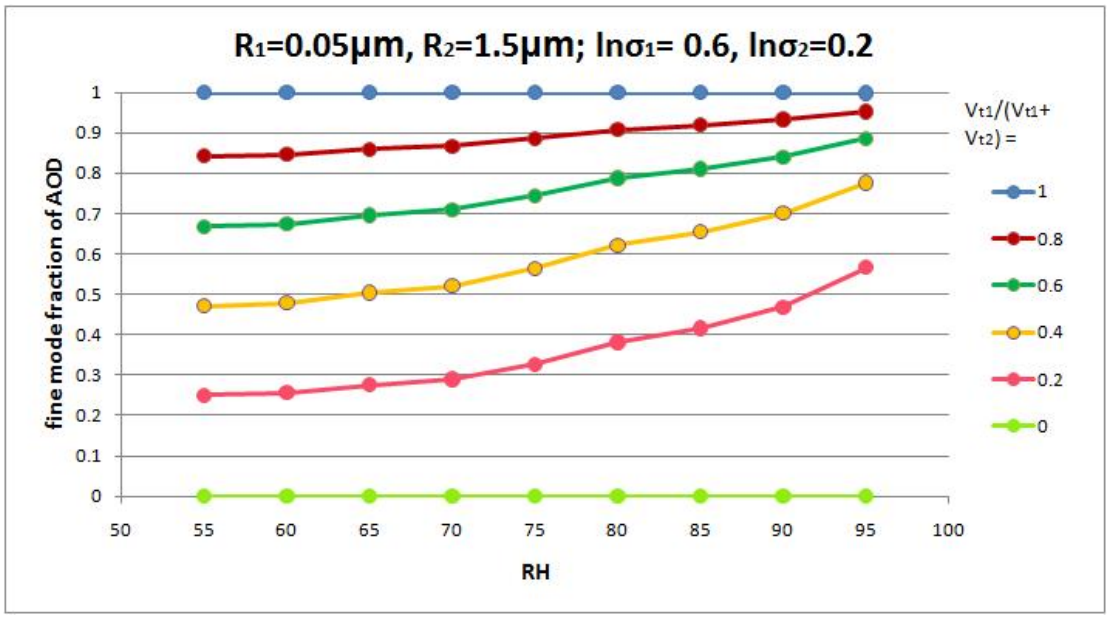

Figure A.20: Fine mode fraction of AOD (Type 1 aerosols) as a function of RH for dry size distributions specified by the parameters R_1=0.05μm, R_2=1.5μm, lnσ_1=0.6,lnσ_2=0.4,$V_{t1}/(V_{t1} + V_{t2})$=1, 0.8, 0.6, 0.4, 0.2, 0.0

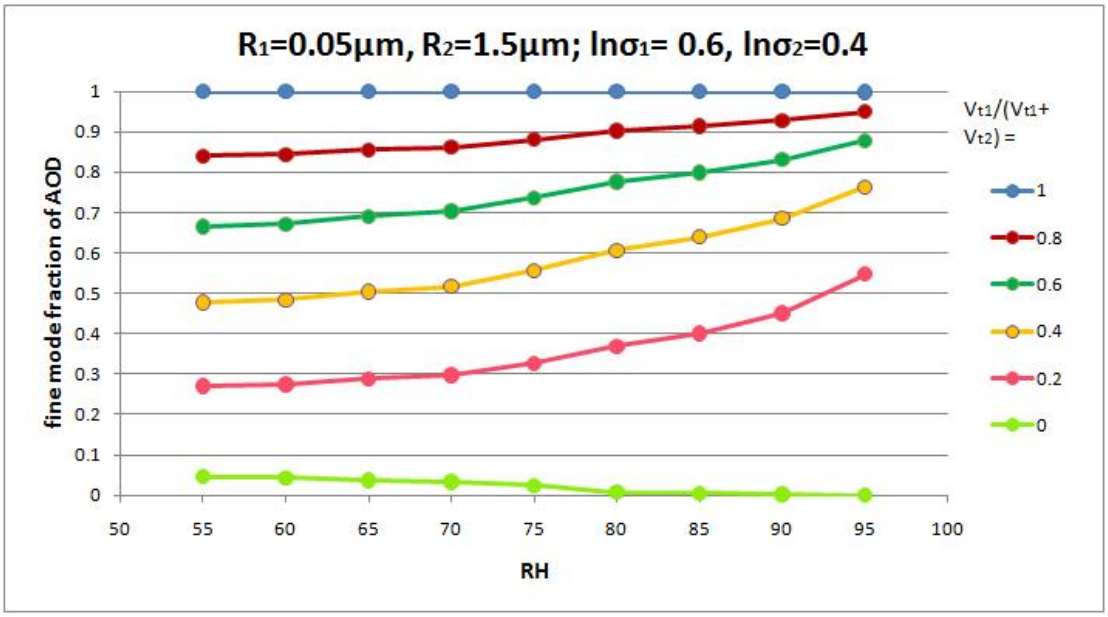

Figure A.21: Fine mode fraction of AOD (Type 1 aerosols) as a function of RH for dry size distributions specified by the parameters R_1=0.05μm, R_2=1.5μm, lnσ_1=0.6,lnσ_2=0.6,$V_{t1}/(V_{t1} + V_{t2})$=1, 0.8, 0.6, 0.4, 0.2, 0.0

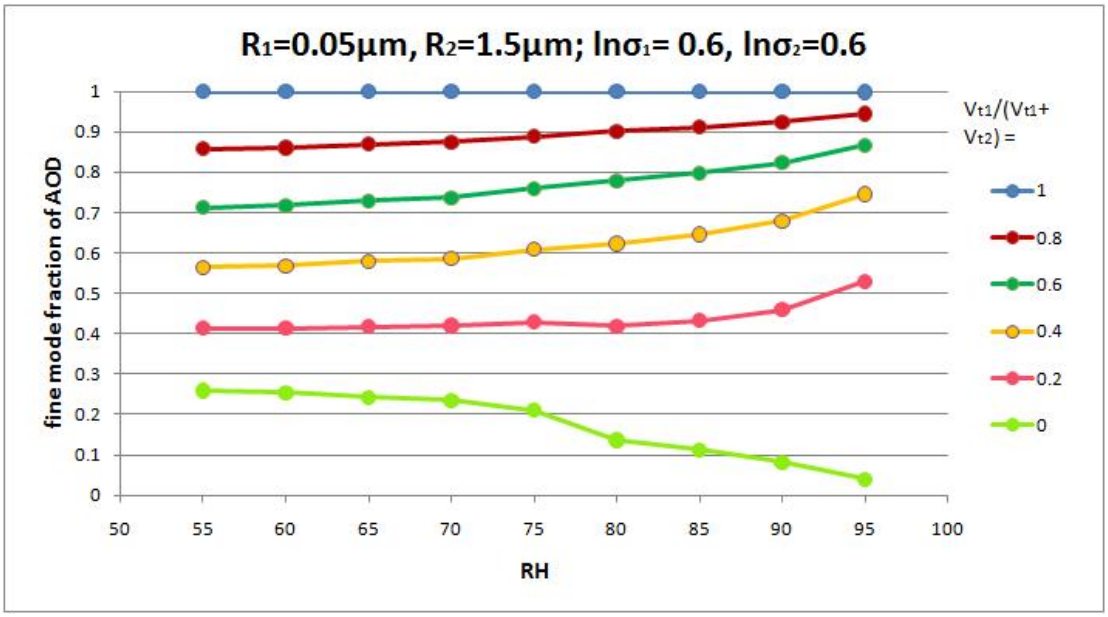

Figure A.22: Fine mode fraction of AOD (Type 1 aerosols) as a function of RH for dry size distributions specified by the parameters R_1=0.05μm, R_2=1.5μm, lnσ_1=0.6,lnσ_2=0.8,$V_{t1}/(V_{t1} + V_{t2})$=1, 0.8, 0.6, 0.4, 0.2, 0.0

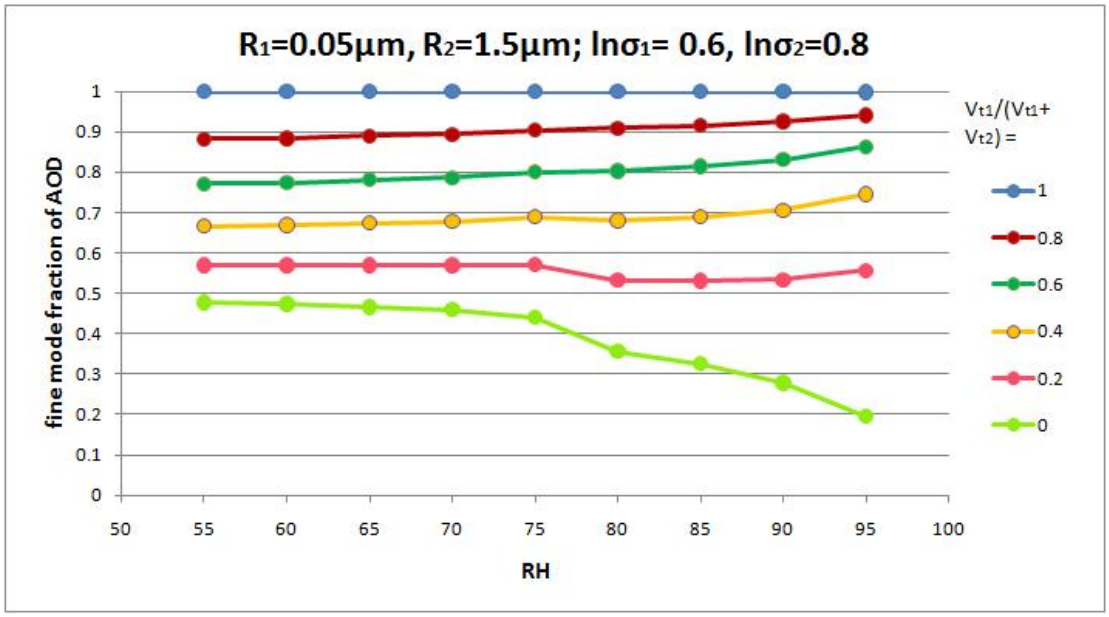

Figure A.23: Fine mode fraction of AOD (Type 1 aerosols) as a function of RH for dry size distributions specified by the parameters R_1=0.05μm, R_2=1.5μm, lnσ_1=0.8,lnσ_2=0.2,$V_{t1}/(V_{t1} + V_{t2})$=1, 0.8, 0.6, 0.4, 0.2, 0.0

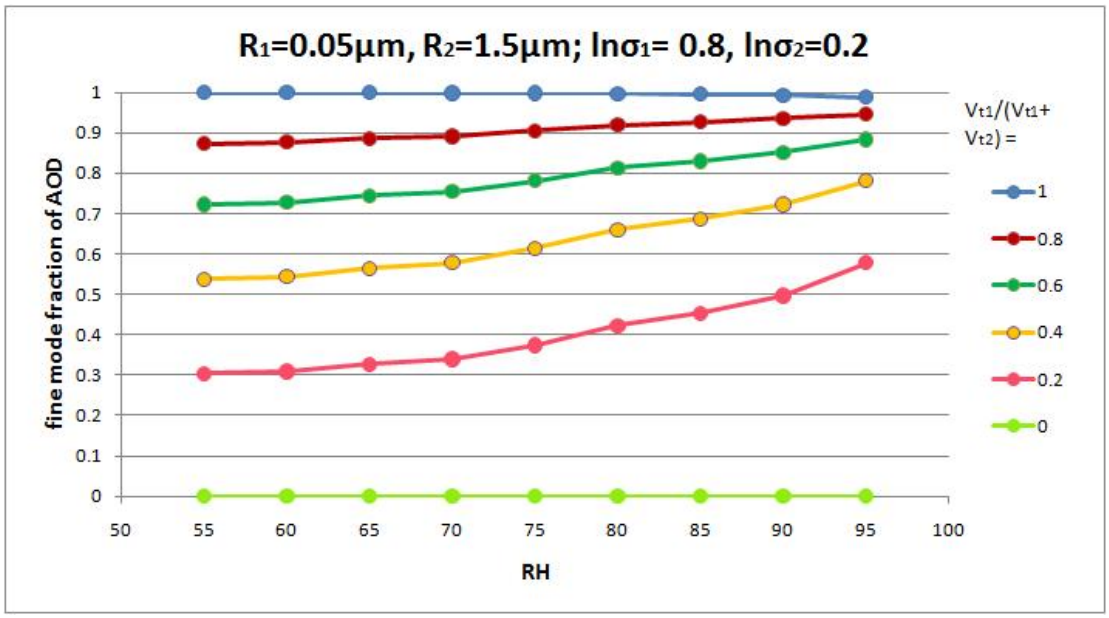

Figure A.24: Fine mode fraction of AOD (Type 1 aerosols) as a function of RH for dry size distributions specified by the parameters R_1=0.05μm, R_2=1.5μm, lnσ_1=0.8,lnσ_2=0.4,$V_{t1}/(V_{t1} + V_{t2})$=1, 0.8, 0.6, 0.4, 0.2, 0.0

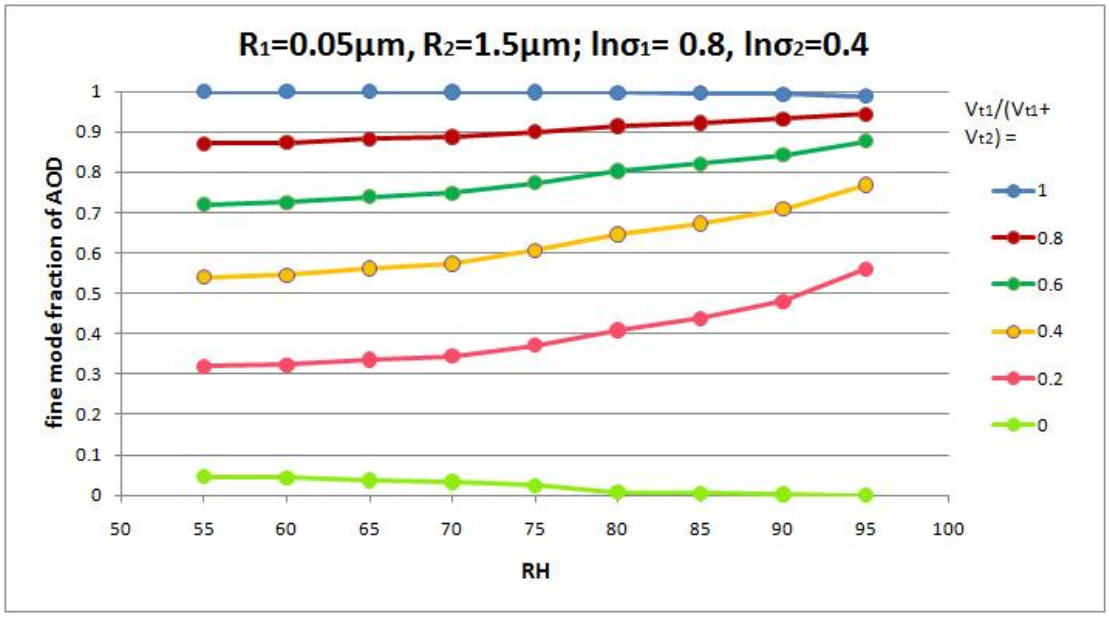

Figure A.25: Fine mode fraction of AOD (Type 1 aerosols) as a function of RH for dry size distributions specified by the parameters R_1=0.05μm, R_2=1.5μm, lnσ_1=0.8,lnσ_2=0.6,$V_{t1}/(V_{t1} + V_{t2})$=1, 0.8, 0.6, 0.4, 0.2, 0.0

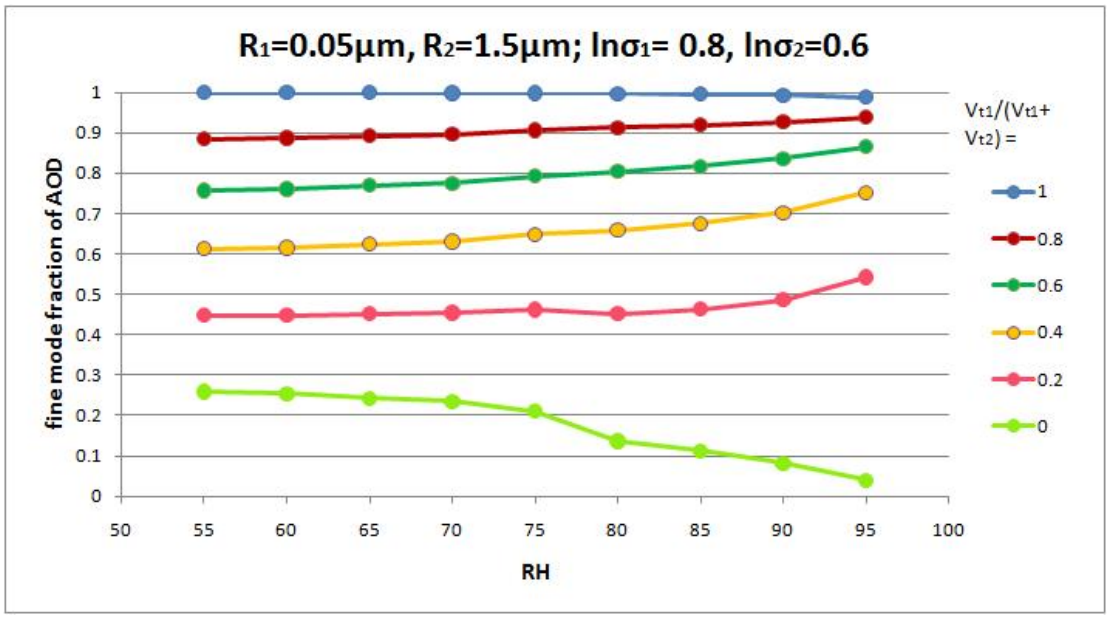

Figure A.26: Fine mode fraction of AOD (Type 1 aerosols) as a function of RH for dry size distributions specified by the parameters R_1=0.05μm, R_2=1.5μm, lnσ_1=0.8,lnσ_2=0.8,$V_{t1}/(V_{t1} + V_{t2})$=1, 0.8, 0.6, 0.4, 0.2, 0.0

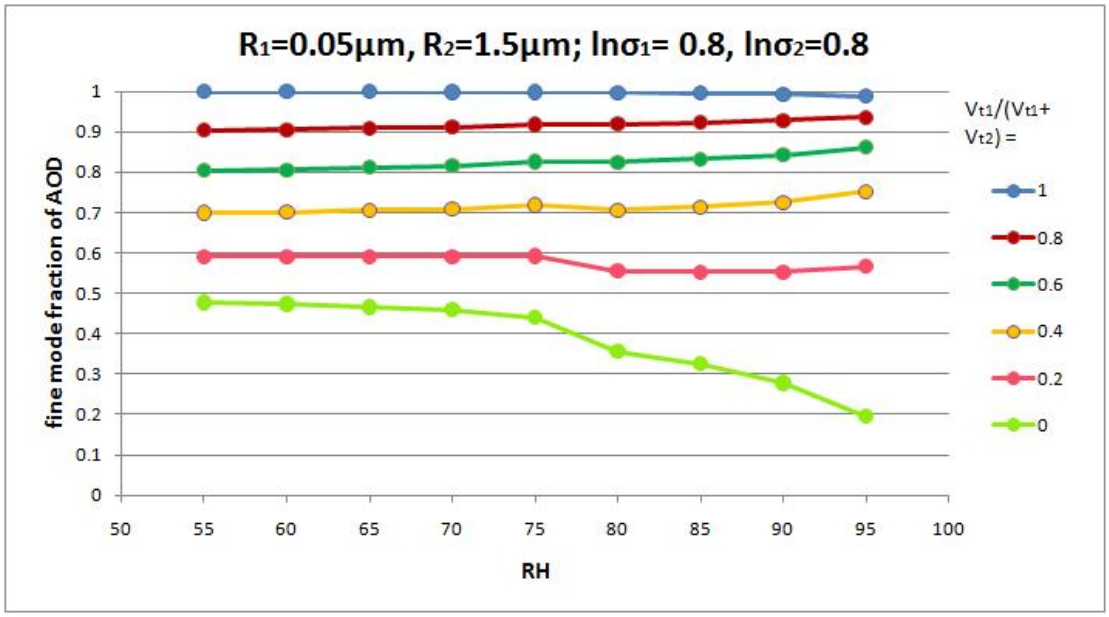

APPENDIX B

VARIATION IN FINE MODE FRACTION OF AOD AS A FUNCTION OF RELATIVE HUMIDITY FOR TYPE 2 AEROSOLS

This Appendix presents the variation in the fine mode fraction of AOD with increasing RH for the 156 different dry aerosol size distributions of composition Type2.

Figure B.1: Fine mode fraction of AOD (Type 2 aerosols) as a function of RH for dry size distributions specified by the parameters R_1=0.005μm, R_2=1μm, lnσ_1=0.4,lnσ_2=0.72,$V_{t1}/(V_{t1} + V_{t2})$=1, 0.8, 0.6, 0.4, 0.2, 0.0

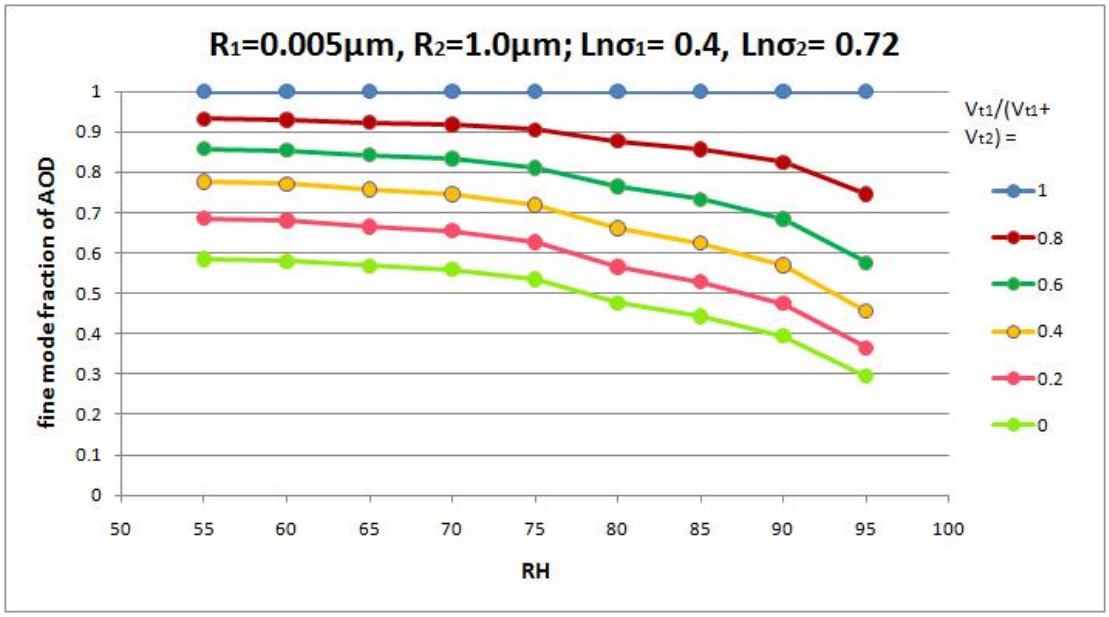

Figure B.2: Fine mode fraction of AOD (Type 2 aerosols) as a function of RH for dry size distributions specified by the parameters R_1=0.005μm, R_2=1.5μm, lnσ_1=0.4,lnσ_2=0.72,$V_{t1}/(V_{t1} + V_{t2})$=1, 0.8, 0.6, 0.4, 0.2, 0.0

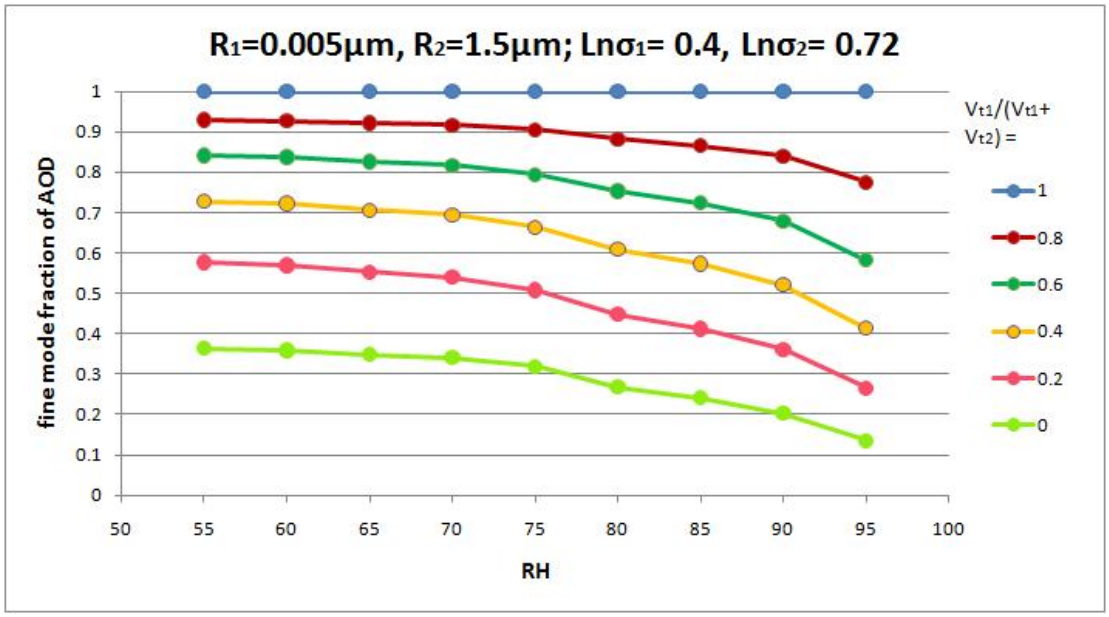

Figure B.3: Fine mode fraction of AOD (Type 2 aerosols) as a function of RH for dry size distributions specified by the parameters R_1=0.005μm, R_2=2.0μm, lnσ_1=0.4,lnσ_2=0.72,$V_{t1}/(V_{t1} + V_{t2})$=1, 0.8, 0.6, 0.4, 0.2, 0.0

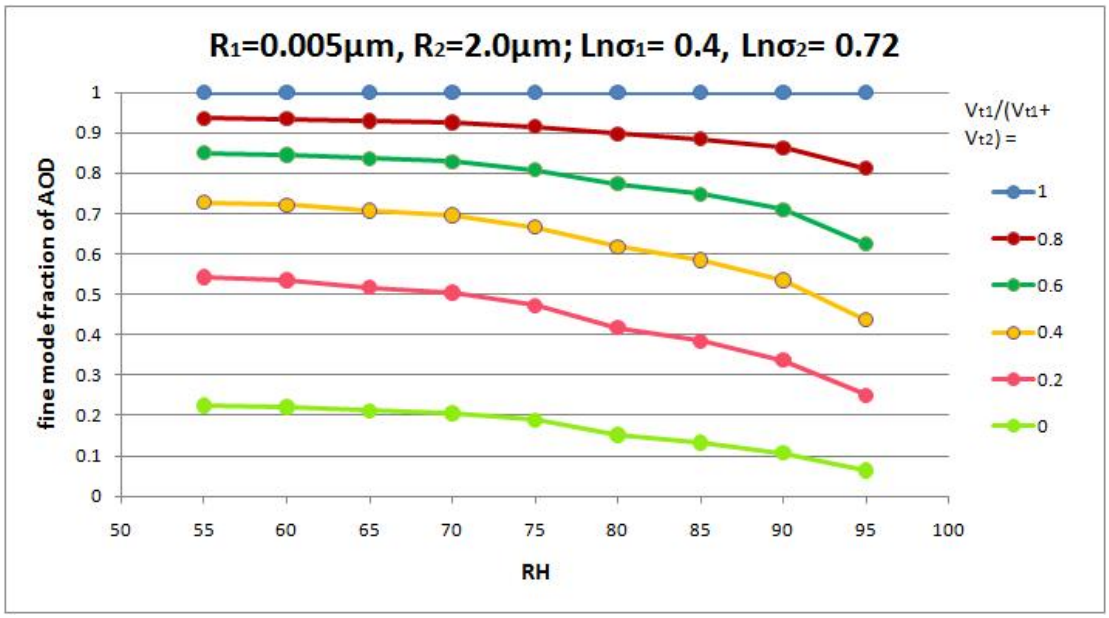

Figure B.4: Fine mode fraction of AOD (Type 2 aerosols) as a function of RH for dry size distributions specified by the parameters R_1=0.005μm, R_2=2.5μm, lnσ_1=0.4,lnσ_2=0.72,$V_{t1}/(V_{t1} + V_{t2})$=1, 0.8, 0.6, 0.4, 0.2, 0.0

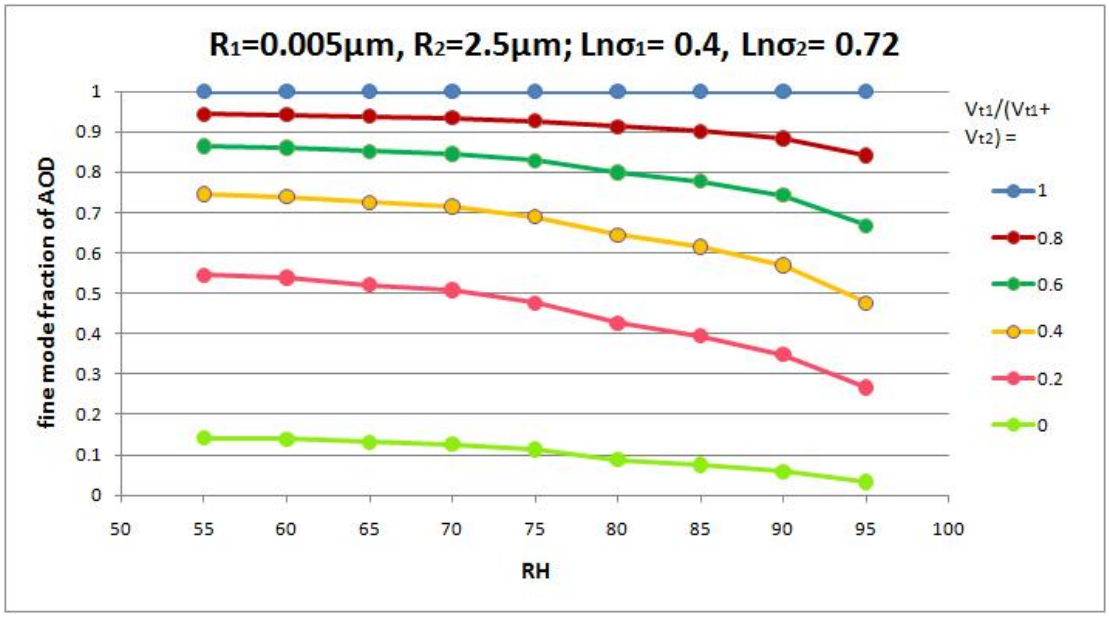

Figure B.5: Fine mode fraction of AOD (Type 2 aerosols) as a function of RH for dry size distributions specified by the parameters R_1=0.005μm, R_2=3.0μm, lnσ_1=0.4,lnσ_2=0.72,$V_{t1}/(V_{t1} + V_{t2})$=1, 0.8, 0.6, 0.4, 0.2, 0.0

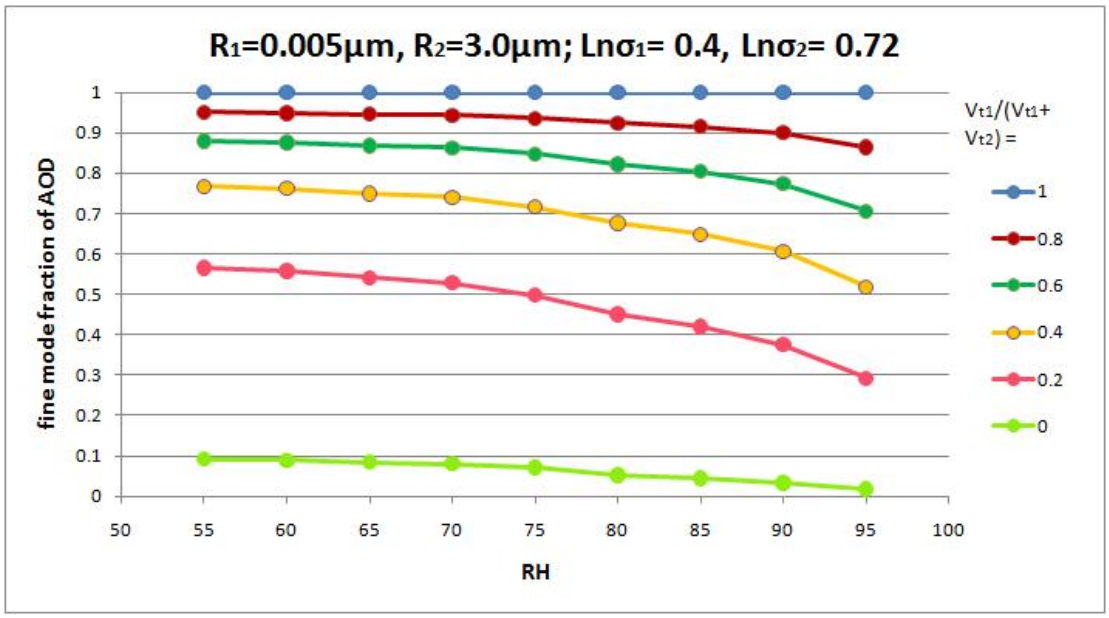

Figure B.6: Fine mode fraction of AOD (Type 2 aerosols) as a function of RH for dry size distributions specified by the parameters R_1=0.05μm, R_2=1.0μm, lnσ_1=0.4,lnσ_2=0.72,$V_{t1}/(V_{t1} + V_{t2})$=1, 0.8, 0.6, 0.4, 0.2, 0.0

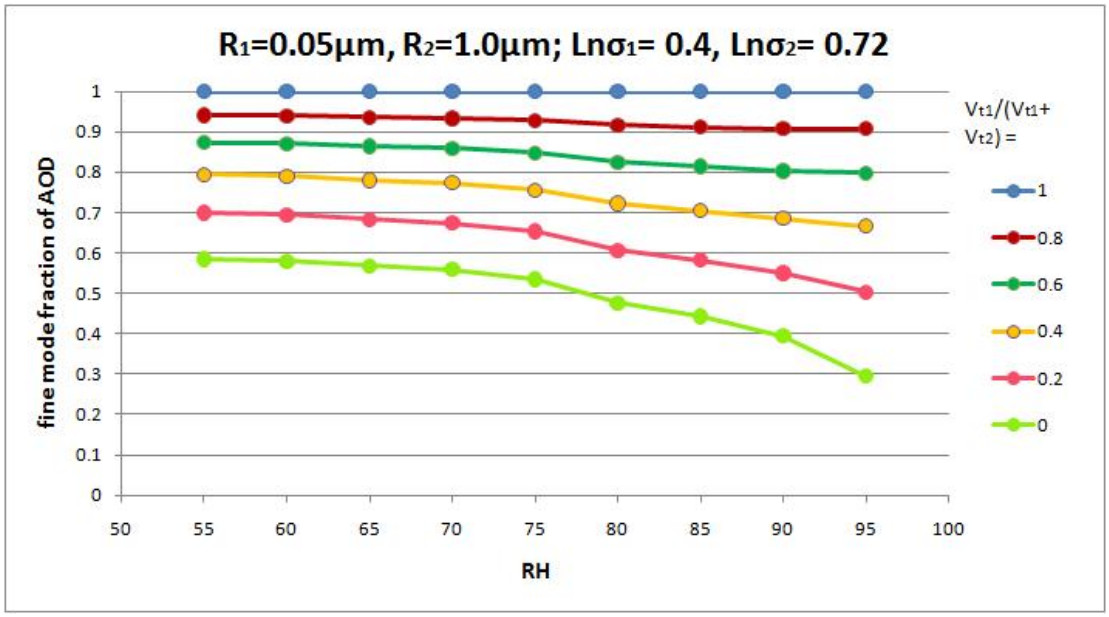

Figure B.7: Fine mode fraction of AOD (Type 2 aerosols) as a function of RH for dry size distributions specified by the parameters R_1=0.05μm, R_2=1.5μm, lnσ_1=0.4,lnσ_2=0.72,$V_{t1}/(V_{t1} + V_{t2})$=1, 0.8, 0.6, 0.4, 0.2, 0.0

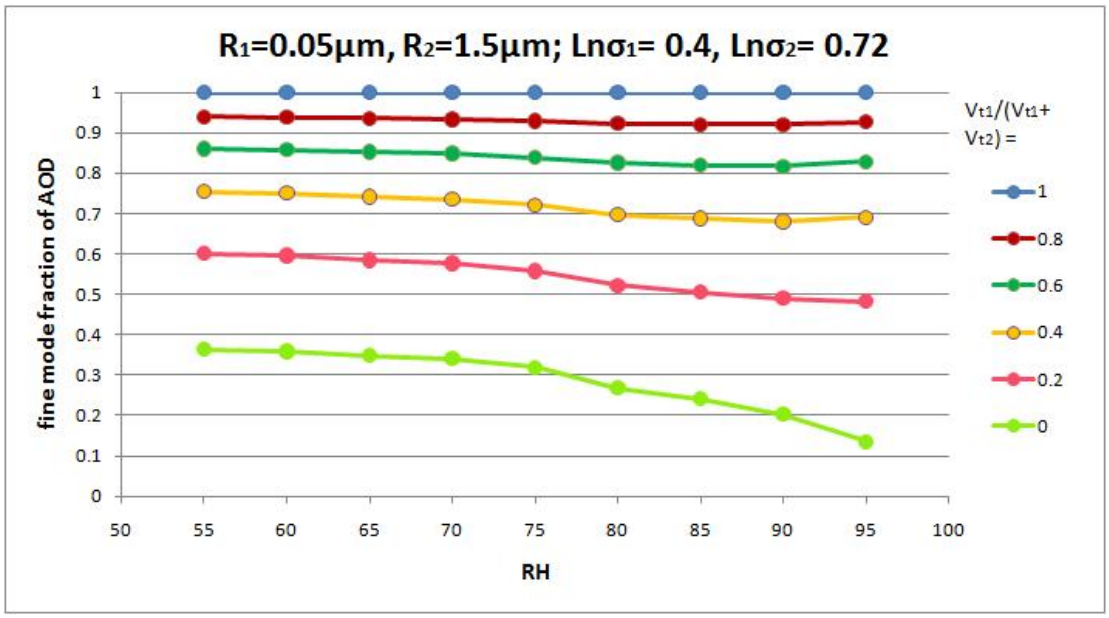

Figure B.8: Fine mode fraction of AOD (Type 2 aerosols) as a function of RH for dry size distributions specified by the parameters R_1=0.05μm, R_2=2.0μm, lnσ_1=0.4,lnσ_2=0.72,$V_{t1}/(V_{t1} + V_{t2})$=1, 0.8, 0.6, 0.4, 0.2, 0.0

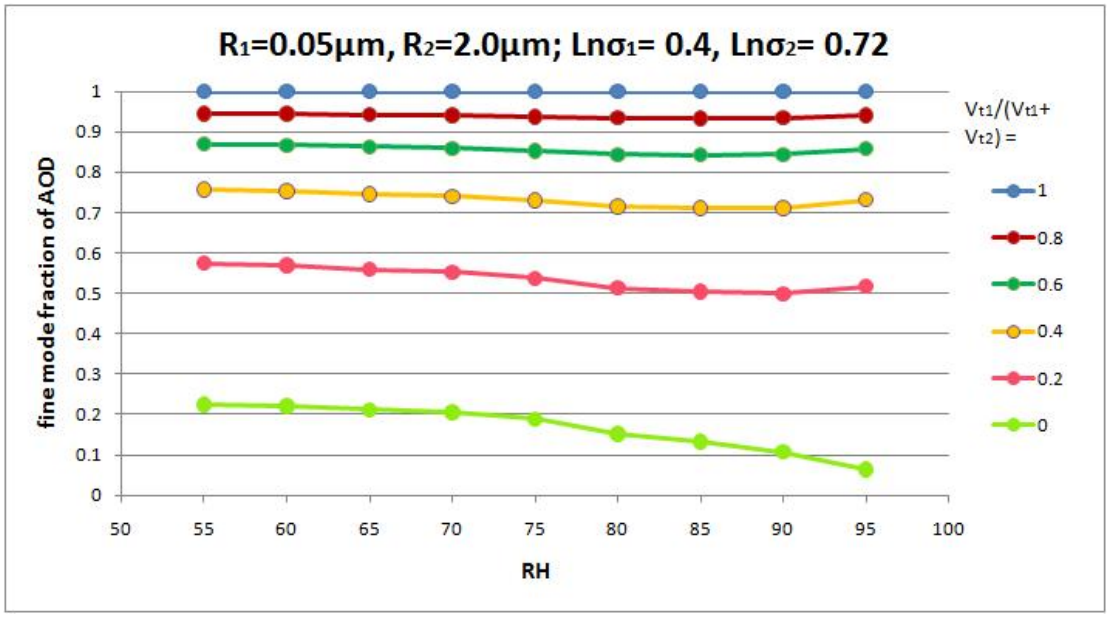

Figure B.9: Fine mode fraction of AOD (Type 2 aerosols) as a function of RH for dry size distributions specified by the parameters R_1=0.05μm, R_2=2.5μm, lnσ_1=0.4,lnσ_2=0.72,$V_{t1}/(V_{t1} + V_{t2})$=1, 0.8, 0.6, 0.4, 0.2, 0.0

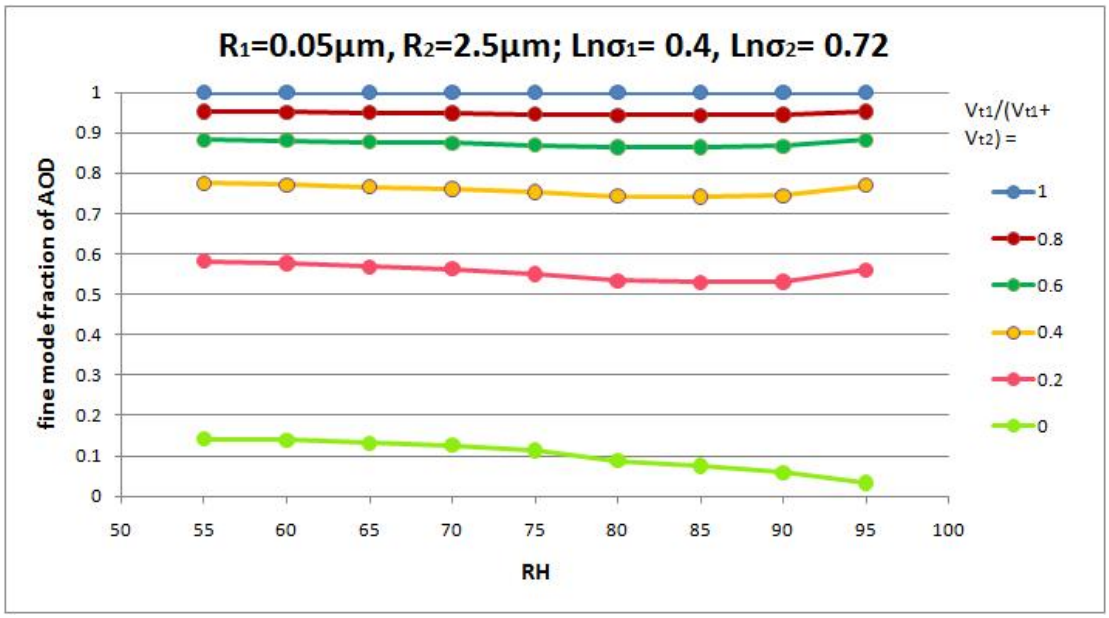

Figure B.10: Fine mode fraction of AOD (Type 2 aerosols) as a function of RH for dry size distributions specified by the parameters R_1=0.05μm, R_2=3.0μm, lnσ_1=0.4,lnσ_2=0.72,$V_{t1}/(V_{t1} + V_{t2})$=1, 0.8, 0.6, 0.4, 0.2, 0.0

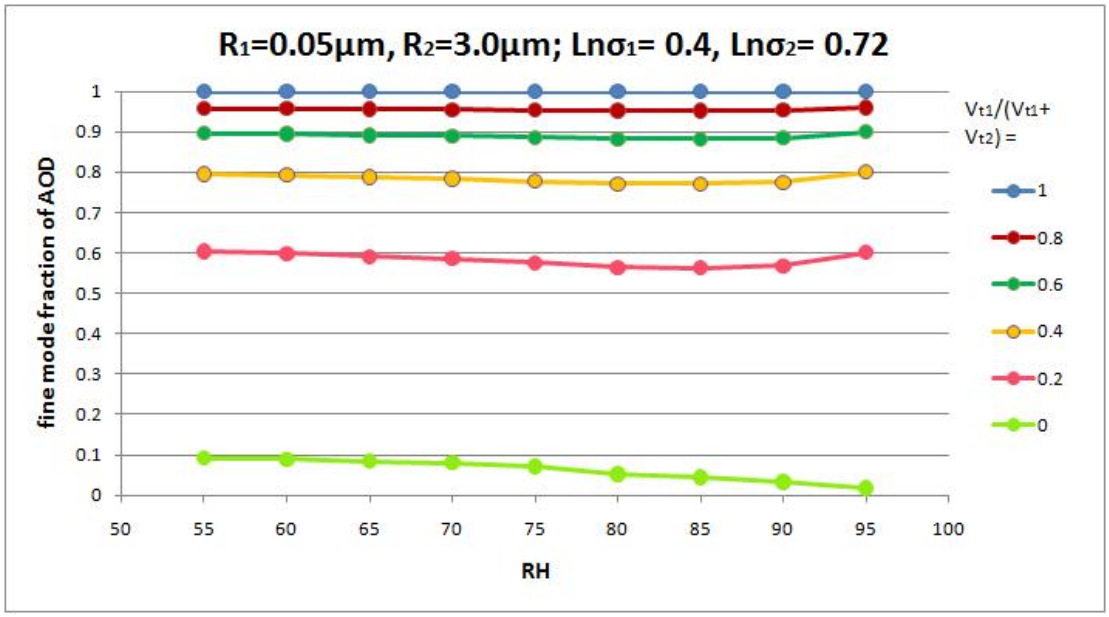

Figure B.11: Fine mode fraction of AOD (Type 2 aerosols) as a function of RH for dry size distributions specified by the parameters R_1=0.05μm, R_2=1.5μm, lnσ_1=0.2,lnσ_2=0.2,$V_{t1}/(V_{t1} + V_{t2})$=1, 0.8, 0.6, 0.4, 0.2, 0.0

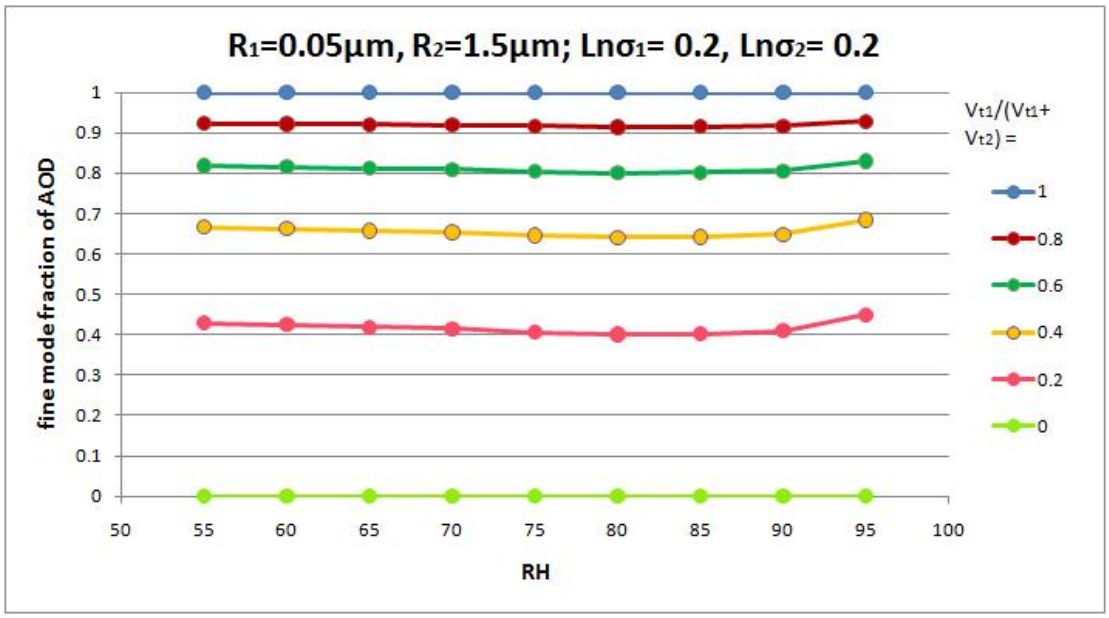

Figure B.12: Fine mode fraction of AOD (Type 2 aerosols) as a function of RH for dry size distributions specified by the parameters R_1=0.05μm, R_2=1.5μm, lnσ_1=0.2,lnσ_2=0.4,$V_{t1}/(V_{t1} + V_{t2})$=1, 0.8, 0.6, 0.4, 0.2, 0.0

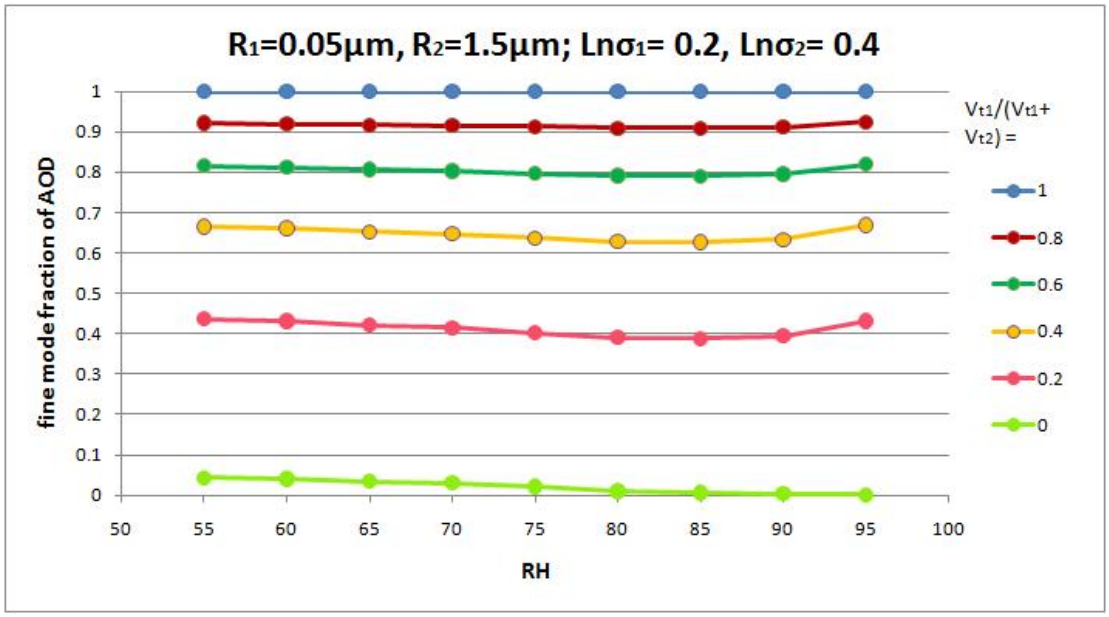

Figure B.13: Fine mode fraction of AOD (Type 2 aerosols) as a function of RH for dry size distributions specified by the parameters R_1=0.05μm, R_2=1.5μm, lnσ_1=0.2,lnσ_2=0.6,$V_{t1}/(V_{t1} + V_{t2})$=1, 0.8, 0.6, 0.4, 0.2, 0.0

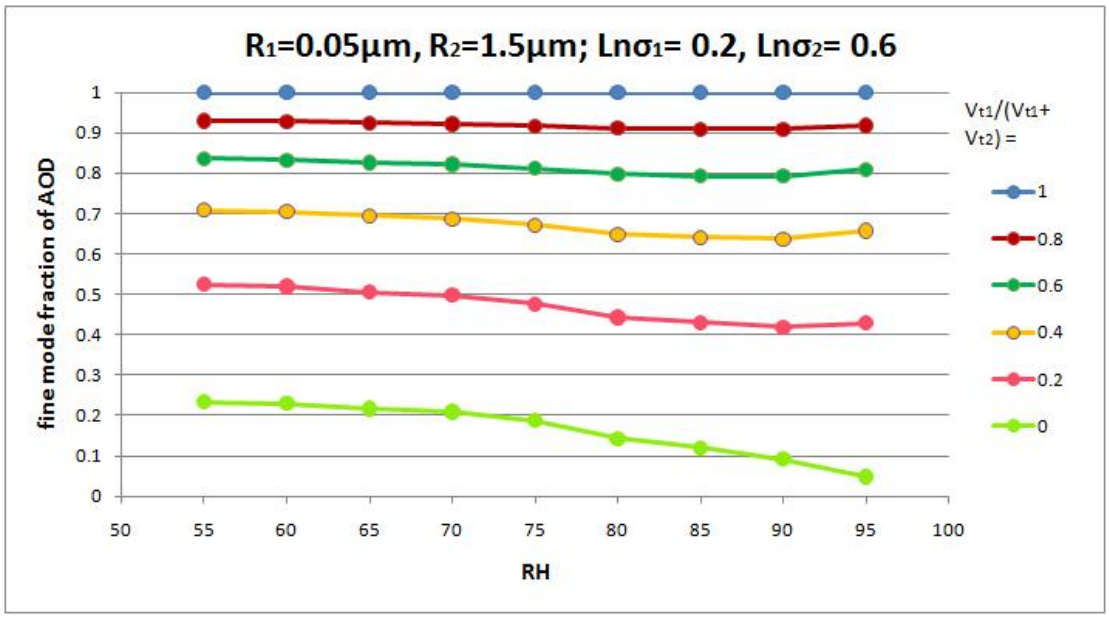

Figure B.14: Fine mode fraction of AOD (Type 2 aerosols) as a function of RH for dry size distributions specified by the parameters R_1=0.05μm, R_2=1.5μm, lnσ_1=0.2,lnσ_2=0.8,$V_{t1}/(V_{t1} + V_{t2})$=1, 0.8, 0.6, 0.4, 0.2, 0.0

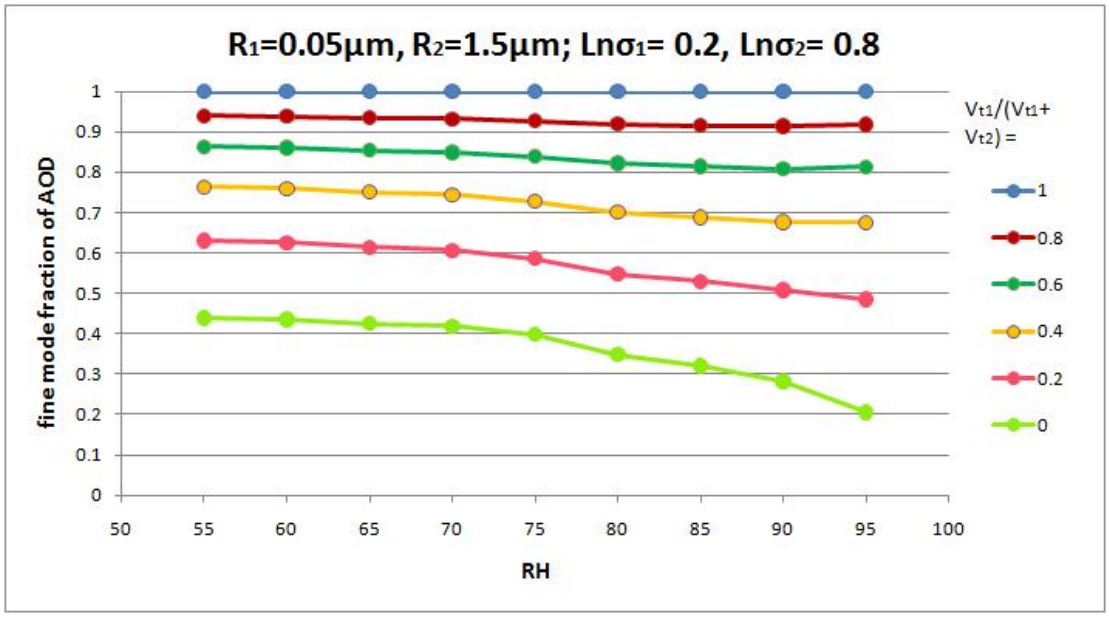

Figure B.15: Fine mode fraction of AOD (Type 2 aerosols) as a function of RH for dry size distributions specified by the parameters R_1=0.05μm, R_2=1.5μm, lnσ_1=0.4,lnσ_2=0.2,$V_{t1}/(V_{t1} + V_{t2})$=1, 0.8, 0.6, 0.4, 0.2, 0.0

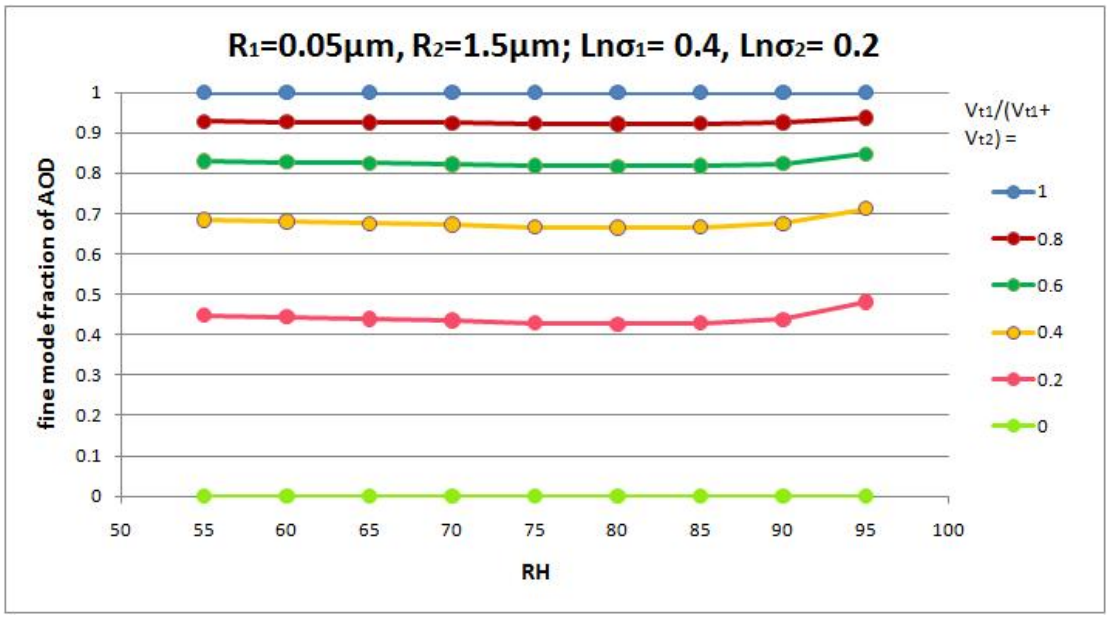

Figure B.16: Fine mode fraction of AOD (Type 2 aerosols) as a function of RH for dry size distributions specified by the parameters R_1=0.05μm, R_2=1.5μm, lnσ_1=0.4,lnσ_2=0.4,$V_{t1}/(V_{t1} + V_{t2})$=1, 0.8, 0.6, 0.4, 0.2, 0.0

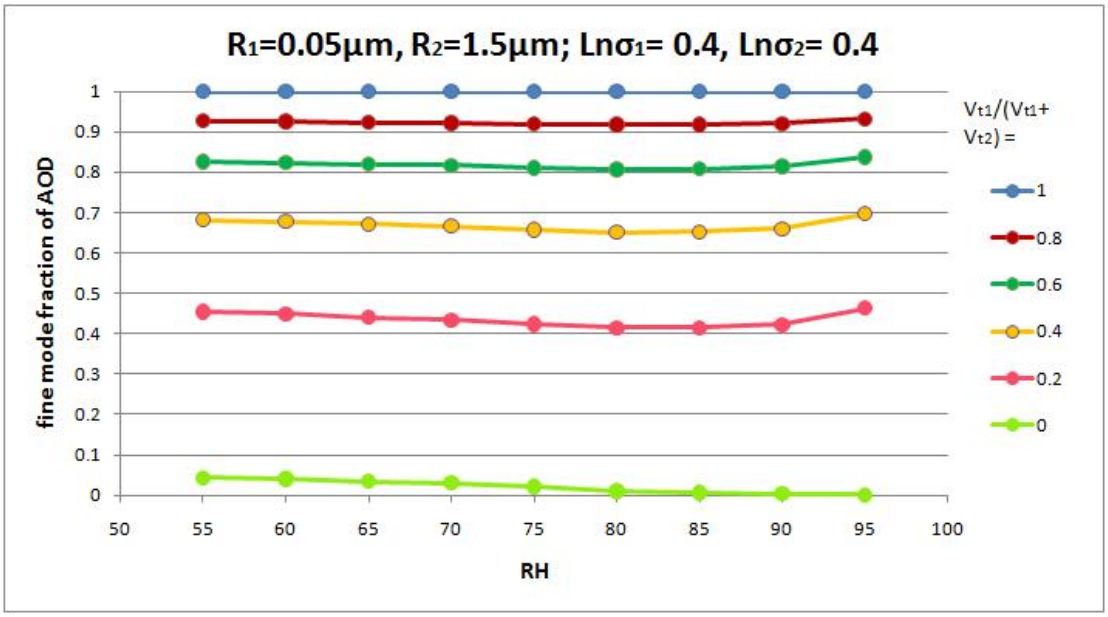

Figure B.17: Fine mode fraction of AOD (Type 2 aerosols) as a function of RH for dry size distributions specified by the parameters R_1=0.05μm, R_2=1.5μm, lnσ_1=0.4,lnσ_2=0.6,$V_{t1}/(V_{t1} + V_{t2})$=1, 0.8, 0.6, 0.4, 0.2, 0.0

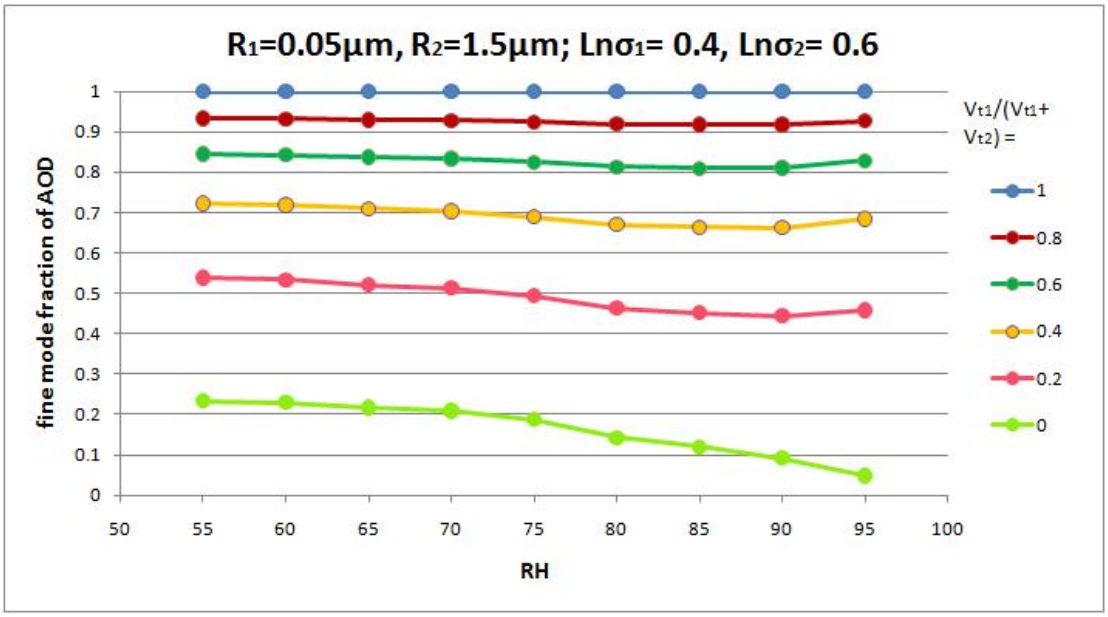

Figure B.18: Fine mode fraction of AOD (Type 2 aerosols) as a function of RH for dry size distributions specified by the parameters R_1=0.05μm, R_2=1.5μm, lnσ_1=0.4,lnσ_2=0.8,$V_{t1}/(V_{t1} + V_{t2})$=1, 0.8, 0.6, 0.4, 0.2, 0.0

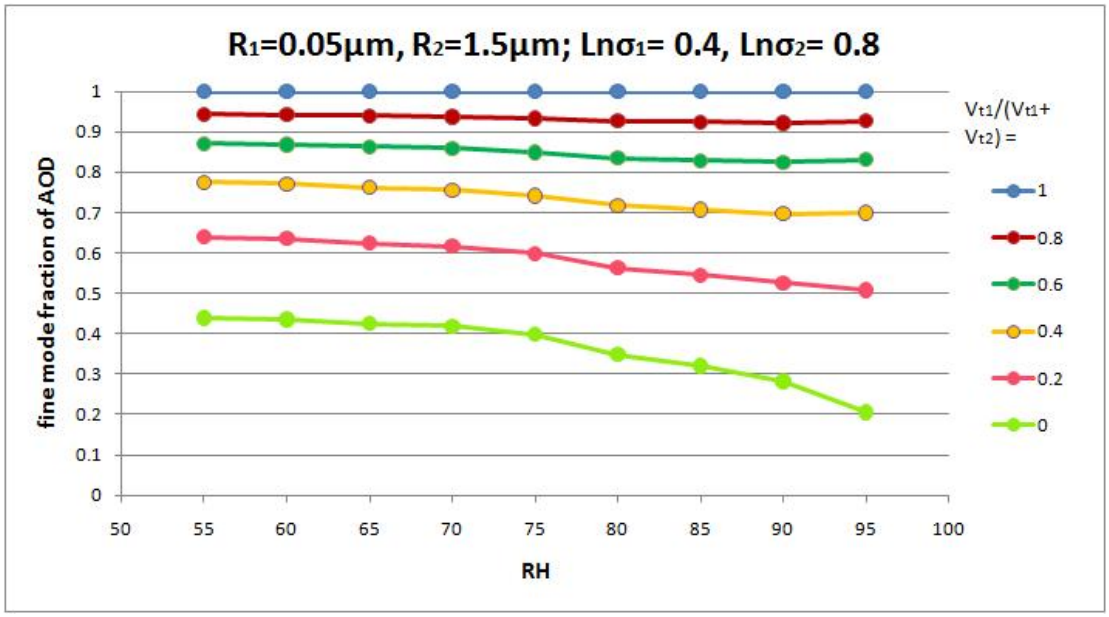

Figure B.19: Fine mode fraction of AOD (Type 2 aerosols) as a function of RH for dry size distributions specified by the parameters R_1=0.05μm, R_2=1.5μm, lnσ_1=0.6,lnσ_2=0.2,$V_{t1}/(V_{t1} + V_{t2})$=1, 0.8, 0.6, 0.4, 0.2, 0.0

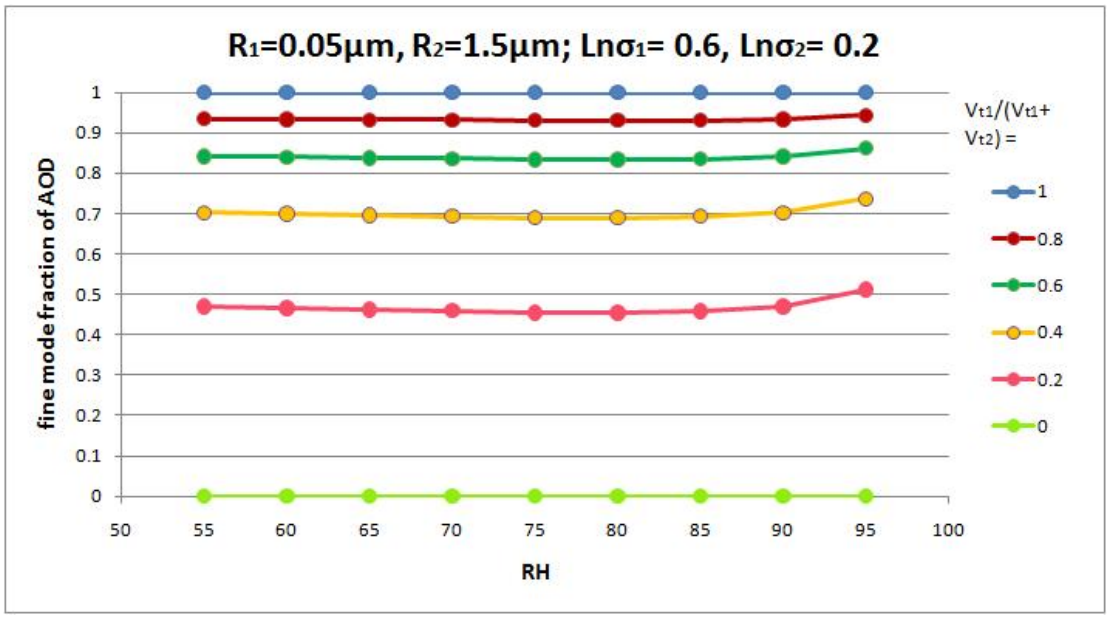

Figure B.20: Fine mode fraction of AOD (Type 2 aerosols) as a function of RH for dry size distributions specified by the parameters R_1=0.05μm, R_2=1.5μm, lnσ_1=0.6,lnσ_2=0.4,$V_{t1}/(V_{t1} + V_{t2})$=1, 0.8, 0.6, 0.4, 0.2, 0.0

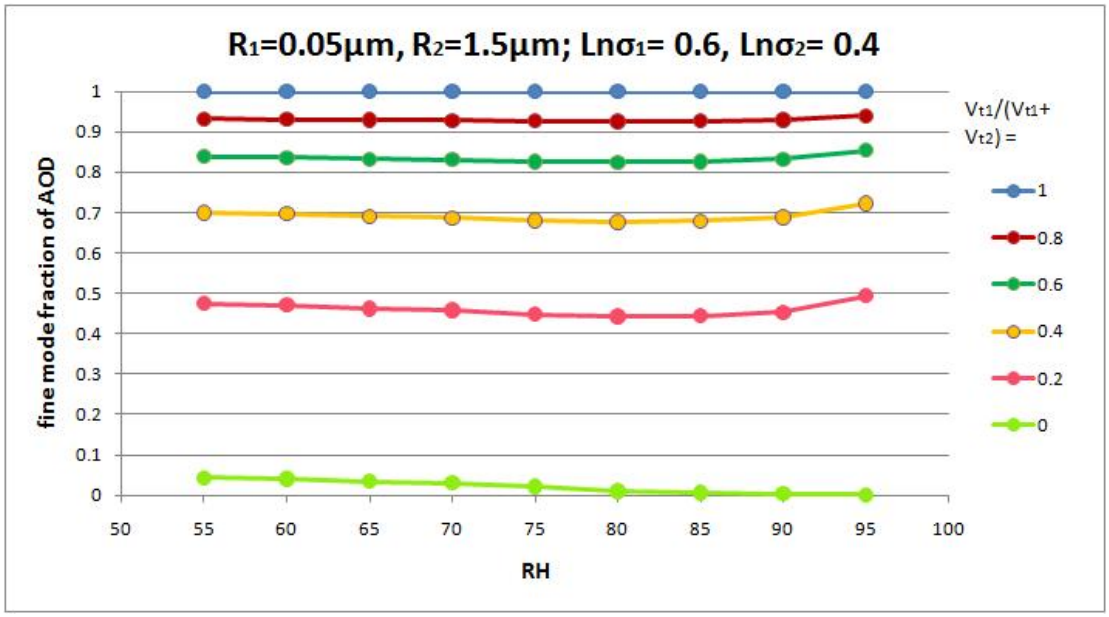

Figure B.21: Fine mode fraction of AOD (Type 2 aerosols) as a function of RH for dry size distributions specified by the parameters R_1=0.05μm, R_2=1.5μm, lnσ_1=0.6,lnσ_2=0.6,$V_{t1}/(V_{t1} + V_{t2})$=1, 0.8, 0.6, 0.4, 0.2, 0.0

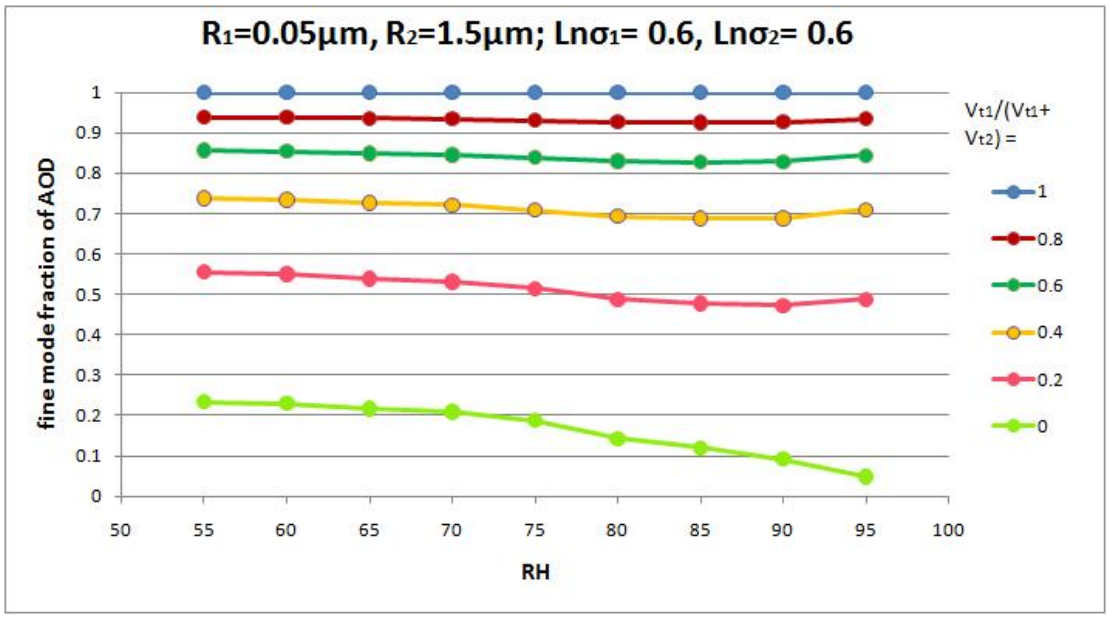

Figure B.22: Fine mode fraction of AOD (Type 2 aerosols) as a function of RH for dry size distributions specified by the parameters R_1=0.05μm, R_2=1.5μm, lnσ_1=0.6,lnσ_2=0.8,$V_{t1}/(V_{t1} + V_{t2})$=1, 0.8, 0.6, 0.4, 0.2, 0.0

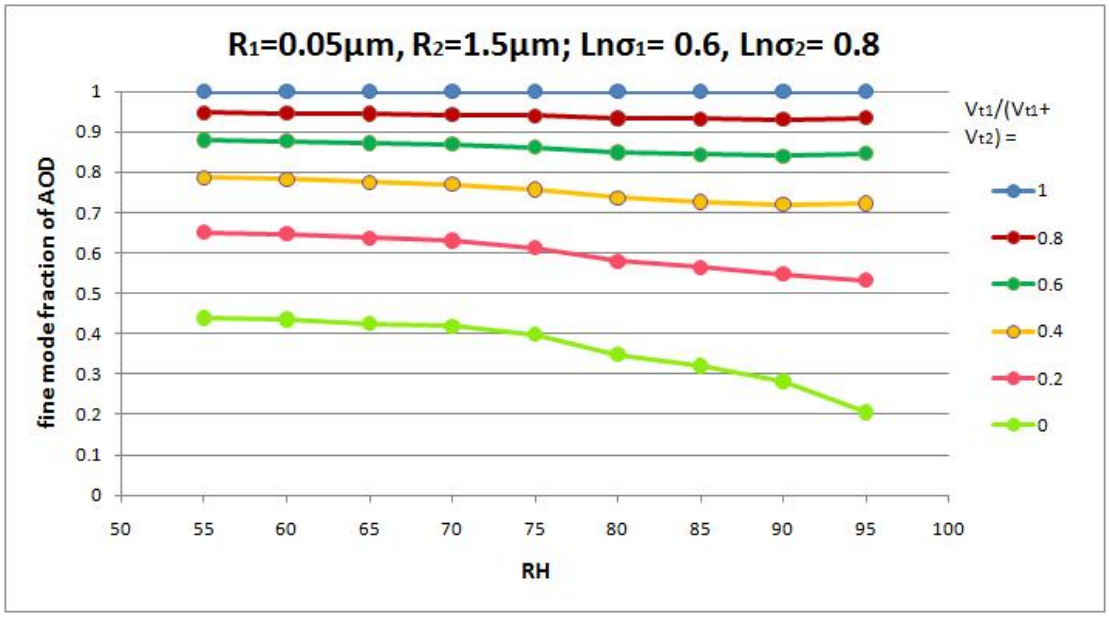

Figure B.23: Fine mode fraction of AOD (Type 2 aerosols) as a function of RH for dry size distributions specified by the parameters R_1=0.05μm, R_2=1.5μm, lnσ_1=0.8,lnσ_2=0.2,$V_{t1}/(V_{t1} + V_{t2})$=1, 0.8, 0.6, 0.4, 0.2, 0.0

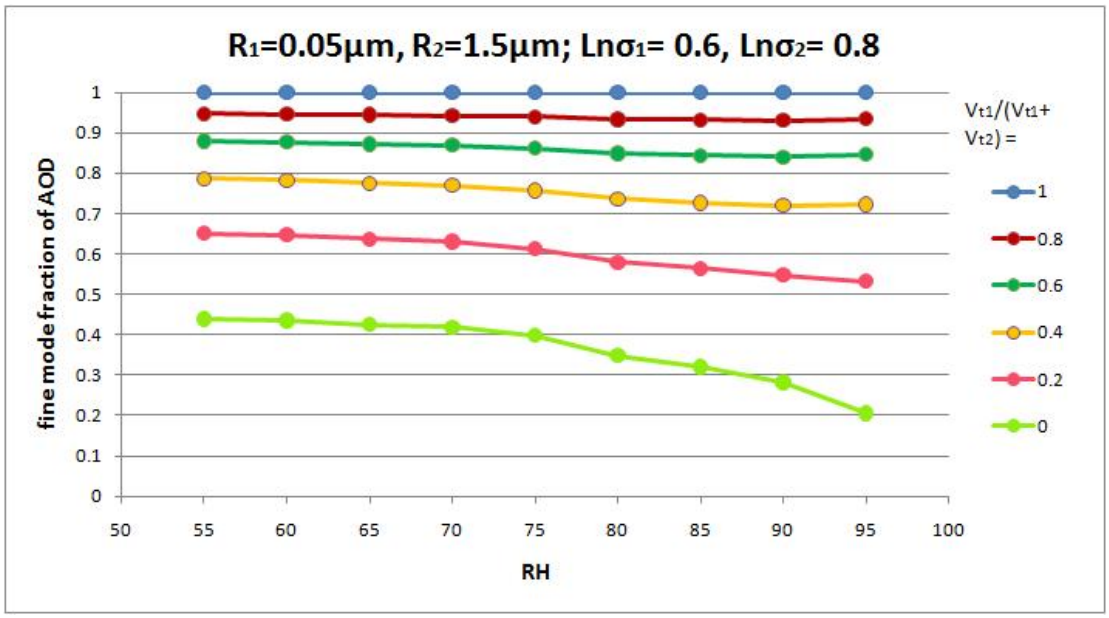

Figure B.24: Fine mode fraction of AOD (Type 2 aerosols) as a function of RH for dry size distributions specified by the parameters R_1=0.05μm, R_2=1.5μm, lnσ_1=0.8,lnσ_2=0.4,$V_{t1}/(V_{t1} + V_{t2})$=1, 0.8, 0.6, 0.4, 0.2, 0.0

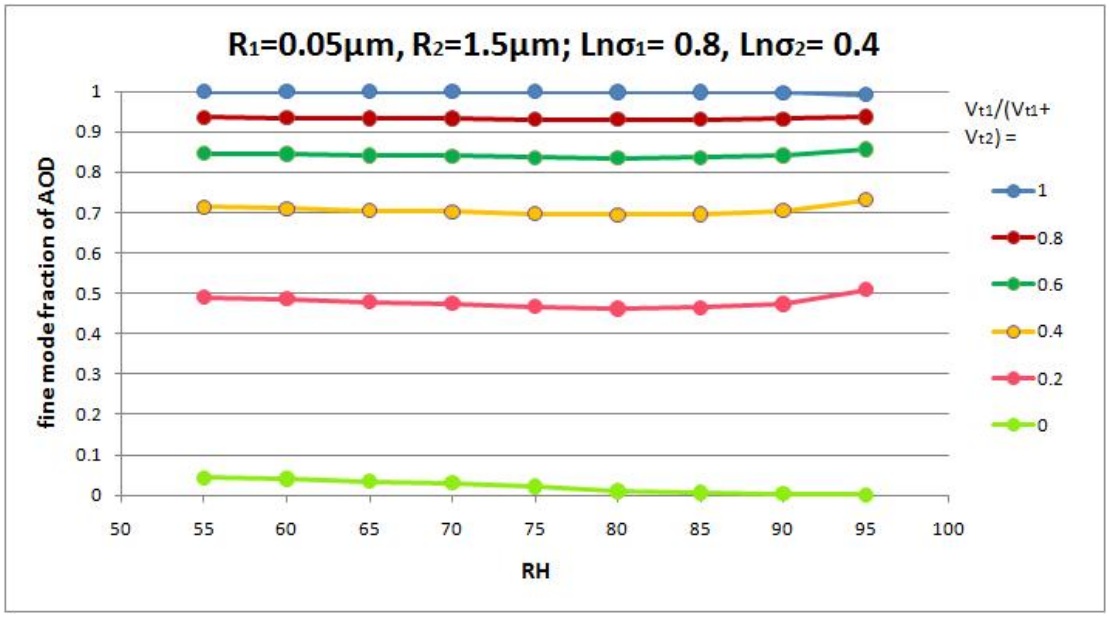

Figure B.25: Fine mode fraction of AOD (Type 2 aerosols) as a function of RH for dry size distributions specified by the parameters R_1=0.05μm, R_2=1.5μm, lnσ_1=0.8,lnσ_2=0.6,$V_{t1}/(V_{t1} + V_{t2})$=1, 0.8, 0.6, 0.4, 0.2, 0.0

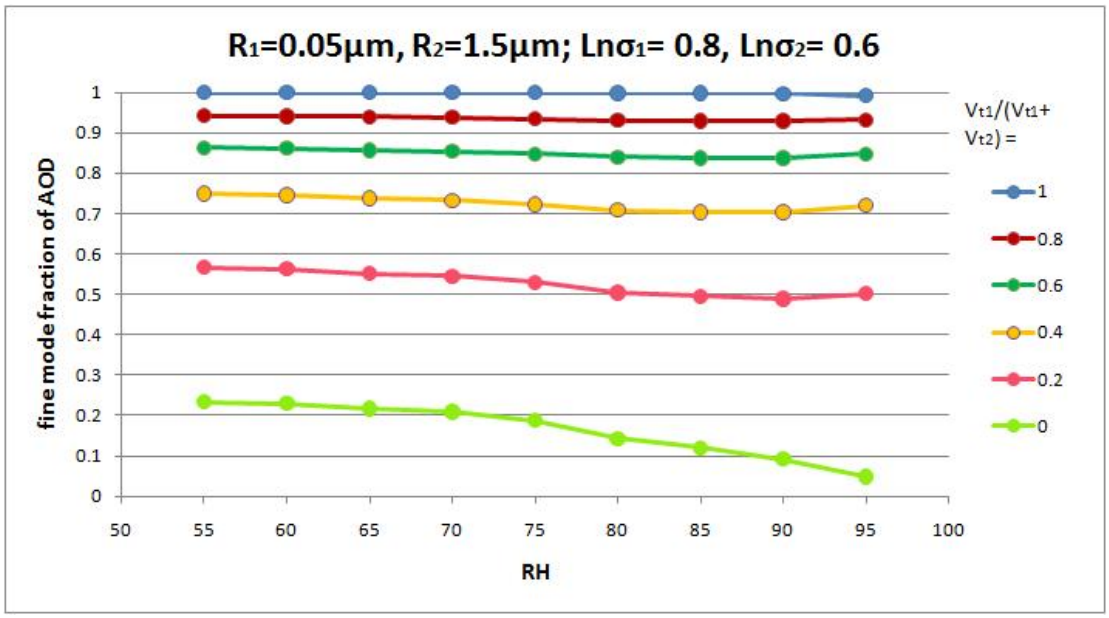

Figure B.26: Fine mode fraction of AOD (Type 2 aerosols) as a function of RH for dry size distributions specified by the parameters R_1=0.05μm, R_2=1.5μm, lnσ_1=0.8,lnσ_2=0.8,$V_{t1}/(V_{t1} + V_{t2})$=1, 0.8, 0.6, 0.4, 0.2, 0.0

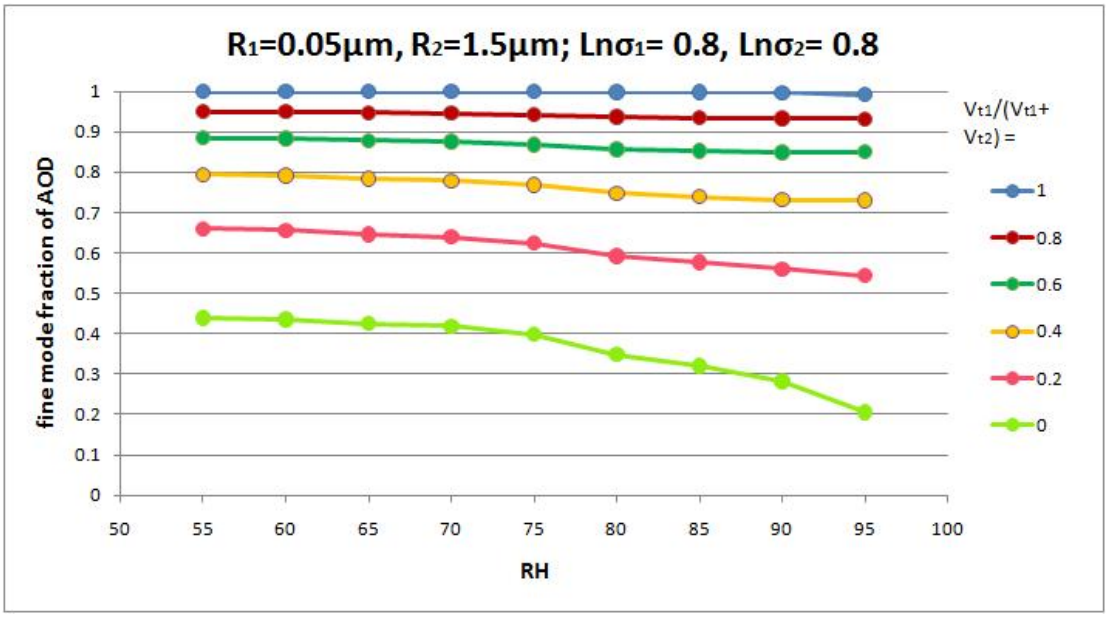

REFERENCES

Adachi, K., Freney, E., & Buseck, P. (2011). Shapes of internally mixed hygroscopic aerosol particles after deliquescence, and their effect on light scattering. *Geophysical Research Letters*, 38(13), L13804.

Andreae, M. & Merlet, P. (2001). Emission of trace gases and aerosols from biomass burning. *Global biogeochemical cycles*, 15(4), 955–966.

Ångström, A. (1929). On the atmospheric transmission of sun radiation and on dust in the air. *Geografiska Annaler*, 11, 156–166.

Bian, H., Chin, M., Rodriguez, J., Yu, H., Penner, J., & Strahan, S. (2009). Sensitivity of aerosol optical thickness and aerosol direct radiative effect to relative humidity. *Atmos. Chem. Phys*, 9, 2375–2386.

Bohren, C. & Huffman, D. (1983). Absorption and scattering of light by small particles. *Research supported by the University of Arizona and Institute of Occupational and Environmental Health. New York, Wiley-Interscience, 1983, 541 p.*, 1.

Bond, T. & Bergstrom, R. (2006). Light absorption by carbonaceous particles: An investigative review. *Aerosol Science and Technology*, 40(1), 27–67.

Brosset, C. (1976). Air borne particles: black and white episodes. *Ambio*, 5(4), 157–163.

Charlson, R., Schwartz, S., Hales, J., Cess, R., Coakley, J., Hansen, J., & Hofmann, D. (1992). Climate forcing by anthropogenic aerosols. *Science*, 255(5043), 423.

Cheng, M. T. & Tsai, Y. I. (2000). Characterization of visibility and atmospheric aerosols in urban, suburban, and remote areas. *The Science of the total environment*, 263(1-3), 101–114.

Cheng, Y. F., Wiedensohler, A., Eichler, H., Su, H., Gnauk, T., Brggemann, E., Herrmann, H., Heintzenberg, J., Slanina, J., Tuch, T., Hu, M., & Zhang, Y. H. (2008). Aerosol optical properties and related chemical apportionment at xinken in pearl river delta of china. *Atmospheric Environment*, 42(25), 6351–6372.

Chu, D., Kaufman, Y., Zibordi, G., Chern, J., Mao, J., Li, C., & Holben, B. (2003). Global monitoring of air pollution over land from the earth observing system-terra moderate resolution imaging spectroradiometer (modis). *J. Geophys. Res*, 108(D21).

Day, D. & Malm, W. (2001). Aerosol light scattering measurements as a function of relative humidity: a comparison between measurements made at three different sites. *Atmospheric Environment*, 35(30), 5169–5176.

Dey, S. & Di Girolamo, L. (2010). A climatology of aerosol optical and microphysical properties over the indian subcontinent from 9 years (2000–2008) of multiangle imaging spectroradiometer (misr) data. *Journal of Geophysical Research*, 115(D15), D15204.

Dockery, D. W., Pope, C. A., Xu, X., Spengler, J. D., Ware, J. H., Fay, M. E., Ferris, B. G., & Speizer, F. E. (1993). An association between air pollution and mortality in six u.s. cities. *New England Journal of Medicine*, 329(24), 1753–1759. doi: 10.1056/NEJM199312093292401.

Ebert, M., Weinbruch, S., Rausch, A., Gorzawski, G., Helas, G., Hoffmann, P., & Wex, H. (2002). Complex refractive index of aerosols during lace 98 as derived from the analysis of individual particles. *Journal of geophysical research*, 107(D21), 8121.

Eldering, A., Ogren, J. A., Chowdhury, Z., Hughes, L. S., & Cass, G. R. (2002). Aerosol optical properties during indoex based on measured aerosol particle size and composition. *J.Geophys.Res.*, 107, 8001.

Finlayson-Pitts, B. & Pitts, J. (2000). *Chemistry of the upper and lower atmosphere: Theory, experiments, and applications*. Academic Pr.

Fitzgerald, J. (1984). Effect of relative humidity on the aerosol backscattering coefficient at 0.694-and 10.6-μm wavelengths. *Applied optics*, 23(3), 411–418.

Fuzzi, S., Decesari, S., Facchini, M., Matta, E., Mircea, M., & Tagliavini, E. (2001). A simplified model of the water soluble organic component of atmospheric aerosols. *Geophys. Res. Lett*, 28(21), 4079–4082.

Garland, R., Ravishankara, A., Lovejoy, E., Tolbert, M., & Baynard, T. (2007). Parameterization for the relative humidity dependence of light extinction: Organic-ammonium sulfate aerosol. *Journal of Geophysical Research*, 112(D19), D19303.

Hänel, G. (1976). The properties of atmospheric aerosol particles as functions of the relative humidity at thermodynamic equilibrium with the surrounding moist air. *Adv. Geophys*, 19(1), 73–188.

Horvath, H. (1995). Size segregated light absorption coefficient of the atmospheric aerosol. *Atmospheric Environment*, 29(8), 875–883.

Jeong, M., Li, Z., Andrews, E., & Tsay, S. (2007). Effect of aerosol humidification on the column aerosol optical thickness over the atmospheric radiation measurement southern great plains site. *J. Geophys. Res*, 112.

Kaufman, Y., Koren, I., Remer, L., Rosenfeld, D., & Rudich, Y. (2005a). The effect of smoke, dust, and pollution aerosol on shallow cloud development over the atlantic ocean. *Proceedings of the National Academy of Sciences of the United States of America*, 102(32), 11207.

Kaufman, Y., Remer, L., Tanré, D., Li, R., Kleidman, R., Mattoo, S., Levy, R., Eck, T., Holben, B., Ichoku, C., et al. (2005b). A critical examination of the residual cloud contamination and diurnal sampling effects on modis estimates of aerosol over ocean. *Geoscience and Remote Sensing, IEEE Transactions on*, 43(12), 2886–2897.

Kaufman, Y., Tanré, D., & Boucher, O. (2002). A satellite view of aerosols in the climate system. *Nature*, 419(6903), 215–223.

Kim, J., Lee, J., Song, C., Kim, S., Chun, Y., Sohn, B., & Holben, B. (2010). Characteristics of aerosol types from aeronet sunphotometer measurements. In *AGU Fall Meeting Abstracts*, volume 1 (pp.$\tilde{0}$8).

Kleidman, R., O'Neill, N., Remer, L., Kaufman, Y., Eck, T., Tanré, D., Dubovik, O., & Holben, B. (2005). Comparison of moderate resolution imaging spectroradiometer (modis) and aerosol robotic network (aeronet) remote-sensing retrievals of aerosol fine mode fraction over ocean. *Journal of geophysical research*, 110(D22), D22205.

Köhler, H. (1936). The nucleus in and the growth of hygroscopic droplets. *Trans. Faraday Soc.*, 32, 1152–1161.

Koren, I., Remer, L., Kaufman, Y., Rudich, Y., & Martins, J. (2007). On the twilight zone between clouds and aerosols. *Geophysical research letters*, 34(8), L08805.

Kotchenruther, R. A., Hobbs, P. V., & Hegg, D. A. (1999). Humidification factors for atmospheric aerosols off the mid-atlantic coast of the united states. *J.Geophys.Res.*, 104, 2239–2251.

Laird, N. F. (2005). Humidity halos surrounding small cumulus clouds in a tropical environment. *Journal of the Atmospheric Sciences*, 62(9), 3420–3425. doi: 10.1175/JAS3538.1; M3: doi: 10.1175/JAS3538.1; 19.

Li-Jones, X., Maring, H., & Prospero, J. (1998). Effect of relative humidity on light scattering by mineral dust aerosol as measured in the marine boundary layer over the tropical atlantic ocean. *Journal of geophysical research*, 103, 31.

Liu, Z., Liu, D., Huang, J., Vaughan, M., Uno, I., Sugimoto, N., Kittaka, C., Trepte, C., Wang, Z., Hostetler, C., & Winker, D. (2008). Airborne dust distributions over the tibetan plateau and surrounding areas derived from the first year of calipso lidar observations. *Atmos.Chem.Phys.*, 8(16), 5045–5060. J1: ACP.

Loeb, N. & Schuster, G. (2008). An observational study of the relationship between cloud, aerosol and meteorology in broken low-level cloud conditions. *Journal of Geophysical Research*, 113(D14), D14214.

Lu, M.-L., Wang, J., Flagan, R. C., Seinfeld, J. H., Freedman, A., McClatchey, R. A., & Jonsson, H. H. (2003). Analysis of humidity halos around trade wind cumulus clouds. *Journal of the Atmospheric Sciences*, 60(8), 1041–1059. doi: 10.1175/1520-0469(2003)602.0.CO;2; M3: doi: 10.1175/1520-0469(2003)602.0.CO;2; 19.

Markowicz, K. M. (2003). Influence of relative humidity on aerosol radiative forcing: An ace-asia experiment perspective. *Journal of geophysical research*, 108(D23).

Nessler, R., Weingartner, E., & Baltensperger, U. (2005). Effect of humidity on aerosol light absorption and its implications for extinction and the single scattering albedo illustrated for a site in the lower free troposphere. *Journal of Aerosol Science*, 36(8), 958–972.

Nilsson, B. (1979). Meteorological influence on aerosol extinction in the 0.2–40-μm wavelength range. *Applied Optics*, 18(20), 3457–3473.

ONeill, N., Eck, T., Smirnov, A., Holben, B., & Thulasiraman, S. (2003). Spectral discrimination of coarse and fine mode optical depth. *J. Geophys. Res*, 108, 4559.

Phalen, R. (1984). *Inhalation studies: foundations and techniques*. CRC Press Inc., Boca Raton, FL.

Platt, C. M. R. & Gambling, D. J. (1971). Laser radar reflexions and downward infrared flux enhancement near small cumulus clouds. *Nature*, 232(5307), 182–185. M3: 10.1038/232182a0; 10.1038/232182a0.

Pope, C. (2007). Mortality effects of longer term exposures to fine particulate air pollution: review of recent epidemiological evidence. *Inhalation toxicology*, 19(S1), 33–38.

Pope, C., Burnett, R., Thun, M., Calle, E., Krewski, D., Ito, K., & Thurston, G. (2002). Lung cancer, cardiopulmonary mortality, and long-term exposure to fine particulate air pollution. *JAMA: the journal of the American Medical Association*, 287(9), 1132.

Pope, C. A., Dockery, D. W., & Schwartz, J. (1995). Review of epidemiological evidence of health effects of particulate air pollution. *Inhalation toxicology*, 7(1), 1–18. doi: 10.3109/08958379509014267; M3: doi: 10.3109/08958379509014267; 19.

Pósfai, M. & Buseck, P. (2010). Nature and climate effects of individual tropospheric aerosol particles.

Radke, L. & Hobbs, P. (1991). Humidity and particle fields around some small cumulus clouds. *Journal of Atmospheric Sciences*, 48, 1190–1193.

Rees, M. H. (1989). *Physics and chemistry of the upper atmosphere*, volume 1. Cambridge Univ Pr.

Rosenfeld, D. (1999). Trmm observed first direct evidence of smoke from forest fires inhibiting rainfall. *Geophysical Research Letters*, 26(20), 3105.

Rosenfeld, D. (2000). Suppression of rain and snow by urban and industrial air pollution. *Science*, 287(5459), 1793.

Schuster, G., Dubovik, O., & Holben, B. (2006). Angstrom exponent and bimodal aerosol size distributions. *Journal of geophysical research*, 111(D7), D07207.

Schwartz, J., Dockery, D. W., & Neas, L. M. (1996). Is daily mortality associated specifically with fine particles? *Journal of the Air Waste Management Association*, 46(10), 927–939.

Seinfeld, J. & Pandis, S. (1998). *Atmospheric chemistry and physics: from air pollution to climate change*. Wiley New York.

Su, W., Schuster, G. L., Loeb, N. G., Rogers, R. R., Ferrare, R. A., Hostetler, C. A., Hair, J. W., & Obland, M. D. (2008). Aerosol and cloud interaction observed from high spectral resolution lidar data. *J.Geophys.Res.*, 113, D24202.

Tackett, J. & Di Girolamo, L. (2009). Enhanced aerosol backscatter adjacent to tropical trade wind clouds revealed by satellite-based lidar. *Geophys. Res. Lett*, 36, 14.

Tang, I. (1996). Chemical and size effects of hygroscopic aerosols on light scattering coefficients. *Journal of geophysical research*, 101(D14), 19245.

Tang, I. & Munkelwitz, H. (1994). Water activities, densities, and refractive indices of aqueous sulfates and sodium nitrate droplets of atmospheric importance. *Journal of Geophysical Research*, 99(D9), 18801–18808.

Twohy, C., Coakley Jr, J., & Tahnk, W. (2009). Effect of changes in relative humidity on aerosol scattering near clouds. *Journal of Geophysical Research*, 114(D5), D05205.

Twomey, S. (1974). Pollution and the planetary albedo. *Atmospheric Environment (1967)*, 8(12), 1251–1256.

Twomey, S. (1977). The influence of pollution on the shortwave albedo of clouds. *Journal of the Atmospheric Sciences*, 34(7), 1149.

Veselovskii, I., Whiteman, D., Kolgotin, A., Andrews, E., & Korenskii, M. (2009). Demonstration of aerosol property profiling by multiwavelength lidar under varying relative humidity conditions. *Journal of Atmospheric and Oceanic Technology*, 26(8), 1543–1557.

Wiscombe, W. (1980). Improved mie scattering algorithms. *Applied optics*, 19(9), 1505–1509.

Wulfmeyer, V. & Feingold, G. (2000). On the relationship between relative humidity and particle backscattering coefficient in the marine boundary layer determined with differential absorption lidar. *Journal of geophysical research*, 105(D4), 4729–4741.

Yoon, S. & Kim, J. (2006). Influences of relative humidity on aerosol optical properties and aerosol radiative forcing during ace-asia. *Atmospheric Environment*, 40(23), 4328–4338.